ISSN 1016-3115

wgn

18 - 4
august 1990

bimonthly journal of the international meteor organization

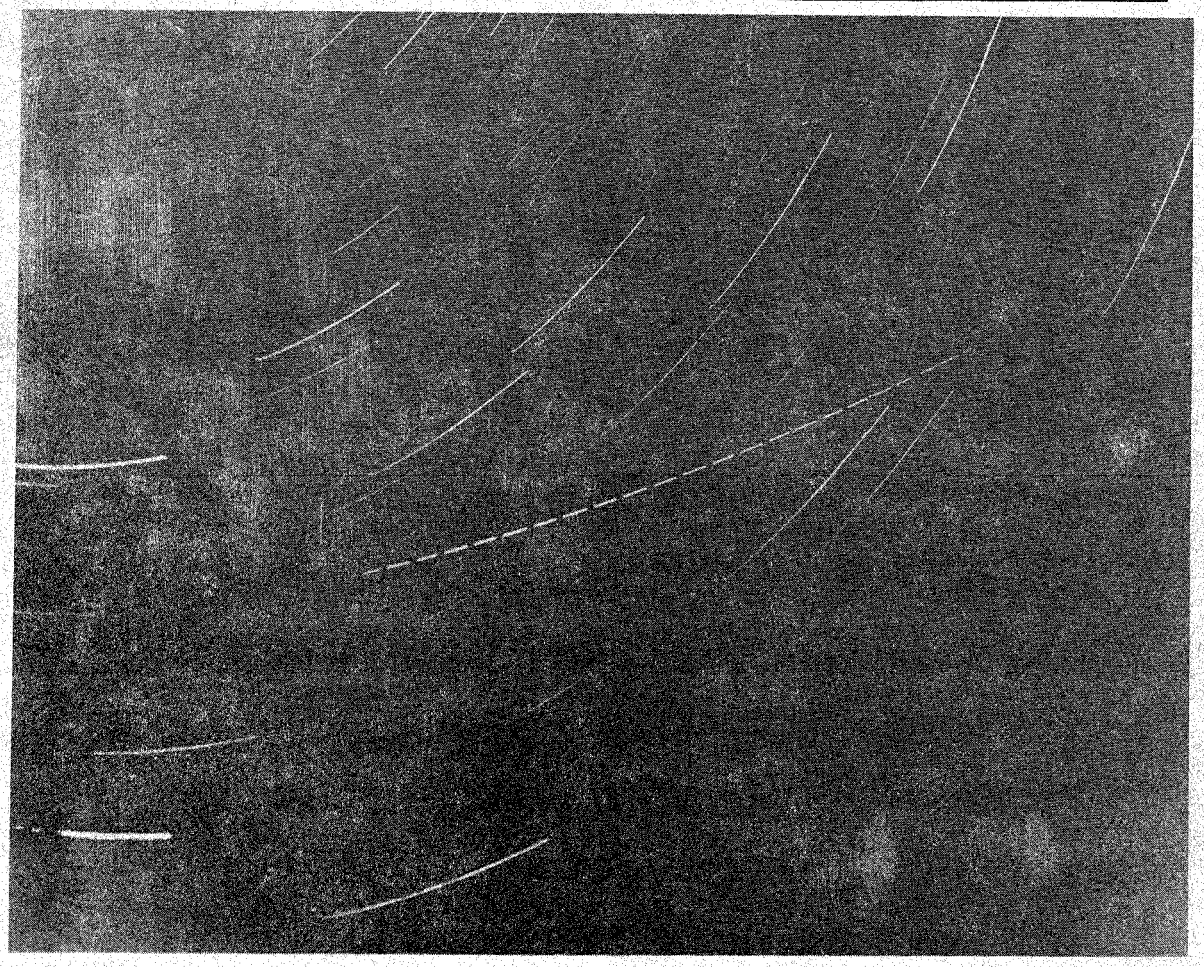

Aquarid fireball of about −5 photographed by Jürgen Rendtel on August 1, 1989, $23^h37^m46^s$ UT, at the Roshen Observatory in Bulgaria. The photograph was exposed from $22^h43^m46^s$ until $23^h41^m31^s$ UT. A fish-eye lens, $f/3.5$, $f = 30$ mm was used in combination with a 400 ASA film. There are 12.5 breaks per second.

In this issue:

In case of non-delivery, return postage guaranteed. Please return to:
v.u.: Marc Gyssens, Heerbaan 74, B-2530 Boechout, Belgium

Afgiftekantoor: 2540 Hove

WGN, volume 18, nr 4, August 1990, pp. 97–166

Contents

Useful Information

The October Issue *(WGN 18:5)*

The *October issue* is expected to be mailed during the first or second week of October. Contributions are due *September 18*. They should be sent to *Marc Gyssens* (or given to him at the *IMW* 1990) or to any member of the editorial board (addresses: inside of back cover).

WGN Subscription/IMO Membership 1991

The subscription rate for volume 19 is 400 BEF for six issues. It is anticipated that volume 19 will contain over 240 pages. Subscriptions should be paid to Ann Schroyens or, for the USA and Canada, to Peter Brown, or, for Japan, to Masahiro Koseki (all addresses on the inside of back cover). Please make sure we retain the full amount due after deduction of bank and/or exchange charges. Therefore it is recommended to pay by international postal money order. Additional gifts are of course welcome.

Administrative Correspondence

All payments should be addressed to Ann Schroyens. Complaints about not receiving *WGN* or changes of address should be sent to Paul Roggemans. Their addresses can be found on the inside of the back cover.

From the Editor-in-Chief

Marc Gyssens

As told, this is once again a thick issue of our journal. The holiday season on the one hand, and professional obligations abroad on my part on the other hand, caused some delays in finishing this issue, for which we apologize. IMO members should find a booklet enclosed about the IMO commissions. Please let us now if you are an IMO member and did not receive the booklet.

At this time, many of us are looking forward to the International Meteor Weekend in Violau, West Germany, which will mark the first anniversary of IMO's official existence. Many results are already achieved, credibility and support from professional astronomers and a well-organized Visual Commission probably being the most important. Furthermore, the political evolution in Eastern Europe during the same period was also very helpful to IMO, in view of the large number of very active meteor workers in that part of the world. These people can now participate much more efficiently in the management of IMO. Still, the fact remains that the workload involved in running IMO still rest on too few shoulders so that many jobs remain undone. Building up the International Meteor Organization requires a commitment which, at present, not enough people seem willing to make. Maybe this is a subject that should be addressed and discussed in Violau.

Meanwhile, I hope that this summer will produce a lot of observations. Please make sure that you follow the various commissions' guidelines in order to enable us to get the maximum out of your observations in global analyses and that you send in your results in time. Also, do not forget WGN!

About IMO Publications

Marc Gyssens

As fall is approaching, we must start thinking about renewing *membership and/or subscription.* As it is our policy to keep our rates as low as possible, we still offer you *WGN* at the same price as this year: 400 BEF. Unfortunately, we are no longer able to guarantee airmail delivery outside Europe for this price. People who wish guaranteed airmail delivery should add 200 BEF. Dues are payable to Ann Schroyens as usual, or to Peter Brown or Masahiro Koseki if you live in North America or Japan, respectively. This year, we experienced a lot of problems with payments from British subscribers. We will try to solve these problems and let you know something concretely in the October issue. Also, there is now the possibility for German subscribers to pay in marks to Ina Rendtel, Jürgen's wife. More information will follow in the next WGN.

The excellent gnomonic *Atlas Brno 2000.0* is also available. They can be ordered from Ann Schroyens at 100 BEF per copy.

The *proceedings* of the International Meteor Weekend in Balatonföldvár, announced in previous issues, are now ready. They too can be ordered from Ann Schroyens at the price of 250 BEF each.

Also, the second issue in the *Observational Reports Series* of *WGN*, the *report on 1989*, is scheduled to appear in the fall. As for the 1988 report, we set the price on 300 BEF.

In you are interested in some or all of this publications, it may be a good idea to make a joint payment for your *IMO/WGN* renewal, the *IMW* 1989 proceedings, the 1988 observational report (if you did not yet order it) and the 1989 report which is to appear. In this way you can save a lot of costs that would otherwise be involved in separate international payments.

In order to avoid misunderstandings, we do recommend you however to accompany your payment with a letter to Paul Roggemans stating what exactly you ordered, how much you paid and to whom and by which means you made the transfer.

Of course, the cheapest way of arranging these matters is to pay cash at the *IMW* in Violau. If you go there, do not miss this opportunity to save money, to avoid late payments, and to help us to update our membership and subscription lists as quickly as possible!

Letters to WGN

compiled by Marc Gyssens

About the editorial policy

Not that many reactions about my editorial comments in the previous issue reached us. Below are the opinions of Alastair McBeath and Peter Brown. Some more comments on this issue by other people would be most welcome! Maybe this topic should also be discussed at the International Meteor Weekend in Violau?

Firstly, should the item "New Evidence for a Cassiopeid Meteor Shower" in *WGN* 18:2 have been published, and should similar items be given a place in future numbers of the Journal ? My answer has to be "yes". If all a journal publishes is "conventional wisdom" then there is no hope for real progress. There must be a place for people to question what is being said, otherwise science simply stagnates; witness for example the extraordinary adherence to the Aristotelian cosmology throughout much of the past 2000 years despite its being wrong in almost every major aspect. This is not, however, to say that we must accept every item without looking at its validity. In the case of the Cassiopeid paper, the editorial disclaimer was useful, and would be essential for any future items, but perhaps publication should have been held for an issue to either clarify the points raised—in particular to obtain much more precise data—or to have a detailed, but not necessarily derogatory, critique prepared with reference to *IMO* results, surely the most reliable source of data on any new shower activity currently available.

Papers of this kind should ideally be presented by the actual observers; a third party is not always conducive to be accurate recording and presentation of the data. This makes such observers rather more accountable for their statements, which may or may not then be borne out by further discussion. It certainly makes obtaining the original information a great deal easier, if nothing else.

The onus must be on the authors to provide as much detail as possible in unusual reports. The recent lengthy discussion on the nature of the "meteor trains" presented in *WGN* 17:4 have largely been possible as the original item did not contain sufficient detail on the observations, thus a number of possible explanations have come to light, and it has not really been practical to rule out any of them. Perhaps the best solution in these cases would be for the author to contact the appropriate *IMO* Commission Director before publishing the paper, to see if others have reported anything similar either at the time or previously. This would prevent the repetitive publication of items on, for instance, curved meteors, which were actually caused by birds catching in street lights—an improbable example, perhaps, but it shows what might happen without some degree of control. If after discussion with the Commission in question the author still wishes to publish, then a forum should be available for them to do so, but of course an additional period would have been allowed for a suitable response piece to have been prepared. This should also ensure that a reasonable factual paper then ensues as well.

At the end of the day, the editor, based on advice, is responsible for what is published in the journal he or she edits. This means that the editor's say is final, and should be treated as such. To ensure that the editor's position is not then undetermined, it is important that contradictory statements should not be issued. The recent closure of the "meteor trains" correspondence in *WGN* 18:2 followed by its re-opening, however briefly, in 18:3 is a case of point. The re-opening was necessary it seems to me because one of the authors did not provide a sufficiently detailed account of the phenomenon they were describing in the first place.

Finally, it is as well to remember that even an incorrect paper or one of dubious value may well be the catalyst which sets in motion a train of thought which eventually lead to deeper understanding of some aspect of our subject. As we cannot possibly tell what might set such a chain of events in motion, we would do well not to discount any item, however unlikely they may seem. While the tale of Newton and the falling apple may well be apocryphal, would we really have wanted to be the person standing in the way of his seeing it?

Alastair McBeath, May 31, 1990

It was very interesting to read Paul's and Ralf's comments about Peter Aneca's paper regarding the Cassiopeid shower.

The paper however, may have received more criticism than it deserved. While it is true that substantial conclusions regarding an outburst of this sort are warranted only when a convincingly large number of independent observations are received I do think Peter Aneca attempted to do this in his paper. By presenting the observation he has brought the data to the attention of those in the meteor community who have the resources to follow it up.

It would have been better perhaps for Peter to communicate the observations to the Visual Commission privately and build a much stronger case for the proposed shower before publishing. Relying on the *BMS* catalog to build a case is quite unacceptable as this source has never been clearly established to have built its database from convincingly rigorous methods of observation.

Of course without plots, as Paul and Ralf point out it is virtually impossible to verify if indeed this was a reputable shower. Only future observations (preferably of a photographic nature) on or about November 4–5 can make up this unfortunate discrepancy. If indeed there is no mention in the other credible sources Peter Aneca lists and there are no other confirming observations as Paul and Ralf suggest and if no future return is noted, then it seems reasonable to assume the shower was a chance lining up perhaps brought about by subjective ideas the observer had after seeing two or three meteors coming from the area around ε-Cassiopeiae.

I am very interested in the possibility that this was a little group of meteoroids (13) all having similar orbits and meeting the Earth by chance as Paul and Ralf suggest. Having not seen this sort of meteoroid swarm mentioned in the literature I am curious as to where this explanation arose.

Peter Aneca is, at worst, guilty of merely jumping the gun and publishing this observation before consulting with other workers and looking through many sources.

The point raised by Ralf and Paul about he editorial board's responsibility is a very valid one. While I would not call the work "nonsense" I think a limited form of review of major articles might be in order for *WGN*. Notes and straight observational reports should continue going in to *WGN* as before and had Peter Aneca's paper gone in instead as a short note mentioning the observation and asking observers to watch on this date I think no harm would have been done. I would like to hear what other members of the editorial board think about the idea of this sort of a limited review system.

Peter Brown, June 6, 1990

About radio observing

Jeroen Van Wassenhove has some comments on two articles in previous issues of WGN regarding radio work.

First, I have some comments on the article of Dr. T.R. Manley in *WGN* 18:2, pp. 66–67. The method of reduction as presented in the article is very simplified. The observations should be corrected with the so-called "Observability Function" [1], which is similar to the application of the ZHR correction for visual work. The observability function is calculated with the program "Forward" (release 3.0), which includes the antenna gain, power of the transmitter and many other parameters. If one applies this correction, one will notice that the so called "M" patterns will change dramatically. Comparing the successive days (using the corrected values) or periods with each other will give a more detailed view of the activity profile than plotting all observations on one time scale (normally, solar longitude is used).

My other comments are about the article "Meteors by Radio" from M.J. Morrow and B.R. Moore in *WGN* 18:3, pp. 90–94. Using tape recorder for automatizing a forward scatter system can be a proper solution but has some disadvantages. Due to the quality of the tape, a lot of meteor reflections (weak ones) are simply not recorded. This number is so significant (5–15%) that we stopped using tape recorders. Even high quality tapes had this disadvantage. Chart recorders on the other hand perform much better and yield more information about the meteor reflection itself. (amplitude, duration). However, external signal sources such as lightening, certain switches, ..., produce a signal which is similar to a meteor reflection. Except when the speed of the chart recorder is rather high, it is not that easy to distinguish the "rubbish" from the meteor reflections (especially with lightening). So I would like to recommend radio observers to keep listening with a headphone, even when they use a chart recorder. It wouldn't be the first time that a Perseid campaign is spoiled due to this. Most people shut down their system when there is heavy lightening because the financial consequences of a lightening strike are high.

[1] Christian Steyaert, "Forward : A General Program for Calculating the Observability Function", *WGN* 15:3, June 1987, pp. 90–93.

Jeroen Van Wassenhove, June 1990

Workshop Visual Commission at the IMW 1990

Ralf Koschack

The Visual Commission Workshop at the International Meteor Weekend in Violau, West Germany, is scheduled on the evening of Friday, September 7. In order to use the time most effectively and to avoid a pointless discussion, I propose to establish a loose program with topics we want to discuss. People having another topic for discussion should contact me on Thursday. If people not participating in the *IMW* have problems they want to see discussed, they can contact me by mail. From my point of view, we should talk about the following issues:

1. The improvement of the new observing report forms published in *WGN* 18:2. In order to print a large number of copies we have to define the final form.
2. Modification of the contents and the format of the annual report on visual data.
3. Since the article about the procedure to determine spatial number densities, population and mass distribution index by means of visual observations, published in *WGN* 18:2 and this issue, covers one of the most important topics of visual work, Jürgen Rendtel and I want to take the opportunity to answer questions and to discuss problems of general interest concerning the subject.

People are asked to propose further topics and to get ready for the points listed above.

Use of the Epoch 2000.0

Jürgen Rendtel

Presently, both epoch 1950.0 and 2000.0 are used in reports, and this may result in more or less severe misunderstandings. To complicate things even further, some observers use the current epoch in articles about their observations!

In order to overcome this situation in *IMO* it was decided *to use epoch* 2000.0 *for all IMO publications from 1991, January 1, onward*, the beginning of the new decade. Please take notice of this and make your own reports and submissions to *WGN* conform with this decision, to avoid possible ambiguities.

For the remainder of this year, the *IMO* standard is still 1950.0.

New Shower Radiant in Delphinus?

communicated by Jürgen Rendtel

The following short information was received from Eva Bojurova, Varna, Bulgaria:

> *An unknown radiant at* $\alpha = 310°, \delta = +20°$ *in Delphinus is under suspicion since July 17, 1990. Diffuse yellowish meteors. Activity: ZHR below 5.*
>
> Telegram received July 26, 1990.

Did anybody else notice something? We ask all observers to check their observations of that period. Please let us now your findings!

Possible Radio Activity in September 1990

Dirk Artoos

Around September 16, 1989, I registered a high peak of echoes (96 signals/0.67 hours) and G.M. Kristensen too detected with his radio a likewise high activity (143 signals/hour). Since my observation of 1989 was carried out around 8^h50^m UT, corresponding to $\lambda_\odot = 172\overset{\circ}{.}91$ (1950.0), a possible maximum activity might occur this year on September 16, around 15^h UT. The suspected radiant is situated northeast of Orion (near Gemini). Please be alert around that period and listen for any unusual activity!

I also ask your special attention around September 26–30. In 1988 and 1989 I registered high activity during daylight hours. The suspected areas of radiants are Auriga and Sextans, but there is no definite answer as to which radiant is active. The suspected radiant in Sextans is at $\alpha = 152°$, $\delta = 0°$, and the suspected radiant near δ Aurigae is at $\alpha = 87\overset{\circ}{.}8$ and $\delta = +54°$. In September 1989 the Danish radio observer G.M. Kristensen had also detected a great activity (196 signals/hour). He reported an activity period from September 25 till October 1.

Therefore please observe visually during the early morning hours. Keep the areas indicated well in sight.

For the radio predictions for 1990, see the observability function in Table 1. The observability function is given for 50° N, 35° N, 0° and 35° S. The value (a percentage) is given for each hour local time for the directions South, West, East and North. 100% corresponds to the best observability, 0% with the radiant under the horizon. For the calculations, a four element antenna at an elevation of 45°, a transmitter distance of 1000 km and a transmitter power of 30 kW were assumed.

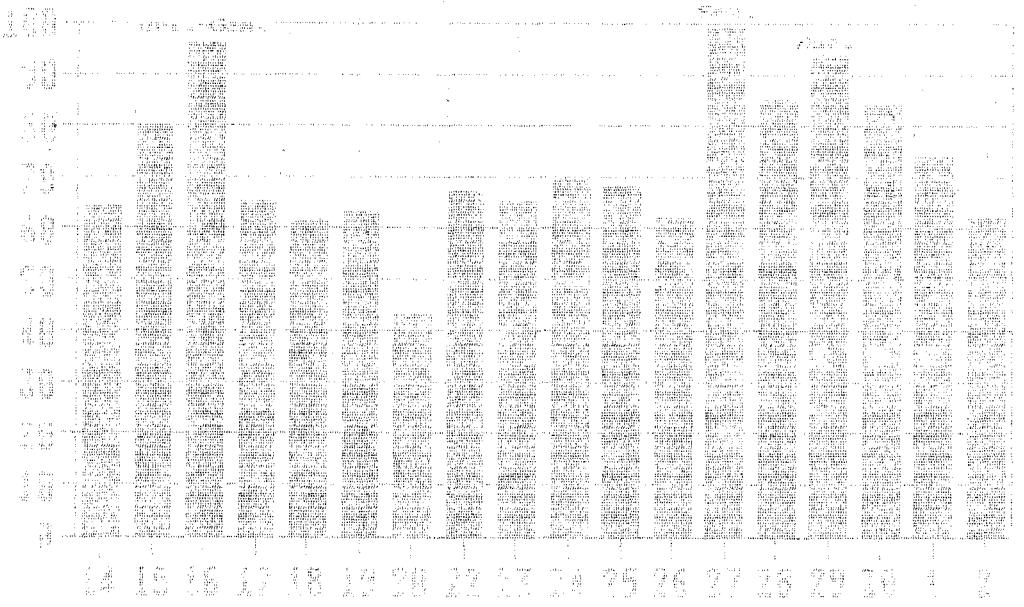

Figure 1 – Radio activity observed in September 1989 by Dirk Artoos at 66.45 MHz with an antenna elevation of 40° and azimuth of 275°. Observations up to September 20 were carried out between 8^h30^m and 9^h10^m UT; afterwards, observations were carried out between 9^h45^m and 10^h15^m UT.

Table 1 – Observability function for a four-element antenna elevated at 45° for each hour of the day (local time), four cardinal directions and four latitudes (100 = best observability, 0 = radiant below the horizon). For the calculations a transmitter distance of 1000 km and a transmitter power of 30 kW was assumed.

Lat.	Dir.	00	01	02	03	04	05	06	07	08	09	10	11	12	13	14	15	16	17	18	19	20	21	22	23
+50	S	0	0	0	0	7	37	65	89	100	96	92	99	96	77	51	22	0	0	0	0	0	0	0	0
+50	W	0	0	0	0	11	59	86	100	96	99	98	96	90	84	71	35	0	0	0	0	0	0	0	0
+50	E	0	0	0	0	10	58	81	89	94	98	100	99	95	94	75	38	0	0	0	0	0	0	0	0
+50	N	0	0	0	0	6	29	52	73	96	100	97	99	89	62	41	16	0	0	0	0	0	0	0	0
+35	S	0	0	0	0	10	46	77	97	94	59	47	81	100	89	61	27	0	0	0	0	0	0	0	0
+35	W	0	0	0	0	12	59	85	100	95	94	91	87	83	81	73	37	0	0	0	0	0	0	0	0
+35	E	0	0	0	0	12	58	77	79	82	86	90	92	100	89	70	34	0	0	0	0	0	0	0	0
+35	N	0	0	0	0	8	36	61	79	99	98	95	100	85	71	48	21	0	0	0	0	0	0	0	0
00	S	0	0	0	0	10	51	84	100	94	46	0	78	100	94	68	31	0	0	0	0	0	0	0	0
00	W	0	0	0	0	14	62	87	100	98	88	0	5	40	73	86	49	0	0	0	0	0	0	0	0
00	E	0	0	0	0	29	74	78	50	11	0	0	100	99	98	70	39	0	0	0	0	0	0	0	0
00	N	0	0	0	0	10	51	84	100	93	45	0	77	100	94	68	31	0	0	0	0	0	0	0	0
−35	S	0	0	0	0	8	36	61	79	99	98	95	100	85	71	48	21	0	0	0	0	0	0	0	0
−35	W	0	0	0	0	11	59	85	100	95	94	91	87	83	81	73	37	0	0	0	0	0	0	0	0
−35	E	0	0	0	0	12	58	77	79	82	86	90	92	100	89	70	34	0	0	0	0	0	0	0	0
−35	N	0	0	0	0	9	45	77	99	100	66	44	68	89	81	57	25	0	0	0	0	0	0	0	0

Table 1 – Angular velocity (°/s) as a function of the altitude of the meteor's beginning point h_b and the distance D between the end point and the radiant for various values of a stream's geocentric velocity V_∞. H_b is the altitude of the meteor's beginning point above the Earth's surface.

	$V_\infty = 20$ km/s, $H_b = 100$ km					$V_\infty = 25$ km/s, $H_b = 100$ km				
	$h_b = 10°$	20°	40°	60°	90°	10°	20°	40°	60°	90°
$D = 5°$	0.2	0.3	0.6	0.9	1.0	0.2	0.4	0.8	1.1	1.3
10°	0.3	0.7	1.3	1.7	2.0	0.4	0.9	1.6	2.2	2.5
20°	0.7	1.3	2.5	3.4	3.9	0.9	1.7	3.2	4.3	4.9
40°	1.3	2.5	4.7	6.3	7.3	1.6	3.2	5.9	8.0	9.3
60°	1.7	3.4	6.3	8.5	9.8	2.2	4.3	8.0	11	13
90°	2.0	3.9	7.3	9.8	11	2.5	4.9	9.3	13	14
	$V_\infty = 30$ km/s, $H_b = 100$ km					$V_\infty = 35$ km/s, $H_b = 100$ km				
	$h_b = 10°$	20°	40°	60°	90°	10°	20°	40°	60°	90°
$D = 5°$	0.3	0.5	1.0	1.4	1.6	0.3	0.6	1.1	1.5	1.7
10°	0.5	1.1	2.0	2.7	3.1	0.6	1.2	2.2	3.0	3.4
20°	1.1	2.1	4.0	5.3	6.2	1.2	2.3	4.3	5.8	6.7
40°	2.0	4.0	7.4	10	12	2.2	4.3	8.2	11	13
60°	2.7	5.3	10	14	16	3.0	5.8	11	15	17
90°	3.1	6.2	12	16	18	3.4	6.7	13	17	20
	$V_\infty = 40$ km/s, $H_b = 100$ km					$V_\infty = 50$ km/s, $H_b = 110$ km				
	$h_b = 10°$	20°	40°	60°	90°	10°	20°	40°	60°	90°
$D = 5°$	0.3	0.7	1.3	1.7	2.0	0.4	0.8	1.5	2.0	2.3
10°	0.7	1.4	2.6	3.5	4.0	0.8	1.6	2.9	3.9	4.6
20°	1.4	2.7	5.0	6.8	7.9	1.6	3.1	5.8	7.8	9.0
40°	2.6	5.0	9.5	13	15	2.9	5.8	11	15	17
60°	3.5	6.8	13	17	20	3.9	7.8	15	20	23
90°	4.0	7.9	15	20	23	4.6	9.0	17	23	26
	$V_\infty = 60$ km/s, $H_b = 115$ km					$V_\infty = 66$ km/s, $H_b = 115$ km				
	$h_b = 10°$	20°	40°	60°	90°	10°	20°	40°	60°	90°
$D = 5°$	0.5	0.9	1.7	2.3	2.6	0.5	1.0	1.9	2.5	2.9
10°	0.9	1.8	3.4	4.5	5.2	1.0	2.0	3.7	5.0	5.8
20°	1.8	3.5	6.7	9.0	10	2.0	3.9	7.3	10	11
40°	3.7	6.7	13	17	20	3.7	7.3	14	18	21
60°	4.6	9.0	17	23	26	5.0	10	18	25	29
90°	5.3	10	20	26	30	5.8	11	21	29	33
	$V_\infty = 70$ km/s, $H_b = 126$ km									
	$h_b = 10°$	20°	40°	60°	90°					
$D = 5°$	0.5	0.9	1.8	2.4	2.8					
10°	1.0	1.9	3.6	4.8	5.5					
20°	1.9	3.7	7.0	9.4	11					
40°	3.6	7.0	13	18	21					
60°	4.8	9.4	18	24	28					
90°	5.5	11	21	28	32					

Estimating a Meteor's Angular Velocity

Ralf Koschack

Reliable observations of minor showers require considering all criteria of shower association (see [1]). The angular velocity ω of a meteor is such an important criterion. Since all meteors belonging to a same shower enter the Earth's atmosphere at the same velocity V_∞ and start to light up at similar altitudes H_b above Earth's surface, the angular velocity of a shower meteor is completely determined if one knows the elevation h_b of its beginning point and the distance D between its end point and the radiant D. Table 1 on p. 103 shows the relationship between ω, h_b and D for some values of V_∞. For details of calculation, please refer to [1].

In order to take into account the angular velocity ω as a criterion for shower membership identification, ω has to be estimated in degrees per second and compared to the expected value. Therefore, use Table 1 on the previous page. This table will be published annually until the first available opportunity to include it in the *IMO Handbook for Visual Meteor Observations*.

But how can ω be estimated in degrees per second ? Estimating duration and calculating ω by means of path length is difficult. It is much better to convert the sensation of the meteor's velocity directly into degrees per second. While watching a meteor, the observer stores the phenomenon usually as a whole in his memory. Then he fixes the path and estimates the magnitude. Now it is possible to estimate ω also: in thought, the observer makes the meteor move for one second. Then its path length is ω in degrees per second. One becomes able to estimate ω directly without this procedure after observing a number of meteors if one has the "scale" in his head. Estimates by experienced observers differ by no more than 50%.

References

[1] Koschack R., "Visual Observations of Minor Showers and Association of Shower Meteors", *Proceedings of the IMW 1989*, Balatonföldvár, 1990.

Visual Observers' Notes: September–October 1990

Jeff Wood

1. Introduction

Following the excellent activity of the previous two months, observers tend to feel let down when rates return to normal during September and October. Because of this, nowhere near as much observational work has been carried out during this time even though there is much to see.

Table 1 on the next page gives a list of the active showers that occur in these months and Table 2 shows the observing conditions moon-wise. The illuminated part of the Moon is always given for 0^h UT on the date indicated. The dates of the phases of the Moon are also given in UT.

2. α-Aurigids

This northern hemisphere shower reaches maximum on September 1. Rates are variable from year to year. The α-Aurigids are noted for producing fast moving yellow fireballs many of which have a train. The *IMO* requests observers to give this shower special attention in 1990. Further details on the α-Aurigids are to be found in [1,2].

Table 1 – A list of some of the meteor showers to be seen during September and October 1990.

Shower	Activity	Max	Radiant			Drift		V_∞	r	ZHR
			α	δ	Diam.	$\Delta\alpha$	$\Delta\delta$			
π-Eridanids	Aug 20–Sep 05	Aug 28	52°	−15°	6°	+0.8	+0.2	59	2.8	
α-Aurigids	Aug 24–Sep 05	Sep 01	84°	+42°	5°	+1.1	0.0	66	2.5	15
Piscids S	Aug 15–Oct 14	Sep 24	8°	0°0	8°	+0.9	+0.2	26	3.0	3
κ-Aquarids	Sep 08–Sep 30	Sep 20	339°	−02°	5°	+1.0	+0.2	16	3.0	3
Capricornids (Oct)	Sep 20–Oct 14	Oct 03	303°	−10°	5°	+0.8	+0.2	15	2.8	3
σ-Orionids	Sep 10–Oct 26	Oct 05	86°	−03°	5°	+1.2	0.0	65	3.0	3
Draconids	Oct 06–Oct 10	Oct 09	262°	+54°	5°			20	2.6	storm
ε-Geminids	Oct 14–Oct 27	Oct 19	104°	+27°	5°	+1.0	0.0	71	3.0	5
Orionids	Oct 02–Nov 07	Oct 22	95°	+16°	10°	+1.2	+0.1	66	2.9	30
Taurids S	Sep 15–Nov 26	Nov 03	50°	+13°	10°/5°			27	2.3	12
Taurids N	Sep 13–Dec 01	Nov 13	58°	+22°	10°/5°			29	2.3	8
Puppid/Velids	Oct 15–Jan 22	several	120°	−45°	20°/5°			40	2.9	

Table 2 – Moonlight and observing conditions in September–October 1990.

Date	k	Date	k
Friday August 24	0.16+	Friday September 28	0.59+
Friday August 31	0.75+	Friday October 5	0.99−
Friday September 7	0.95−	Friday October 12	0.41−
Friday September 14	0.27−	Friday October 19	0.00+
Friday September 21	0.04+	Friday October 26	0.42+

New Moon:	August 20, September 19, October 18
First Quarter:	August 28, September 27, October 26
Full Moon:	September 5, October 4, November 2
Last Quarter:	September 11, October 11, November 9

3. Southern Piscids

This weak ecliptic stream is active from August 15 through to October 14. Rates are generally one or two meteors per hour, but on occasions have passed 5 per hour around the maximum which occurs on September 24.

Observers are encouraged to monitor this stream. They should face the radiant area and plot all Southern Piscids seen taking care to distinguish them from the sporadic background. In particular, the angular velocity must be taken into account using the tables in the preceding article. The geocentric velocity of the Southern Piscids equals $V_\infty = 26$ km/s.

Table 3 – Radiant positions of the Southern Piscids.

Date	α	δ	Date	α	δ
Sep 15	0°	−02°	Sep 30	13°	+01°
Sep 20	4°	−01°	Oct 05	17°	+02°
Sep 25	9°	00°	Oct 15	26°	+04°

4. κ-Aquarids

This minor ecliptical stream has an activity period from September 8 to 30. It reaches a maximum ZHR of 3 on September 21. Since its period of activity and its radiant position is similar to that of the Southern Piscids, both showers can be observed simultaneously. With favorable Moon conditions in 1990 observers are urged to make them a priority this year. They should make their center of field of view somewhere around $\alpha = 345°$ to $0°$ and $\delta = -20°$ to $+20°$. All possible shower meteors should be plotted. Shower association should be carried out very carefully taking note of direction of travel, path length and appropriate angular velocity. For the last criterion, use the table in the preceding article. The geocentric velocity for the κ-Aquarids equals $V_\infty = 16$ km/s.

Table 4 – Radiant positions of the κ-Aquarids.

Date	α	δ	Date	α	δ
Sep 15	334°	−03°	Sep 25	344°	−01°
Sep 20	339°	−02°	Sep 30	349°	00°

5. October Capricornids

The October Capricornids were discovered in 1972 and provide variable activity from year to year. They are active from September 20 through to October 14 with an overall maximum on October 3, close to Full Moon.

Intending observers should ensure that they face the radiant position and plot all possible shower meteors. Care should be taken in identifying these meteors. At maximum the October Capricornid radiant is situated at $\alpha = 303°$ and $\delta = -10°$. Angular velocities are comparable to these of the κ-Aquarids.

6. Comet Findlay radiant

Observations during September and October have indicated that there is some evidence of meteor activity from the area of the predicted Comet Findlay radiant. Although there will be some interference from the Moon during early October, southern hemisphere observers are requested to make observations of the Comet Findlay radiant a priority in 1990. Since they can be observed simultaneously with the October Capricornids, southern observers should endeavor to monitor both. To do this they should have a center of field of view situated around $\alpha = 285°$ and $\delta = -20°$. which is midway between both shower radiants. The Comet Findlay radiant should be monitored from September 20 through to October 20. The radiant area is from $\alpha = 260°$ to $280°$ and $\delta = -30°$ to $-42°$. All possible shower members should be plotted and great care should be taken in identifying any meteors coming from the radiant area as such. The angular velocity of meteors originating from the Comet Findley radiant is comparable to these of the κ-Aquarids ($V_\infty \approx 15$ km/s).

7. σ-Orionids

This shower is active from September 10 through to October 26. Its maximum ZHR of 3 meteors per hour occurs on October 5 which means that the Moon interferes greatly with the strongest period of activity in 1990. The σ-Orionids have their radiant in the Belt of Orion and so after maximum great care needs to be taken to distinguish them from the October Orionids. This year, the *IMO* is particularly interested in the σ-Orionid activity profile for the period September 18 to October 3 when the skies should be moon-free. Observers in both hemispheres should watch during the last few hours before sunrise and have a center of field situated no more than 30° west or northwest of the radiant. All possible shower members should be plotted

and care taken in identifying them. The geocentric velocity equals $V_\infty = 65$ km/s. Please use the table in the preceding article for shower membership identification.

Table 5 – Radiant positions of the σ-Orionids.

Date	α	δ	Date	α	δ
Sep 15	71°	−03°	Oct 15	93°	−03°
Sep 25	79°	−03°	Oct 25	101°	−03°
Oct 05	86°	−03°			

8. Draconids

The October Draconids reach a sharp predicted maximum at 15^h UT on October 10. Due to the Moon, the early evening hours when the Moon is either set or low on the eastern horizon are to be preferred for the viewing. The Draconids can only be seen from the northern hemisphere and provide extremely variable rates from the ZHR 0 to storm proportions. Situated at a radiant of $\alpha = 262°$ an $\delta = +54°$, the Draconids should be monitored from October 9 to 11 to see if there are any unusual outbursts of activity (probably unlikely) and to determine the structure of the stream. Intending observers should plot all stream members seen unless the ZHR rises above 10 when classified counts may be taken. They should have their center of field of view located no more than 40° from the radiant position. The diameter of the Draconid radiant is 5°. The geocentric velocity of the Draconids equals $V_\infty = 20$ km/s. Please use the table in the preceding article for shower membership identification.

9. Orionids

This major shower has very favorable Moon conditions in 1990 and is a must on the meteor observer's calendar. The Orionids have a complex radiant structure with the center of activity being located just north of the star Betelgeuse at maximum. The Orionids are associated with Comet Halley and, like the η-Aquarids, display a plateau-like maximum. This can vary from year to year but is generally from October 20 to 25. The Orionid maximum occurs on October 22 with a ZHR that is usually in the range of 20 to 30 meteors per hour. Orionids are best observed during the latter part of the night when the radiant altitude rises above 20°. They are observable in both hemispheres and all possible Orionid meteors should be plotted unless the ZHR exceeds 10. Thereafter, classified counts may be taken. The *IMO*'s aims for the 1990 Orionid watch is for ZHR and population index profiles. The geocentric velocity of the Orionids equals $V_\infty = 66$ km/s. Please use the table in the preceding article for shower membership identification.

Table 6 – Radiant positions of the Orionids.

Date	α	δ	Date	α	δ
Oct 10	80°	+14°	Oct 25	98°	+15°
Oct 15	86°	+15°	Oct 30	104°	+16°
Oct 20	92°	+15°			

10. Taurids

This shower is broken up into several substreams, the most important of which are called the Northern and the Southern Taurids respectively. The Taurids have one of the longest periods of activity known and last from September 13 through to December 1. They reach a broad maximum in late October and early November. The maximum of November 3 (Southern Taurids) and November 13 (Northern Taurids) given in the radiant list were derived from radio meteor and photographic meteor orbital elements and not visual observations. The latter give an uncertain picture. At maximum, Taurid activity is often very erratic with rates ranging from 1–2 meteors per hour to as high as 10 or 15 meteors per hour.

In September and October, the Taurids are best observed during the middle and latter parts of the night. They are noted for their many fireballs. These are frequently yellow and orange in color, but all of the other colors are also well represented. This together with their relatively low geocentric velocity means that they can be recorded more easily on film than most other showers. Perhaps you could try and photograph some for the *IMO* Photographic Meteor Database.

Since they have a great longevity of activity, the Taurids have parts of their activity period moon-free and others greatly affected by the Moon. They can be easily seen from both hemispheres. When observing the Taurids, all possible shower members should be plotted. In order to distinguish meteors from the both branches the center of field of view should be located between 20° and 40° east or west of the radiant at the same declination.

In September the most favorable center of field of view is around $\alpha = 0°$ and $\delta = +10°$ to $+15°$. This way, κ-Aquarid, Southern Piscid, Northern Taurid and Southern Taurid radiants can all be observed simultaneously. In October the most favorable field of view is located at $\alpha = 80°$ and $\delta = +20°$ which enables both the Taurid radiants together with the Orionid, σ-Orionid and the ε-Geminid radiant to be monitored at the same time.

The *IMO* is particularly looking to obtain Taurid ZHR profiles and to investigate the population index during the 1990 Taurid watch. The geocentric velocity of the Taurids is about 30 km/s; the table in the preceding article must be used for shower membership identification.

Table 7 – Radiant positions of the Taurids.

Date	Taurids North		Taurids South	
	α	δ	α	δ
Sep 20	29°	+16°	25°	+10°
Sep 30	37°	+17°	29°	+10°
Oct 10	41°	+18°	36°	+10°
Oct 20	46°	+19°	41°	+11°
Oct 30	51°	+20°	48°	+13°

11. ε-Geminids

This shower is active from October 16 to 27 with a maximum of 5 meteors per hour on October 19. As with the Orionids, Moon conditions are favorable in 1990 and the shower is to be targeted for investigation by the *IMO*. The ε-Geminids can be seen during the last few hours before sunrise in both hemispheres where they often produce fast blue or white trained meteors. The ε-Geminids have angular velocities similar to those of the Orionids and the table in the preceding article should be consulted when identifying possible shower members. The ε-Geminids should only be observed when the radiant reaches an elevation of 20° or more.

All possible shower members should be plotted. In order to effectively distinguish Orionids, σ-Orionids, Taurids and ε-Geminids, the center of the observer's field of view must be located around $\alpha = 80°$ and $\delta = +20°$.

References

[1] J. Wood, "Observers' Notes: July–August 1990", *WGN* 18:3, June 1990, pp. 77–81.

[2] J. Rendtel, "The α-Aurigid Meteor Shower", *WGN* 18:3, June 1990, pp. 81–84.

The Structure of the Geminid Meteor Shower

O. Belkovich, V. Martynenko, A. Levina and A. Grishchenyuk

The authors compare the Geminid activity of various years and conclude that the Geminids are a stable shower.

The problem of the structure, stability and activity of the Geminid meteor shower is still subject to discussion. An attempt to solve the problem has been undertaken on the basis of long period (1971–1989) visual observations carried out by groups of 5 to 8 experienced observers. As a result of the processing of the observations, the ZHR profile of meteors brighter than magnitude +3 with respect to solar longitude was obtained. Two corrections were taken into account: the zenith distance of the shower's radiant and losses of faint meteors. It is known that:

$$N = Q_0 \left(\frac{M}{M_0}\right)^{s-1} S_n T \tag{1}$$

where N is the number of observed meteors with masses greater than M, Q_0 is the meteor flux density, i.e., the number of meteors in a unit area normal to a vector of the meteroid velocity in a unit time, S_n is a normal collecting area and T is the time of observation. The collecting area for visual observations S is a section of a cone of view by a horizontal plane at the mean altitude of the meteor zone (about 82 km for the Geminids). The normal collecting area is:

$$S_n = S \cos Z \tag{2}$$

with Z the zenith distance of radiant. The maximum brightness I of a meteor is given by:

$$I = CM \cos Z \tag{3}$$

with C a constant. Let M_0 be the mass of a meteor of brightness I at $Z = 0°$. Then:

$$I = CM_0 \tag{4}$$

We have from (3) and (4):

$$\frac{M}{M_0} = \cos Z \tag{5}$$

and now from (1), (2) and (5):

$$N = Q_0 ST \cos^s Z \tag{6}$$

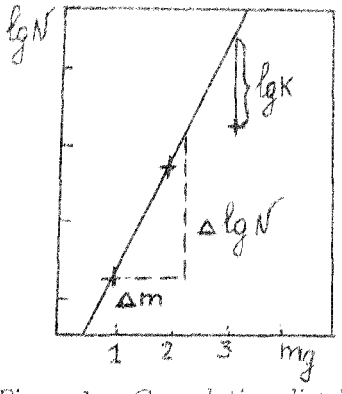

Figure 1 — Cumulative distribution of observed meteor magnitudes.

Figure 1 shows a cumulative distribution of observed meteor magnitudes. The dots on the graph are concentrated along a straight line up to magnitude +2. Then, due to a loss of fainter meteors, the dots are deviating from the line. The second correction k can now be found from the graphs as the difference between the ordinate values for the dot on the graph and the point on the line corresponding to magnitude +3. (If there would be no loss of fainter meteors, the dot would actually be located on the line.)

The exponent s of the mass distribution of meteor bodies is calculated as:

$$s = 1 + 1.67 \frac{\Delta \ln N}{\Delta m} \tag{7}$$

The coefficient $1.67 = 2.5x$ has been taken from Levin [1], who estimated the value of x as 0.7. Our value of 0.67 has been found from the comparison of values of s found from visual data and radar data (solid line) [2]. See also Figure 2.

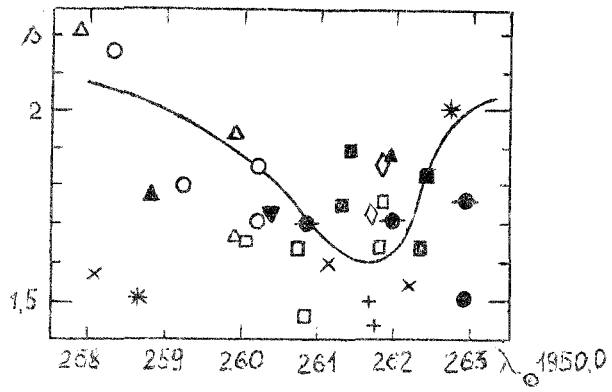

Figure 2 — The value of s as a function of solar longitude.

Expression (6) can be reduced to zenithal hourly rates by taking into account the correction factor k:

$$N_z = Q_0 S k = \frac{N k}{T \cos^s Z} \qquad (8)$$

Since magnitude +3 has been chosen as a limit, M_0 corresponds to Geminid meteors of +3 with $Z = 0$. Values of s and k have been found for every night of observation, but the nights were divided by nearly hour intervals and N_z has been calculated for each of them; mean values $\overline{N}_z$ were then calculated for every night.

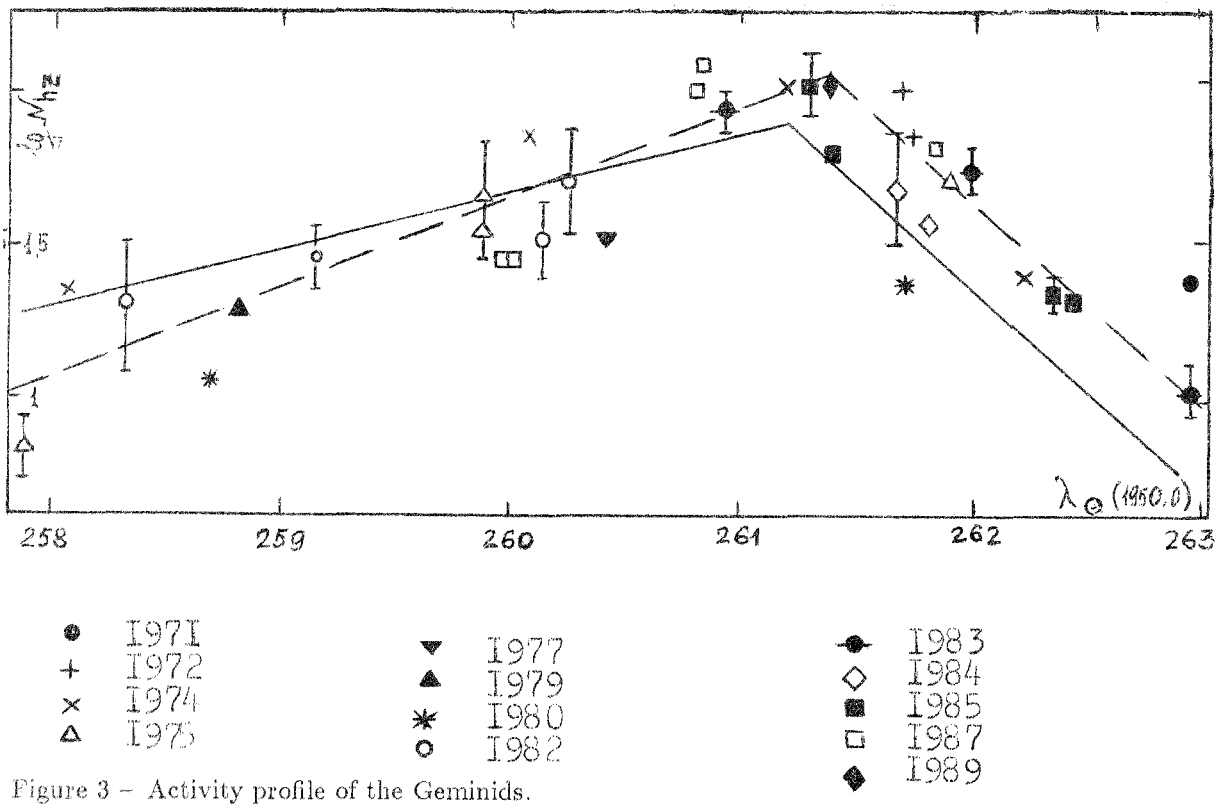

Figure 3 – Activity profile of the Geminids.

The mean values of $\overline{N}_z$ as a function of the solar longitude $\lambda_\odot$ for the Geminid meteor shower are shown in Figure 3 for every night of different years. The logarithmic scale has been chosen for convenience because many meteors showers have an exponential rise and fall of activity; in this way, shower activity can be represented by two straight lines (dashed lines). The shower is stable in structure and activity for all years of observation. The same conclusion has been made by Belkovich [2]. Flux density of the Geminids obtained from radar observations [2] are shown in Figure 3 by solid lines. Some differences in slopes of the left branches of the activity lines and the maxima positions are due to the difference of the minimum detectible meteoroid masses for the visual and the radio method. The maximum rate is $\overline{N}_z = 120$ and occurs at solar longitude $\lambda_\odot = 261°.42$ (1950.0).

References

[1] B.Yu. Levin, "Physical Theory of Meteors and Meteor Matter in the Solar System".

[2] O.I. Belkovich, *Solar System Res.*, 1986, nr. 2, p. 142.

Meteor Colors

Ulrich Sperberg

Some basic ideas concerning the calculation of the color index of meteor streams, using only visual observations, are described. The relation between color index and magnitude is discussed. A formula to calculate a standardized color index is proposed.

1. Introduction

Whenever visual meteors were observed, also the color of some, especially of bright meteors, is recorded. Although this information is considerably uncertain and, since for one and the same meteor, various observers record different colors, the material permits some interesting investigations.

In the reports of observer groups, often color distributions in percent are given. These distributions contradict each other and are less informative. To quantify the color, normally the *color index (CI)* is used. It can be especially easy determined if the meteor is photographed in two spectral ranges [1,2]. The color index can also be determined by simultaneous photographic and visual observations [3,4,5] or on the basis of visual observations through different color filters [6].

Several analyses have shown that the color index is a linear function of magnitude. Weaker meteors are redder than brighter meteors. The slope ρ of the reddening function CI (as a function of magnitude) differs depending on the method of determination and the spectral range. In Table 1, some slopes and their corresponding magnitude ranges are given.

Table 1 – Slopes of the reddening function.

Author	ρ_V	$m_{\min}$	$m_{\max}$
Jacchia 1957 [4]	0.49	+1.0	−1.5
Davis 1963 [7]	0.35	+2.5	−1.5
Davis 1963 [7]	0.39	+2.5	−1.5
Hajdukova 1967 [6]	0.29	+5.0	−1.0
Ceplecha 1959 [1]	0.43		
Kohoutek 1963 [2]	0.14		
Hajdukova 1967 [6]	0.47		
Hajdukova 1972 [8]	0.58		
Stohl, Hajdukova 1979 [9]	0.43	+5.0	−2.0

The quantity ρ_V indicates the slope using the magnitude m in the visual range, ρ_P is the slope using m in the photographic range. According to Stohl and Hajdukova [9] ρ_V and ρ_V can be transformed into each other as follows:

$$\rho_V = \frac{\rho_P}{1-\rho_P} \qquad \text{and} \qquad \rho_P = \frac{\rho_V}{1+\rho_V}$$

2. Observation material

This investigation is based on observations of the *AK Meteore* in the GDR. About 300 meteors in the magnitude range −3 to −1 were used. The observations were carried out in the years 1975–1989, the main bulk being obtained during 1985–1989.

3. The method to determine the color index

The visible spectral range is divided in two subranges, a "blue" range with the colors blue, green and violet and a "visual" range with the colors yellow, orange and red.

Assuming that the number of meteors in both ranges is proportional to the intensity of the emission of an average meteor in these ranges, it becomes possible to determine the color index for a meteor stream.

With $CI = m_B - m_V$, m_B being the magnitude in the blue range and m_V the magnitude in the visual range, and the well-known formula:

$$m_2 - m_1 = 2.5 \log \frac{I_1}{I_2}$$

the I being intensities, we obtain:

$$CI = 2.5 \log \frac{N_V}{N_B}$$

where N_B and N_V are the numbers of meteors in both ranges.

By calculating the color index for different magnitudes and different streams the relationship with the magnitude is found. Using the least square method, the slope of the reddening function is obtained. Figure 1 shows this for the sporadic meteors.

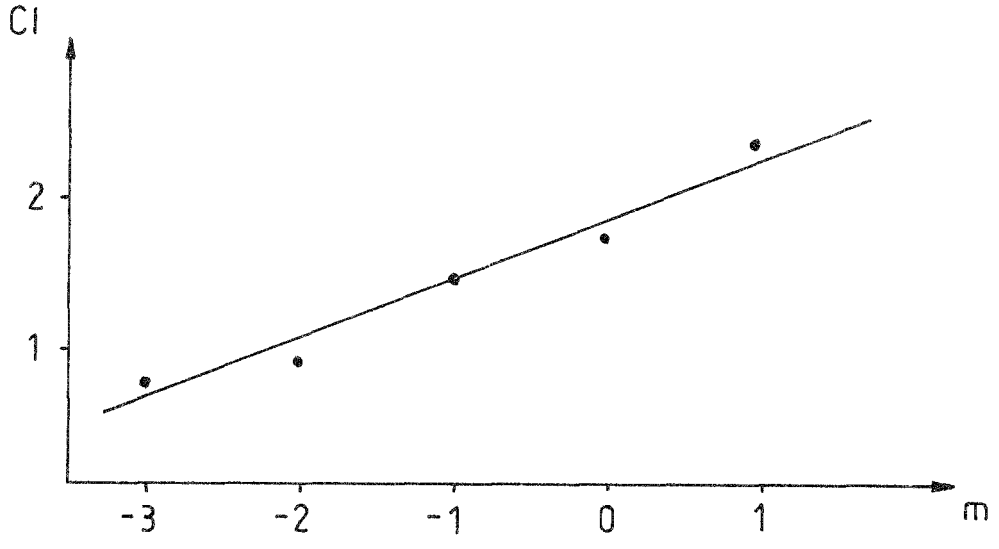

Figure 1 – The color index CI as a function of the magnitude m for sporadic meteors.

In Table 2 the slope and the magnitude range for some streams are given. In this table, k is the correlation coefficient and N the total number of meteors. Although k is low, the slopes seem to be identical, except for the Taurids.

Table 2 – Color index and slope for some meteor streams.

Stream	ρ_V	k	$m_{\min}$	$m_{\max}$	N	CI^θ
Spor	0.39	0.979	+1	−3	1660	1.78
Per	0.32	0.850	+1	−3	990	2.07
Gem	0.37	0.862	+1	−3	128	0.61
Vir	0.39	0.899	+1	−2	49	2.55
Tau	0.55	0.895	+1	−1	89	2.47
Qua					47	2.68
Ori					26	2.95

For further calculations, a stream independent value of 0.37 is used for ρ_V. In order to regard the color index as a stream property, it is necessary to reduce to the same magnitude, preferably magnitude 0 with:

$$CI_0 = 2.5 \log \frac{N_V(m)}{N_B(m)} + \rho_V m$$

Transformation leads to:

$$CI_0 = 2.5 \log \frac{N_V(m) 10^{0.4 \rho_V m}}{N_B(m)}$$

Furthermore, it is necessary to reduce to the true number of meteors with the corresponding magnitude. For this, the probabilities of Koschack and Rendtel [10] are used. With $N = N_{\mathrm{obs}} p(\Delta m)^{-1}$, the previous formula becomes:

$$CI_0 = 2.5 \log \frac{N_V(m) 10^{0.4 \rho_V m} p(\Delta m)^{-1}}{N_B(m) \cdot p(\Delta m)^{-1}}$$

The probabilities $p(\Delta m)$ do not influence the CI value before the next step.

When the number of meteors is small, it is often not possible to calculate CI_0 because of $N_B = 0$. Nevertheless the CI can be calculated after summation of all magnitude classes according to:

$$CI^{\theta} = 2.5 \log \frac{\sum_{m=+1}^{-3} \left(N_V(m) 10^{0.4 \rho_V m} p(\Delta m)^{-1} \right)}{\sum_{m=+1}^{-3} \left(N_B(m) p(\Delta m)^{-1} \right)}$$

4. Results

The values for CI^{θ} are also given also in Table 2. They must be regarded as preliminary values because of the low total number of stream meteors. Only for the Perseids and for the sporadic meteors, the CI^{θ} is of a higher reliability.

The strongly different value for the Geminids also seems to be real. Hajdukova too reported about this [11].

Using meteors fainter than magnitude +1 is unfavorable. The perception of the color is of great uncertainty and the CI becomes nearly constant.

References

[1] Z. Ceplecha, *Bull. Astron. Inst. Czechosl.* 13, 1959, p. 39.
[2] L. Kohoutek, *Bull. Astron. Inst. Czechosl.* 14, 1963, p. 172.
[3] P.M. Millman, D. Hoffleit, *Harvard Ann.* 105, 1937, p. 601.
[4] L. Jacchia, *Astronomical Journal* 62, 1957, p. 358.
[5] Z. Ceplecha, *Bull. Astron. Inst. Czechosl.* 9, 1958, p. 225.
[6] M. Hajdukova, *Bull. Astron. Inst. Czechosl.* 18, 1967, p. 187.
[7] J. Davis, *Monthly Notices Royal Astr. Society* 126, 1963, p. 39.
[8] M. Hajdukova, *Bull. Astron. Inst. Czechosl.* 23, 1972, p. 350.
[9] J. Stohl, M. Hajdukova, *Bull. Astron. Inst. Czechosl.* 30, 1979, p. 13.
[10] R. Koschack, *WGN* 18, 1990, p. 44.
[11] M. Hajdukova, *Bull. Astron. Inst. Czecosl.* 25, 1974, p. 365.

Sporadic Meteor Colors

Alastair McBeath

An analysis of visual colors recorded for sporadic meteors between 1984–1988 as observed by the JAS Meteor Section is presented and discussed. Little evidence is found to support the view that these colors provide an insight into the nature of meteoroids.

1. Introduction

That visual color occur at all in meteors is well known. Even complete novice observers with no prior knowledge of meteoric phenomena have reported them from time to time, but analyses of such colors and what they may tell us about the various meteor populations are less common.

In this paper, an analysis of sporadic meteor colors recorded by reliable JAS Meteor Section observers between 1984 to 1988 is presented, an adjunct to the data given in [1]. None of the observers treated as reliable in that earlier paper were found to suffer from eye complaints such as color-blindness, although about one third of them routinely wore glasses whilest meteor watching. As no significant difference was found in color results between users and non-users of glasses, the 5660 sporadic meteors which formed the basis for [1] were re-analyzed for colors without adjustment.

2. Results

Not all observers whose data were used in the color analysis recorded colors for every meteor seen. Of those who did, the vast majority were noted as being white. As the human eye operates in monochrome vision unless sufficiently stimulated by light to allow cones of the retina to function, "white" becomes the equivalent of "no color", so that all "white" meteors and those without any color notes were treated as being effectively uncolored.

In all, 908 sporadics exhibited a noticeable color, and five specific shades were observed: red, orange, yellow, green and blue. Table 1 shows a breakdown of this data by magnitude class, with the corrected mean magnitude for a limiting magnitude +6.5 sky ($\overline{m}_{6.5}$ and the percentage of all sporadic meteors showing colors (%) are also given.

Table 1 – Sporadic color magnitude distributions for the period 1984–1988.

Color	-3^-	−2	−1	0	+1	+2	+3	+4	$+5^+$	Tot	$\overline{m}_{6.5}$	%
Red	0	1	0	2	4	12	7	5	0	31	+2.95	0.5
Orange	0	3	7	18	13	11	5	2	0	59	+1.55	1.0
Yellow	16	26	35	115	175	176	140	15	2	700	+2.03	12.4
Green	2	0	1	1	0	1	0	1	0	6	−0.04	0.1
Blue	8	5	22	44	23	4	4	1	1	112	+0.64	2.0
Total	26	35	65	180	215	204	156	24	3	908	+1.85	16.0

Some meteors (about 5% of the colored total) produced multiple colors, most of which were a color plus white, and these were dealt with as belonging to the color class only. Roughly 1% (11 meteors) showed contrasting colors, particularly yellow-blue (5) and orange-red (3). In these cases, the first noted color only was recorded.

Table 2 – Percentages of all sporadic meteors which showed colors between 1984–1988 by magnitude class.

Magnitude	-3^-	−2	−1	0	+1	+2	+3	+4	$+5^+$
Percentage	63.4	63.6	58.6	46.8	30.9	17.7	9.5	2.1	0.7

Table 2 gives the proportions of colored meteors as a percentage of all sporadic meteors per magnitude class, and Table 3 gives the numbers and percentages of colored sporadics for each year.

Table 3 – Breakdown of colored sporadic numbers per year, 1984–1988.

Color	1984	1985	1986	1987	1988
Red	8	9	5	5	4
Orange	11	17	16	4	11
Yellow	141	141	123	183	112
Green	1	2	1	1	1
Blue	32	30	20	13	17
Total	193	199	165	206	145
%	18.4	13.7	10.4	25.3	18.9

3. Discussion

As only 16% of sporadics showed a distinct color, it is most unlikely that this can be seen as representative of the entire population. However, further consideration is necessary to help to determine whether the colored sporadic group can be treated as providing information on some part of the sporadic meteoroid flux or not.

A number of specific items stand out from Table 1. The quantity of yellow meteors is out of all proportion to the figures for the other colored groups, and indeed accounts for almost 80% of the colored sporadics. The paucity of green meteors (a mere 0.7% of the colored meteors) is also striking. From visual star colors, it seems that stars fainter than approximately magnitude +1.5 appear white or colorless to the naked eye, so the number of faint ($m \geq +2$) red, orange and yellow meteors are rather curious too.

The decreasing trend in the numbers of sporadic colored meteors with fainter magnitudes (Table 2) provides some support for a magnitude +1.5 color "cutoff" point, although a significant part of the sporadic component remains white or uncolored even for the fireball-class magnitudes. Brighter meteors do tend to be perceived as colored much of the time, however. Table 3 indicates that the overall proportions of meteors in separate color groupings remain relatively constant over time. An inverse relationship between sporadic color and train percentages per year is apparent (compare to [1], Table 2), but this is almost certainly mere coincidence.

In order to determine whether the effects seen in Table 1 are genuine or simply result from the peculiarities of the human eye, several possibilities are considered in the following sections.

4. Color perception

The most obvious aspect to examine is the eye's perception of different colors in poor lighting conditions, as it is clear from experiments that this sensitivity changes for the photopic (light-adapted) or scotopic (dark adapted) vision [2]. For this purpose, we can numerically define the relative luminous efficiency of the scotopic eye, V'_λ. This parameter varies by wavelength as shown in Table 4. Scotopic vision is most efficient ($V'_\lambda = 1.0$) at $\lambda = 507$ nm, in the blue-green part of the spectrum.

It might be expected that V'_λ would have some bearing on the numbers of differently colored sporadics seen, and this does seem to apply to some extent for blue, orange and red, albeit in general terms. Whether V'_λ can be used to determine what portion of the flux in each of these three color classes is actually being observed is uncertain, but as several other selection effects may operate (see Sections 5 and 6), this can probably not be meaningfully calculated. What is clear is the absence of any obvious correlation between V'_λ and the quantities of yellow and

green sporadics observed.

Table 4 – Mean V'_λ parameters correlated to colors and their approximate wavelength ranges (based on [2], Table VII, p. 415).

Color	λ – range (nm)	V'_λ
Red	670–700	0.0001
Orange	630–670	0.001
Yellow	560–630	0.09
Green	490–560	0.77
Blue	430–490	0.56
Violet	400–430	0.08

A perusal of any good visual astronomy text—cfr. [3]—will show that all of the brighter stars (magnitude at least +1) exhibit a naked-eye color representative of their spectral class. At some point between magnitudes +1 and +2, visual color ceases to be visible. The actual cutoff is difficult to determine precisely, but is probably around +1.5. For instance, Pollux (β Gem) is a K0 class star of +1.2 and appears distinctly yellow to most observers, while Dubhe (α UMa) is a K0 star of +1.8 and shows no perceptible color to the unaided eye. Assuming this holds true for meteors as well, rapid fall-off in the numbers of colored events between the +1 and +2 categories should be seen. This is very much the case for blue sporadics, but orange meteors show this feature rather less well, and for red it is totally absent, the cutoff here probably being somewhere around +3.

From V'_λ, it follows that the perceived brightness of red and orange objects of equal luminosity should be suppressed with regard to shorter wavelengths, red more so than orange, which is exactly what is found. The fact that most comparison stars for estimating meteor magnitudes are chosen from the B, A, and F spectral classes, which appear essentially white to the eye, probably helps further to account for this. It seems that the magnitude of red meteors is probably being underestimated by approximately 1.5 magnitudes, while orange sporadic brightnesses are being reduced by an average of one magnitude or so.

5. Contrast effects

Color contrasts in the eye varies across the spectrum. It is poorest for blue-violet, blue-green, and yellow-white, especially when seen in poor light against a dark background with no immediate adjacent comparisons. The problem is particularly bad for faint light sources. This phenomenon can probably go some way towards explaining the absence of violet meteors, the few green sporadics and the yellow meteor excess.

Any violet meteors which occurred have presumably been subsumed into the blue color category, or possibly lost in the darkness of the sky itself. Many green meteors may well have suffered the same result due to the contrast-poor overlap between the two shades blue and green as well. The high sensitivity of the scotopic eye to green could then account for the few "genuine" green sporadics rather than their total loss, though it remains surprising that so few bright (negative magnitude) green events should have been noted, since contrast would be expected to have less effect in these cases.

The distribution of yellow meteors is not easy to explain, as any adjustment should, according to V'_λ, be far less than for orange meteors, whereas a shift of two full magnitudes would be required to cause the color cutoff to fall between +1 and +2. This plus the very large number of yellow-class meteors overall tend to support the view that many yellow meteors are simply the result of poor yellow-white color distinction, where colorless meteors are mistakenly assigned the color yellow in the eye. How large a fraction of yellow meteors could be thus affected

is difficult to estimate, although increasingly fewer "errors" would be expected with brighter meteors. The majority of fainter meteors and increasingly smaller numbers of brighter objects could therefore be removed by this mechanism.

Contrast may actually enhance the number of red and particularly orange meteors seen, as both are made more obvious by a dark background. This could lead to rather more meteors of these colors being observed than simple comparison with V'_λ might suggest.

6. Persistence of vision

With swifter meteors, those whose atmospheric velocities are in excess of about 40 km/s, persistence of vision often causes the object to appear as lines or streaks of light, rather than moving points. The effectively enlarged area of light so produced may well be more frequently perceived as colored than as a smaller point would be, which would tend to work to the benefit of fainter meteors. Although too few contributing observers regularly reported relative meteor speeds to allow a thorough examination of this facet, data from those who did have suggested there is no real preference for meteors of a certain color to be associated with a particular relative velocity. As many blue sporadics appeared to be "fast" as "slow" for example. Thus, any effect of this kind probably affects sporadic meteors of all color classes equally since velocity distribution should be random.

7. After-image colors

An accompaniment to the persistence of vision, light "held" by the retina after the source has moved takes on its "opposite" or after-image color. These opposites are red $\leftrightarrow$ green and blue $\leftrightarrow$ yellow. For this to be noticeable, however, the light source needs to be strong enough to temporarily saturate part of the retina, and as this is likely only with brighter meteors, primarily fireballs, it probably plays very part in determining the colors of the sporadic flux. The chief exception to this is the saturation of the eye with dark blue light from the sky, which may further enhance the number of white meteors seeming to be yellow. Flicking the eyes from the night sky to a small piece of faintly illuminated white card allows this to be seen well, for instance.

8. Atmospheric filtering and absorption

Color changes brought about by atmospheric effects would be most obvious only for meteors seen through haze, cloud, mist, smoke or at large zenith distances. Owing to the selection criteria used to isolate the sporadic data as suitable for the analysis, it is extremely unlikely that any but a very small minority of the meteors were affected in any way by such phenomena, and they can be effectively ignored in this discussion.

9. Meteor spectra

There must be doubts as to whether spectra obtained only from exceptionally bright meteors can actually provide reliable information on what may be found with the majority of visual meteors, which are considerably fainter, particularly as many spectra are of shower meteors, which may be different to the sporadic meteor component in any case. However, [4] indicates that most spectra show sodium (Na I) multiplets, which would produce visual yellow light, perhaps suggesting a possibility for more yellow meteors to be seen. Fast meteors occasionally show the "forbidden" green oxygen (O I) line at 557.7 nm too, though this is thought to be atmospheric in origin. This rarity may perhaps account for the lack of green meteors in the analysis, though other elements could probably fill this gap, e.g. magnesium (Mg I). The human eye is certainly not sensitive enough to give precise spectral data, so any correlation between meteor colors and a possible major meteoroid chemical elements in this way must remain speculative.

10. Conclusion

From the above discussion, it can be seen that there are a number of possible effects which may operate together in some combination to produce the observed color balance in the minority of sporadic meteors which show colors. Most significant seem to be the effect of color perception and contrast in the human eye. Very little of what was recorded needs to be explained in terms other than these, with the possible exceptions of the green and, to some extent, yellow meteor fluxes, though how significant these two features are remains open to question.

Whether shower meteor colors are any more useful in providing data on their parent bodies has still to be determined, but it will be necessary to take into account the sensitivity of the eye when performing any future visual color analyses.

References

[1] A. McBeath, "An Analysis of Sporadic Meteors", *WGN* 17:6, December 1989, pp. 267–272.
[2] H.A.E. Keitz, "Light Calculations and Measurements (2nd revised edition)", Macmillan, London, 1971.
[3] R. Burnham Jr., "Burnham's Celestial Handbook (3 vols.)", Dover, New York, 1978.
[4] V.A. Bronshten, "Physics of Meteoric Phenomena", D.Reidel, Dordrecht, Holland, 1983.

Erratum on Determination of Spatial Number Densities and Mass Index from Visual Meteor Observations (I)

Ralf Koschack and Jürgen Rendtel

The following modifications should be made in the text in *WGN* 18:2, April 1990, pp. 44–58.

- Equation (1), p. 46 should read:

$$A_{\mathrm{red}} = \sum_i A_i \, r^{5 \log \frac{100 \text{ km}}{d_i} - \varepsilon_i} \tag{1}$$

  (add an index i to the variable d).

- On p. 47, items 4 and 5 have to be read as follows:

  4. determination of A_R for each distance class using (1);
  5. summing up the values of A_R in order to get A_{red}; and

- Equation (3) is not sufficient. We fitted again using 3 parameters and found:

$$A_{\mathrm{red}}(r) = 37\,200 \text{ km}^2 (r - 1.3)^{-0.748} \tag{3}$$

  which is absolutely sufficient for $1.8 \leq r \leq 3.5$.

- On p. 51, the second sentence has to be read as follows: For example, we put together the meteors of the class $m = +3$ seen under $5.75 \leq \mathrm{lm} < 6.25$ and of ... (change the bounds of the inequality).

Please change the passages mentioned in your issue. We apologize for the inconvenience.

Determination of Spatial Number Density and Mass Index from Visual Meteor Observations (II)

Ralf Koschack and Jürgen Rendtel

7. Probabilities of perception of individual observers

We used data obtained during double count observations with shifted field centers (0°, 20°, 35°) of seven experienced observers. Their contribution and experience can be seen from Table 8. The lack of observations with field centers shifted by 35° for SEIHO and BALPE is unfavorable for the final analysis. Therefore the results for both observers are more uncertain.

Table 8 – Contribution and experience of the observers included in the current study.

Observer	First Observation	Until end 1989: Man hours	Until end 1989: Meteors	Fields shifted by: 0°	Fields shifted by: 20°	Fields shifted by: 35°	Total
R. Arlt	1982	730	8500	139	385	207	731
P. Baldauf	1982	350	8000	107	275		382
A. Knöfel	1978	920	10500	170	504	125	799
R. Koschack	1981	880	26500	218	551	378	1147
I. Rendtel	1979	1070	19670	348	834	469	1651
J. Rendtel	1972	2470	28460	404	522	127	1053
H. Seipelt	1981	300	5950	101	384		485

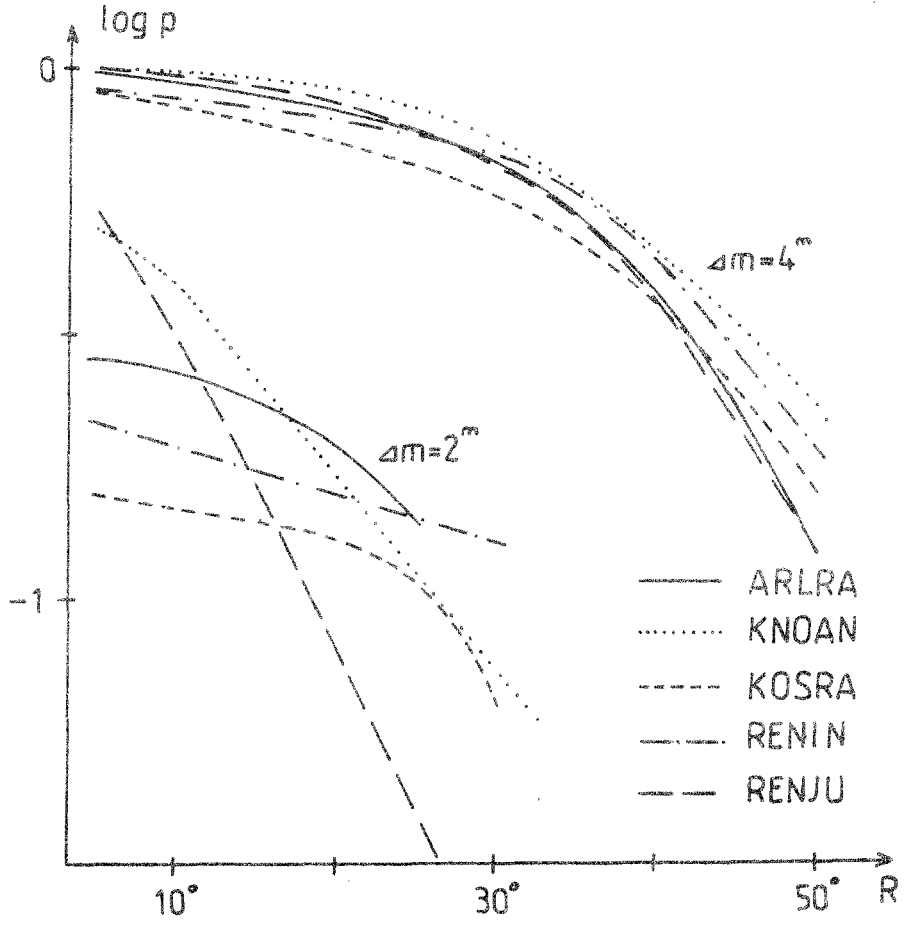

Figure 13 –Individual perceptions $p(R)$ for several values of Δm.

During the analysis we found that the "original" double count observations (identical field centers) do not allow many conclusions while the data of fields shifted by 35° deliver important values for the outer distance classes. Therefore, it would be better to have as much 35° as 20° data. But nevertheless the material available is suitable for the determination of the probabilities of perception $p(\Delta m)$. The method described in Section 3 is now applied to the data of every single observer. It is not necessary to divide the data into several lm-groups since the limiting magnitude for a certain observer does not differ significantly among the observations. An averaging and weighing with n is sufficient. After the first step we find nearly smooth curves. Scatters as they can be seen in Figure 7 do not occur. This is a hint for a good certainty. Furthermore this may indicate individual differences.

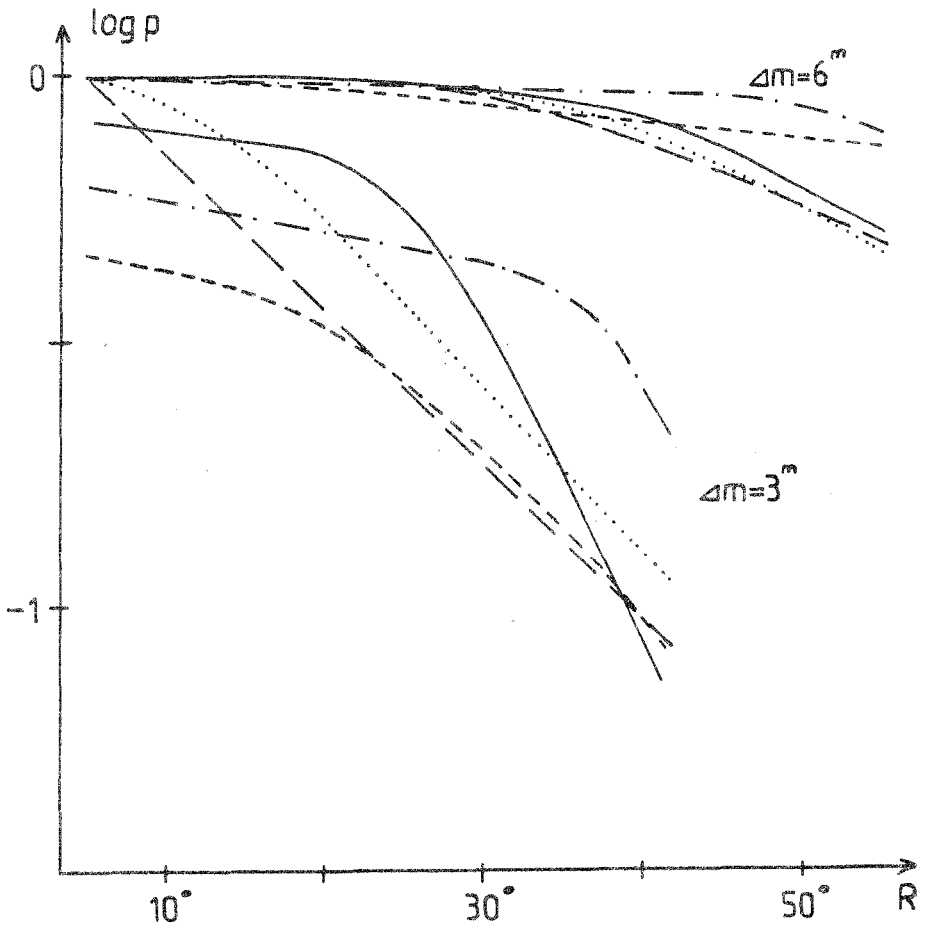

Figure 14 –Individual perceptions $p(R)$ for several values of Δm.

In Figures 13 and 14, we show curves of the probability of perception $p(\Delta m, R)$ as a function of the distance R for individual observers and for different Δm. Obviously, we find two "types of observers":

1. concentration on the center of the field of view (high perception there), steep decrease to the outer regions of the field (RENJU, KNOAN); and
2. a "wide-angle view" with a nearly constant perception over a larger portion which decreases more slowly outwards (KOSRA, RENIN, ARLRA).

The probabilities $p(\Delta m, R)$ are then averaged over the whole field according to equation (5). We obtain $p(\Delta m)$ for $\Delta m > 2$. As described in Section 3 we derive $p(\Delta m)$ for $\Delta m < 2$ from sporadic magnitude distributions in August 1988 and 1989. Due to the high activity, the nights of August 10–11 until 13–14 are excluded. For the calculation, personal $p(\Delta m)$ are already used. We found differing average r-values for the sporadic meteors (Table 9); a point to which we will return later.

Table 9 – Average values of r for sporadic meteors.

Observer	r_{avg}
ARLRA	2.76
KONAN	2.89
KOSRA	3.27
RENIN	2.87
RENJU	3.32

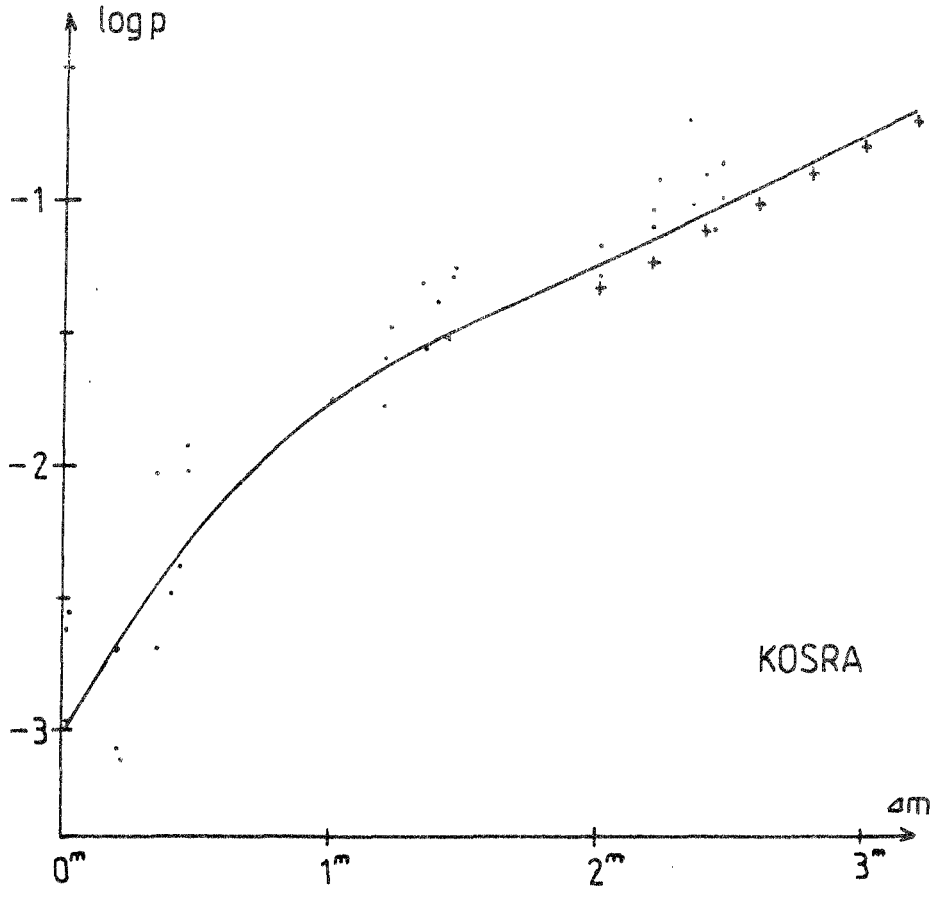

Figure 15 –Fitting of the $p(\Delta m)$ obtained by double count observations (crosses) and those derived from magnitude distributions (points) in the transition range for one observer.

In Figure 15 we show the fit of the curves $p(\Delta m)$ found from the double count observations and those derived from the magnitude distributions. In the region of fitting the latter perception is a little bit higher than the perception calculated from the double count observations.

Figure 16 shows the values of $p(\Delta m)$ for individual observers also given in Table 10.

Equation (12) allows the calculation of the correction factor $c(r)$ for every individual observer, too. The results are summarized in Table 11.

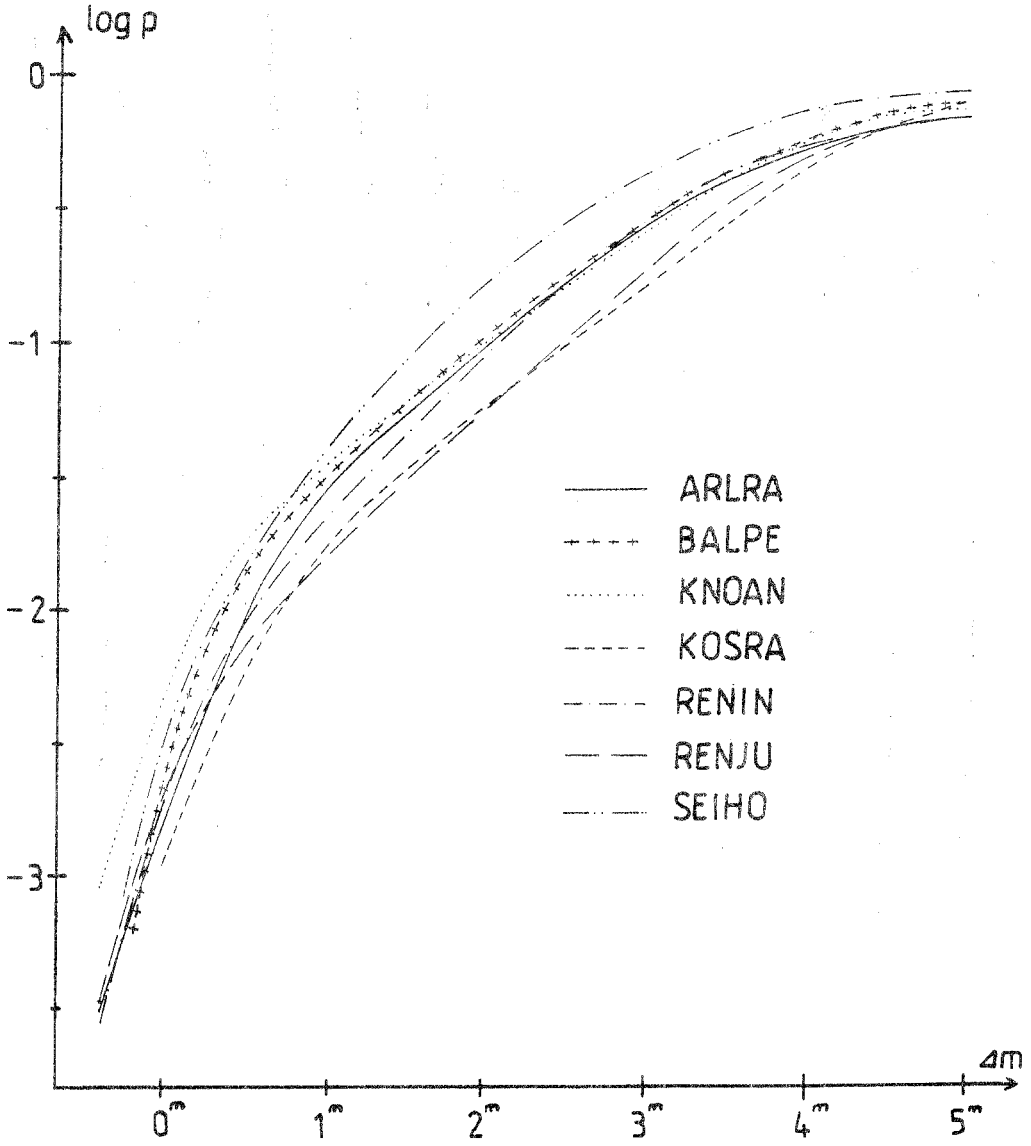

Figure 16 –Probabilities of perception $p(\Delta m)$ as an average over the field of view (52°5 radius) for individual observers.

Table 10 – $p(\Delta m)$ for the individual observers.

Δm	ARLRA	BALPE	KNOAN	KOSRA	RENIN	RENJU	SEIHO
−0.4	0.00031		0.00091		0.00029	0.00033	
+0.0	0.0015	0.0025	0.0048	0.0011	0.0020	0.0020	0.0035
+0.5	0.010	0.014	0.018	0.0058	0.0091	.0074	0.014
+1.0	0.028	0.032	0.035	0.017	0.022	0.015	.040
+1.5	0.052	0.060	0.059	0.034	0.045	0.030	0.087
+2.0	0.095	0.11	0.10	0.058	0.089	0.055	0.17
+2.5	0.17	0.19	0.16	0.10	0.18	0.10	0.28
+3.0	0.28	0.29	0.26	0.17	0.30	0.19	0.44
+3.5	0.40	0.44	0.41	0.28	0.44	0.35	0.58
+4.0	0.51	0.59	0.59	0.46	0.54	0.51	0.73
+4.5	0.63	0.72	0.70	0.66	0.64	0.64	0.81
+5.0	0.71	0.78	0.75	0.79	0.74	0.69	0.86
+6.0	0.84	0.88	0.83	0.84	0.92	0.80	0.91
+7.0	0.92	0.94	0.92	0.89	0.99	0.92	0.96
+7.5	0.99	0.99	0.99	0.99	1.00	0.99	1.00

Table 11 – The correction factor $c(r)$ calculated from the $p(\Delta m)$ of the individual observers.

Observer	$r = 2.0$	$r = 2.5$	$r = 3.0$	$r = 3.5$
ARLRA	9.04	14.6	20.3	25.7
BALPE	8.07	12.8	17.5	21.9
KNOAN	8.41	13.2	17.6	21.6
KOSRA	11.2	19.6	28.8	37.9
RENIN	8.80	14.5	20.5	26.4
RENJU	10.9	18.8	27.5	36.1
SEIHO	6.50	10.0	13.4	16.8

8. Reliability of individual perceptions obtained

Significant differences in the coefficients $c(r)$ should be found within the individual rates. For different observers we find similar shapes of the curves $p(\Delta m)$ in Figure 16. The differences of the individual curves $p(\Delta m)$ against an averaged curve can be expressed as a shift in Δm by an amount of Δlm. For the rates this results in the relations:

$$\mathrm{HR}_{\mathrm{avg}} = r^{-\Delta \mathrm{lm}} \mathrm{HR}_{\mathrm{obs}} \tag{28}$$

$$\Delta \mathrm{lm} = \frac{\log \mathrm{HR}_{\mathrm{obs}} - \log \mathrm{HR}_{\mathrm{avg}}}{\log r} \tag{29}$$

The values of $c(r)$ for the 5 observers with complete data and certain $p(\Delta m)$ (ARLRA, KNOAN, KOSRA, RENIN, RENJU) are averaged to $c(r)_{\mathrm{avg}}$. Then we may calculate the individual shifts Δlm compared to the average, which are summarized in Table 12:

$$\Delta \mathrm{lm} = \frac{\log c_{\mathrm{avg}} - \log c_{\mathrm{obs}}}{\log r} \tag{30}$$

Table 12 – Individual shifts Δlm against the average of ARLRA, KNOAN, KOSRA, RENIN and RENJU.

r	ARLRA	BALPE	KNOAN	KOSRA	RENIN	RENJU	SEIHO
2.0	+0.09	+0.25	+0.20	−0.21	+0.13	−0.18	+0.57
2.5	+0.09	+0.24	+0.21	−0.22	+0.10	−0.18	+0.51
3.0	+0.09	+0.22	+0.21	−0.23	+0.08	−0.19	+0.47
3.5	+0.08	+0.21	+0.22	−0.22	+0.06	−0.19	+0.43
Δlm	+0.09	+0.23	+0.21	−0.22	+0.09	−0.18	+0.50

For most observers the shift Δlm is not depending on the population index r. The maximal deviation from their average shift Δlm corresponds to an error of 3.8% (RENIN), and 9% (SEIHO), whose results are more uncertain due to the smaller amount of data. Conclusion:

Individual deviations from a standard perception function $p(\Delta m)$ may be expressed by Δlm.

We then compared the values of Δlm found from application of equation (30) to the individual $p(\Delta m)$ with those derived from the rates according to equation (29).

1. Δlm *from sporadic rates:*
The average of the population index in Table 9 is $r_{\mathrm{Spor}} = 3.1$. Sporadic hourly rates were calculated for 37 intervals (average duration approximately 2.5 hours, $c_{\mathrm{tot}} < 1$) of the observations in August 1988 and 1989 in Bulgaria (SEIHO only 1988). Results between August 10–11 and 13–14 are not included because of the possibility that Perseids are erroneously noted as sporadics. The definition of "sporadic meteors" is identical for all observers (same showers analyzed and excluded). For each interval we calculated an average HR for the 5 observers mentioned above (HR_{avg}). With the help of (29) and using $r = 3.1$ we calculated Δlm for each observer. All Δlm of a given observer are then averaged and given in Table 14 together with the scatter σ.
2. Δlm *from the perception coefficients of the 1988 Perseids [7]:*
Since Roggemans used $r = 2.5$ as standard in [7], we expect systematical errors if lm $\neq 6.5$. Therefore we calculated the population index r_{Per} for 1988 August 10–11, 11–12, and 12–13 (interval analyzed in [7]) for each night and each observer. The average we found is $r_{\mathrm{Per}} = 2.12 \pm 0.2$. The ideal conditions at Mt. Roshen led to limiting magnitudes varying only very little (for averages $\mathrm{lm}_{\mathrm{avg}}$, see Table 13). The coefficients published in [7] have to be corrected to:

$$k(r = 2.12) = k(r = 2.5) \times \left(\frac{2.12}{2.5}\right)^{6.5-\mathrm{lm}_{\mathrm{avg}}} \tag{31}$$

Table 13 – Correction of the perception coefficients $k(r = 2.5)$ given in [7].

Observer	$\mathrm{lm}_{\mathrm{avg}}$	$k(r = 2.5)$	σ	$k(r = 2.12)$	σ
ARLRA	6.51	0.89	0.20	0.89	0.20
BALPE	6.74	0.70	0.18	0.73	0.18
KNOAN	6.51	0.90	0.19	0.90	0.19
KOSRA	7.29	0.74	0.14	0.84	0.15
RENIN	6.90	0.89	0.19	0.91	0.20
RENJU	6.51	0.93	0.15	0.93	0.15
SEIHO	6.05	1.19	0.28	1.10	0.26

The corrected coefficient k for the 5 selected observers are averaged, and the average is then used as a reference for the individual observers. The Δlm are then:

$$\Delta\mathrm{lm} = \frac{\log k_{\mathrm{obs}} - \log k_{\mathrm{avg}}}{\log 2.12} \tag{32}$$

Table 14 – Comparison of the shifts Δlm obtained from individual $p(\Delta m)$ and rates.

Observer	from $p(\Delta m)$	from Spor		from 1988 Per		Average
	Δlm	Δlm	σ	Δlm	σ	Δlm
ARLRA	+0.09	−0.11	0.18	−0.02	0.18	−0.06
BALPE	+0.23	+0.03	0.21	−0.29	0.25	−0.13
KNOAN	+0.21	−0.04	0.18	0.00	0.30	−0.02
KOSRA	−0.22	+0.08	0.16	−0.09	0.20	0.00
RENIN	+0.09	+0.03	0.16	+0.07	0.30	+0.05
RENJU	−0.18	−0.05	0.20	+0.04	0.20	0.00
SEIHO	+0.50	+0.13	0.39	+0.26	0.40	+0.20

From Table 14, we conclude that the standard deviation σ of Δlm shows the real scatter of the perception of experienced observers. The value $\sigma = 0.20$ corresponds with a scatter of 25% in the ZHR if $r = 3.0$. Be careful with analyses based on only a few ZHR values!

The shift Δlm of the 5 selected observers derived from the rates is nearly zero. It is nearer to the average perception function than Δlm determined from the individual $p(\Delta m)$. Since the results lie within 1σ of the rate-determined values of Δlm, they are not contradicting each other. Recall that r_{Spor} was determined using the individual $p(\Delta m)$. If we compare the results of Table 9 with Figure 15, we find that the observers ARLRA, KNOAN, and RENIN have a smaller gradient in their $p(\Delta m)$ for $\Delta m > 2$ and that they also get smaller values of r. Since all observers were situated at the same site, the population index of the sporadic meteors should be the same for all observers. Differences like those mentioned before should be caused by erroneous values of $p(\Delta m)$. Together with the results given in Table 14 this leads to the following conclusions:

1. *the five observers (ARLRA, KNOAN, KOSRA, RENIN, RENJU) show very similar behavior with respect to perception; and*
2. *the differences of the $p(\Delta m)$ are random errors.*

The two different "types" of observers (see Figures 13 and 14) are real because the effect is significant. If one averages $p(\Delta m, R)$ over the field of view according to (5), the differences equalize. This leads to similar $p(\Delta m)$. Both observers reach the same success at the end. The average perception function for the 5 observers is given in Table 15.

Table 15 – Average perception function $p(\Delta m)$ over a field with $R = 52\overset{\circ}{.}5$. (See explanation in text.)

Δm	−1	0	+1	+2	+3	+4	+5	+6	+7
0.0		0.0023	0.023	0.079	0.24	0.52	0.74	0.85	0.94
0.2		0.0046	0.030	0.10	0.29	0.55	0.77	0.87	0.96
0.4		0.0081	0.039	0.13	0.35	0.64	0.79	0.89	0.98
0.6	0.00046	0.0122	0.049	0.16	0.40	0.67	0.81	0.91	1.00
0.8	0.0011	0.018	0.063	0.20	0.46	0.71	0.83	0.93	1.00

The following examples should clarify how Table 15 must be read:

$$p(\Delta m = -0.4) = p(-1 + 0.6) = 0.00046$$
$$p(\Delta m = -0.2) = p(-1 + 0.8) = 0.0011$$
$$p(\Delta m = +2.4) = p(+2 + 0.4) = 0.13$$

The factor $c(r)$ was obtained by averaging the 5 individual $c(r)$. The confidence interval of 68.3% (1σ-interval) is then $\pm\sigma/\sqrt{n}$, with $n = 5$.

Table 16 – Factors $c(r)$ obtained by averaging individual factors of the five selected observers.

r	1.8	2.0	2.2	2.4	2.6	2.8	3.0	3.2	3.4	3.6	3.8	4.0
$c(r)$	7.34	9.66	12.2	14.8	17.5	20.2	23.0	25.6	28.2	30.8	33.3	35.7
σ	0.80	1.26	1.8	2.5	3.3	4.1	4.9	5.8	6.6	7.5	8.4	9.2
$\pm$	0.36	0.56	0.8	1.1	1.5	1.8	2.2	2.6	3.0	3.4	3.8	4.1

It is possible to use sufficient approximations, which are:

$$c(r) = 13.10r - 16.45 \tag{33}$$
$$\pm = 0.198r^2 + 0.617r - 1.45 \tag{34}$$

Summary:

The perception of each of the 5 selected observers is characterized by the given function $p(\Delta m)$, cfr. Table 15, and the factor $c(r)$, cfr. Table 16, or equation (33), respectively.

9. Application to general meteor shower analysis

We now discuss the application of the above derived correlations to general meteor shower analysis in *IMO*.

We know the perception of five experienced observers well. They are really active observers. Nevertheless, their results represent only a small contribution to the amount of observational data. Thus the question arises how to determine the perception of other observers. Practically it is impossible to organize double count observations for all observers. It would require group observations under favorable circumstances during periods of enhanced activity. Furthermore, such observations are extremely fatiguing, and the numbers included into the present study represent an upper limit even for experienced and enthusiastic observers.

Within *IMO* we find considerable differences among the ZHRs. This is obvious e.g. in [7] and leads to the conclusion that there are differences in the perception. Possible reasons for such systematic differences are:

1. the determination of the limiting magnitude caused by different interpretations and methods; or
2. a differing individual perception.

In Section 8, we showed that individual differences of the perception function may be expressed by a shift Δlm. This may be regarded as a correction of the limiting magnitude lm. If we determine Δlm for individual observers we automatically eliminate one source of differences mentioned above (item 1). For several practical reasons, we propose to define the perception function of the 5 selected observers as the standard perception function. The fact that the authors are included is not the reason, but:

- we know this perception function with good certainty,
- this perception function is almost identical for five active observers, and
- due to the experience of these observers over a long time period, we may assume their perception to be constant.

There are the following possibilities to determine the value of Δlm of other observers:

1. *Determination of* Δlm *using sporadic rates:*
   First, we choose periods without any significant shower activity. Furthermore it is necessary to consider the same showers (*IMO* working list) according to all criteria available. Systematical differences between northern and southern hemisphere are possible. Since the standard observers are situated at the northern hemisphere, one should include only observations carried out at the northern hemisphere into the analysis.

   A possible method may be as follows. We choose a certain interval, say 10 days. For this period we assume the sporadic activity to be constant. Differences will be regarded as random fluctuations. Of course, we have to eliminate the diurnal variation. This effect is of importance especially during long nights in springtime when the elevation of the apex is $-60°$ in the evening and $+10°$ in the morning (cfr. [8]). During short nights or in fall, this effect can be neglected. If we restrict ourselves to data between May and November, the diurnal variation plays no role. Furthermore, a relatively even distribution of observations in the morning and in the evening may diminish the remaining effect.

   Then we calculate a reference rate $\mathrm{HR_{st}}$ for each interval by averaging all observational results of the five standard observers. Each hourly rate HR of another observer could be used to determine the value of Δlm according to:

$$\Delta\mathrm{lm} = \frac{\log \mathrm{HR} - \log \mathrm{HR_{st}}}{\log r} \tag{35}$$

   Random errors may be reduced if we include a sufficient number of observations from each observer. We assume a number of 30 observations of an effective duration $T_{\mathrm{eff}} \approx 2$ hours each. All values of Δlm found for an individual observer will be averaged then.

2. *Determination of* Δlm *using the activity profile of a major shower according to [7]:* Showers which produce a very sharp peak, such as Quadrantids and Lyrids, are not suitable for this method. For our purpose we prefer showers with a wide maximum and a sufficiently high activity. Such showers are the Perseids for the northern hemisphere, and both the Orionids and Geminids for northern and southern hemispheres. We propose the apply the procedure used in [7]. Before calculating the perception coefficients it is necessary to determine the population index r, or a profile of r, respectively. The coefficients found for the standard observers included in the sample are then averaged (k_{st}). The values Δlm can be calculated for individual observers according to

$$\Delta\mathrm{lm} = \frac{\log k - \log k_{\mathrm{st}}}{\log r} \tag{36}$$

   In order to obtain a certain Δlm, k should be based on a sufficient number of ZHR-values (at least 10). Since such an analysis is restricted to a few nights only, systematical effects on Δlm are possible. They may be caused by accidental circumstances of the observations as well as by the actual personal form, or even other effects. We suppose that at least four shower analyses are necessary to obtain a certain individual Δlm. The Δlm-values of all such analyses are to be averaged.

3. *Combination of (1) and (2):*

   In this case only half the number of observations requested for (1) or (2) are necessary.

If a certain individual Δlm for a given observer is determined, one may regard him as standard observer. He has to correct the limiting magnitude he calculates from his observation by Δlm:

$$\mathrm{lm}_{\mathrm{st}} = \mathrm{lm} + \Delta\mathrm{lm} \tag{37}$$

Known individual values of Δlm are stored in the *Visual Meteor Database (VMDB)*. For analysis, the observed lm will be corrected according to (37). This means that there are not any changes for the observer himself. Furthermore, the ZHR calculated by means of the *VMDB* including the individual Δlm can be used to calculate the number density ρ or the flux density Q (taking into account the standard graph $c(r)$).

In the case of a global shower analysis as in [7], the values of Δlm for most observers are not known. How can we overcome this situation? We carry out an analysis as described in [7] until we obtain a ZHR graph and values of the perception coefficient k for individual observers. The values of Δlm of standard observers are already included (equation (37)) at this stage. Then we average the values of k of the included standard observers and obtain $k_{\mathrm{avg}} \pm \Delta k_{\mathrm{avg}}$. The error Δk_{avg} corresponding to a confidence interval of 68.3% is given by

$$\Delta k_{\mathrm{avg}} = \sigma/\sqrt{n} \tag{38}$$

with n the number of standard observers.

The next step is the calibration of the ZHR graph such that $k_{\mathrm{avg}} = 1$. Then we obtain a reduced $\mathrm{ZHR}_{\mathrm{st}}$:

$$\mathrm{ZHR}_{\mathrm{st}} = \mathrm{ZHR} \times k_{\mathrm{avg}} \tag{39}$$

This $\mathrm{ZHR}_{\mathrm{st}}$ enables us to calculate also the number density ρ and the flux density Q using the factor $c(r)$.

10. Reliability and discussion

While the number density ρ is an obvious measure for the construction of a shower, the flux density Q is a more suitable measure for many calculations. The flux density can be calculated according to equation (14) as follows:

$$Q(m \leq 6.5) = \frac{\mathrm{ZHR}_{\mathrm{st}} \times c(r)}{A_{\mathrm{red}}(r)} \tag{40}$$

The introduction of the approximations for $c(r)$ and $A_{\mathrm{red}}(r)$ as well as the calibration of the observed ZHR_o lead to the equations:

$$Q(m \leq 6.5) = \frac{\mathrm{ZHR}_o \times k_{\mathrm{avg}} \times (13.1r - 16.5)(r - 1.3)^{0.748}}{37\,200 \text{ km}^2} \tag{41}$$

$$\rho = \frac{Q}{3600 V_\infty} \tag{42}$$

where V_∞ is expressed in km/s. Equation (18) is valid for Q, of course:

$$Q(M \geq 10^{-3} \text{ g}) = Q(m \leq 6.5) \times r^{9.775 \log \frac{29 \text{ km/s}}{V_\infty}} \tag{43}$$

At the end, the whole procedure looks well and an observer may be happy to see what can be done with serious data. But we have to answer the uncomfortable question: what is its value? Under wich conditions the relations are valid and wich errors should be expected?

Understandings:

- the population index r is more or less constant for visual meteors in the range $0 \leq m \leq 6.5$. This should be the case for visual shower analyses with only very few possible exceptions;
- the population index r lies in the interval $2.0 \leq r \leq 3.5$. For smaller and larger values of r, the simplifications introduced in Sections 2 and 3 lead to greater errors. For all known visual showers, this condition is fulfilled, too.

Estimation of errors:

Both quantities $Q(M \geq 10^{-3} \text{ g})$ and $\rho(M \geq 10^{-3} \text{ g})$ strongly depend on the accuracy of the exponents $a = 3.91$ and $b = 0.92$ in equation (15). We are not able to estimate the certainty and the limits of validity. Possibly the exponents vary from one shower to the next. This will require more research work by professional astronomers.

The quantities $\rho(m \leq 6.5)$ and $Q(m \leq 6.5)$ are more certain because they omit the conversions just mentioned. If not urgently needed, we should restrict to the quantities $\rho(m \leq 6.5)$, or $Q(m \leq 6.5)$, respectively. For these, we now try to estimate the errors. We take as a basis a confidence interval of 68.3% (i.e., 31.7% error probability, 1σ width) and a Gaussian error distribution. The error follows from the total differential of the equations (40) and (41) and the normal law of errors:

$$\Delta Q(m \leq 6.5) = \sqrt{\left(\frac{\partial Q}{\partial \mathrm{ZHR}_o}\Delta \mathrm{ZHR}_o\right)^2 + \left(\frac{\partial Q}{\partial r}\Delta r\right)^2 + \left(\frac{\partial Q}{\partial c}\Delta c\right)^2 + \left(\frac{\partial Q}{\partial k_{\mathrm{avg}}}\Delta k_{\mathrm{avg}}\right)^2 + \left(\frac{\partial Q}{\partial A_{\mathrm{red}}}\Delta A_{\mathrm{red}}\right)^2} \tag{44}$$

and

$$\Delta\rho(m \leq 6.5) = \frac{\Delta Q(m \leq 6.5)}{3600 V_\infty} \tag{45}$$

We now deal with the components of the error. First we have:

$$\frac{\partial Q}{\partial \mathrm{ZHR}_o}\Delta \mathrm{ZHR}_o = \frac{k_{\mathrm{avg}} \times c}{A_{\mathrm{red}}}\Delta \mathrm{ZHR}_o \tag{44.1}$$

ZHR_o is the average of all individual ZHRs. Therefore, we have:

$$\Delta \mathrm{ZHR}_o = \sigma/\sqrt{n} \tag{46}$$

with n the number of ZHR values, or, in the case of a weighed mean (weight $1/c_{\mathrm{tot}}$), we obtain according to [9]:

$$\Delta \mathrm{ZHR}_o = \frac{\sigma}{\sum_{i=1}^{n} \frac{1}{c_i}} \sqrt{\sum_{i=1}^{n} \left(\frac{1}{c_i}\right)^2} \tag{47}$$

with n also the number of ZHR-values. The quantity $\Delta \mathrm{ZHR}_o$ represents :

- differences in the perception of individual observers,
- random fluctuations of the activity, and
- errors, caused by uncertainties in the corrections of limiting magnitude and radiant elevation.

As you know,

$$\mathrm{ZHR}_o = \frac{N}{T_{\mathrm{eff}}} \times \sin^{-1} h_R \times r^{6.5-\mathrm{lm}} \tag{48}$$

If there is only an error in r, we find a scatter in ZHR_o dependent on the limiting magnitude. Furthermore, we obtain a systematical error in the case of a mean limiting magnitude $\overline{\mathrm{lm}} \neq 6.5$. If we know the error on r, we can give error margins depending on $\overline{\mathrm{lm}}$. A similar situation appears in the case of the zenith correction. Notwithstanding, the magnitude of the systematical error cannot be found out since the exact zenith correction is not known. We can reduce the influence of this uncertainty if we include only observations with a radiant elevation $h_R > 20°$ in an analysis. Both errors are partially present in $\Delta\mathrm{ZHR}_o$ already. Taking these into account separately, we would obtain an overestimated error. Therefore we propose to consider the systematical error caused by the correction of lm to be included separately while the elevation correction error is considered to be represented in $\Delta\mathrm{ZHR}_o$ already. Now we introduce a new quantity:

$$\mathrm{ZHR}^* = \frac{\mathrm{ZHR}_o}{r^{6.5-\overline{\mathrm{lm}}}} \tag{49}$$

or

$$\mathrm{ZHR}_o = \mathrm{ZHR}^* \times r^{6.5-\overline{\mathrm{lm}}} \tag{50}$$

respectively. The mean limiting magnitude $\overline{\mathrm{lm}}$ is easy to obtain, and the right-hand side of (50) is then substituted for ZHR_o in equation (41) when the deviation has to be done. Thus we obtain for the second term of equation (44):

$$\frac{\partial Q}{\partial r}\Delta r = \frac{\mathrm{ZHR}^* \times k_{\mathrm{avg}}}{37\,200\ \mathrm{km}^2}\Delta r \left\{ \left[13.1(7.5-\overline{\mathrm{lm}})r^{6.5-\overline{\mathrm{lm}}} - 16.45(6.5-\overline{\mathrm{lm}})r^{5.5-\overline{\mathrm{lm}}} \right] (r-1.3)^{0.748} \right.$$
$$\left. +0.748\left(13.1r^{7.5-\overline{\mathrm{lm}}} - 16.45r^{6.5-\overline{\mathrm{lm}}}\right)(r-1.3)^{-0.252} \right\} \tag{44.2}$$

The third term of equation (44) is:

$$\frac{\partial Q}{\partial c}\Delta c = \frac{\mathrm{ZHR}_o \times k_{\mathrm{avg}}}{A_{\mathrm{red}}}\Delta c \tag{44.3}$$

The quantity Δc represents the error on the factor $c(r)$ which is derived from the standard function $p(\Delta m)$. In the end, this is the uncertainty on the perception function itself. The uncertainty defining the 68.3%-confidence interval was determined in Section 8 (see Table 16 and equation (34)). We have to consider that all 5 estimates were carried out using the same method and the same simplifications. Consequently, errors caused by the procedure have to be summed up. Bearing in mind the whole procedure and the simplifications introduced we assume that an additional 15% error is reasonable. From equations (33) and (34) we then find:

$$\Delta c = 0.198r^2 + 2.582r - 3.921 \tag{51}$$

The fourth term of equation (44) reads:

$$\frac{\partial Q}{\partial k_{\mathrm{avg}}}\Delta k_{\mathrm{avg}} = \frac{\mathrm{ZHR}_o \times c}{A_{\mathrm{red}}}\Delta k_{\mathrm{avg}} \tag{44.4}$$

As already explained in Section 8, the perception of the standard observers is subject to random variations. Thus, also the calibration is effected by an error. For the determination of Δk_{avg}, see equation (38).

The last term of equation (44) reads:

$$\frac{\partial Q}{\partial A_{\mathrm{red}}}\Delta A_{\mathrm{red}} = -\frac{\mathrm{ZHR}_o \times k_{\mathrm{avg}} \times c}{A_{\mathrm{red}}^2}\Delta A_{\mathrm{red}} \tag{44.5}$$

In Section 2 we introduced the following assumptions:

1. $H = 100$ km,
2. an average extinction, and
3. "horizon" at 4° elevation.

If the altitude H differs from 100 km, this leads to an error of maximum 8% (cfr. Table 1). Furthermore, we showed that the deviations from $A_{\mathrm{red}}(h_f = 50°)$ are less than 10% for approximately $2.0 \leq r \leq 3.5$ and $40° \leq h_f \leq 65°$. The elevation of the field center h_f has only little influence on the value of A_{red} (cfr. also Figure 5). In the case of differing h_f, of course , the assumptions (2) and (3) act very differently on A_{red}. Vice versa, we may conclude that in the case of a commonly chosen $h_f = 50°$, any deviations from the assumptions (2) and (3) have only little influence on A_{red}. At the end, we assume an error of 10% to be reasonable to represent the confidence interval of 68.3%:

$$\Delta A_{\mathrm{red}} = 0.1 A_{\mathrm{red}} \tag{52}$$

Now, we examine the contribution of the different errors to the total uncertainty. Therefore we take as an example:

- ZHR = 50,
- $\Delta k_{\mathrm{avg}} = 0.02$ (follows from Table 13 for the example in [7] and should give the order of the effect expected),
- $k_{\mathrm{avg}} = 1$, and
- lm = 6.0 (should represent the real situation).

Table 17 – Dependence of individual error portions on certain conditions. The following constants were chosen: ZHR = 50, $k_{\mathrm{avg}} = 1$, $\Delta k_{\mathrm{avg}} = 0.02$ and lm = 6.0.

nr.	$\Delta\mathrm{ZHR}_o$	$\frac{\Delta\mathrm{ZHR}_o}{\mathrm{ZHR}_o}$ (%)	r	Δr	c	A_{red} (km^2)	$\frac{\partial Q}{\partial \mathrm{ZHR}_o}\Delta\mathrm{ZHR}_o$ ($\times 10^{-3}$)	$\frac{\partial Q}{\partial r}\Delta r$ ($\times 10^{-3}$)	$\frac{\partial Q}{\partial c}\Delta c$ ($\times 10^{-3}$)	$\frac{\partial Q}{\partial k_{\mathrm{avg}}}\Delta k_{\mathrm{avg}}$ ($\times 10^{-3}$)	$\frac{\partial Q}{\partial A_{\mathrm{red}}}\Delta A_{\mathrm{red}}$ ($\times 10^{-3}$)	Q ($\times 10^{-3}$)	ΔQ ($\times 10^{-3}$)	$\frac{\Delta Q}{Q}$ (%)
1	5	10	2.7	0.25	18.92	28 900	3.27	11.5	7.77	0.654	−3.27	32.7	14.6	45
2				0.15			3.27	6.9	7.77	0.654	−3.27	32.7	11.4	35
3				0.35			3.27	16.1	7.77	0.654	−3.27	32.7	18.4	56
4	10	20		0.25			6.54	11.5	7.77	0.654	−3.27	32.7	15.7	48
5	2.5	5		0.25			1.64	11.5	7.77	0.654	−3.27	32.7	14.3	44
6	5	10	2.0	0.25	9.75	48 600	1.00	6.68	2.09	0.2	−1.00	10.0	7.14	71
7				0.15			1.00	4.01	2.09	0.2	−1.00	10.0	4.73	47
8				0.35			1.00	9.35	2.09	0.2	−1.00	10.0	9.69	97
9			3.5	0.25	29.4	20 600	7.13	6.62	18.3	1.43	+7.13	71.3	22	31
10				0.35			7.13	9.27	18.3	1.43	+7.13	71.3	22.9	32
11	25	50		0.25			36	6.62	18.3	1.43	+7.13	71.3	42	58

First, we look at an "average situation" (first line of Table 17). The errors Δr and Δc alone lead to $\Delta Q/Q = 42\%$. All other errors are thus neglectable. The quantity Δc can not be reduced easily. If we determine the population index r with greater/smaller certainty, this increases/decreases the certainty of Q quite reasonably (lines 2 and 3 in Table 17). On the other hand, halving the $\Delta\mathrm{ZHR}_o$ does not improve the accuracy of Q significantly. As becomes obvious from line 5, a $\Delta\mathrm{ZHR}_o$ twice as large as in line 1 does not lead to a remarkable decrease in the accuracy of Q.

Second, we look at a shower with a lower population index ($r = 2.0$, line 6). In this case the contribution of Δr dominates the error on Q: $\Delta Q/Q = 68\%$, and all other errors are neglectable. Again, the quantity Δr is decisive to the certainty of Q (lines 7 and 8). The strong effect of Δr is attributed to the strong contribution of $\frac{dA}{dr}|_{r=2.0}$.

Third, we consider a shower with $r = 3.5$ (line 9). In this case the error Δc is dominating. It contributes with 26% to $\Delta Q/Q$, while the uncertainty Δr is of low effect only. Herewith we confirm the propriety of the decision to omit the nights around the Perseid's maximum for the determination of the perception $p(\Delta m)$. Thus, the values derived ($p(\Delta m)$ and therefore also $c(r)$) are valid for medium (or "normal" activity). Usually then, we find higher values of r, and the influence of errors on $c(r)$ is more important. Near to the maximum of major showers the population index r decreases and errors in $c(r)$ have less influence.

Objective of the observations is the determination of a profile of the quantities Q (or ρ, respectively) through the cross-section of the shower under study. As described for instance in [2], the ZHR is not a suitable measure for the variation of the particle number density through the shower. From Table 17, it becomes obvious that a ZHR of 50 may correspond with $Q = 1.0 \times 10^{-2}$ km^{-2}h^{-1} (if $r = 2.0$), or $Q = 7.13 \times 10^{-2}$ km^{-2}h^{-1} (if $r = 3.5$). Observation and analysis are to be done with the aim of deriving a flux density Q with the greatest accuracy possible.

If we recall the errors, we must consider the following conclusions:

- *In the case of larger r, we should expect more certain values of Q.*
  - *Such greater indices r mostly occur for minor showers. Because of the smaller sample of these showers we obtain r only with a reduced certainty. Since the influence of Δr is smaller for, say, $r \approx 3.5$, it is sufficient to know r with an error of 0.3 to 0.4.*
  - *On the other hand, the ZHR is more uncertain in the case of minor showers. Combined with the smaller effect of Δr, this leads to a comparable error $\Delta Q/Q$ for minor showers and major showers with a small r (cfr. Table 17, line 11).*
- *Major showers are generally characterized by a low value of r. Any further analysis is worthless if r is not known exactly.*
  - *The certainty of the method to obtain ZHR profiles developed in [7] is sufficient. An improvement of the accuracy of the ZHRs can not improve the certainty of Q. Consequently, the determination of the r-profile becomes very important. Therefore the method to calculate a precise population index r is decisive. In the next paragraph, we add some basic ideas to this problem.*

11. Determination of the population index profile

We now deal with the determination of the profile of the population index r along the cross section of a shower.

In [10], a method is described which is also recommended for the use in other publications, e.g., [11]. The basic assumption is that in the case of a given value of r an observer will find a certain average magnitude m of the meteors. From this average magnitude, the population index r is derived. But the relation $r = r(m)$ published in [10] is valid only for certain circumstances, especially a certain limiting magnitude and a certain perception. As soon as the conditions for an observer differ from the "standard" assumed, the relation will change, too. Even stronger, we do not find $r = r(m)$ but $r = r(m, \mathrm{lm}, p(m))$, or $r = r(\mathrm{lm} - \mathrm{m}, p(\Delta m))$. The conditions for the relation published in [10] are:

1. the perception is based on the average of a group of observers at Skalnaté Pleso;
2. the limiting magnitude was not determined , since it was argued to be constant under the conditions at the mountains (1780 m a.s.l.). This may be, but nevertheless lm is specific value for each observer, not an absolute value. The limiting magnitude at the same location may differ from one observer to the next, as it can be seen in Table 13.

It is impossible to use the relation derived at any other location (where a constant limiting magnitude is not fulfilled). The consideration of lm by using $\mathrm{lm} - m$ could be useful, but is impossible, since lm was not determined in [10]. A conversion of the relation from $r = r(m)$ into $r = r(\mathrm{lm} - m)$ is not possible.

Sometimes authors assume that lm = 6.5 for the relation published in [10]. But this is pure speculation! In [10] we read: *The limiting stellar magnitude was generally not recorded because this is quite steady at the high mountain location of Skalnaté Pleso (1780 m above sea-level).*

Another problem arises from the differences in the perception of individual observers , especially for faint meteors which strongly act on the mean magnitude m. Furthermore, the procedure is of no help as far as the certainty of the population index r is concerned. The scatter of m is not a suitable measure because the greatest source of error is the type of the relation $r = r(m)$. Consequently, this procedure is not useful for the accuracy of r requested for our purposes.

Another method is described in [5]. Since until now this note has only been published in Dutch (English version ready for publication now), we summarize the most essential points here. A computer simulation is used to test the consistence and efficiency of several procedures to determine r. The most favorable method was found to be as follows. We start from a magnitude distribution, and calculate the true number of meteors in each magnitude class:

$$\varphi(m) = \frac{n(m)}{p(\mathrm{lm} - m)} \tag{53}$$

These values are used to obtain a cumulative magnitude distribution:

$$\Phi(m) = \sum_{x=-\infty}^{m} \varphi(x) \tag{54}$$

The expression:

$$\Phi(m) = Cr^m \tag{55}$$

is linearized by the equation:

$$\log \Phi(m) = m \log r + \log C \tag{56}$$

Using the least squares method we calculate a linear expression from the observed $\Phi(m)$:

$$\log \Phi(m) = am + b \tag{57}$$

from wich we obtain:

$$r = 10^a \tag{58}$$

The certainty of r is determined as a function of the number of meteors included in the magnitude distribution. Using a computer 400 magnitude distributions are simulated with $n = 10$, $n = 20$, $n = 40$, $n = 100$, $n = 200$, and $n = 400$ meteors each and with a value of $r = 3.0$. The simulated magnitude distributions are then used to calculate r as described before. The resulting values of r show a Gaussian distribution and we can calculate the standard deviation σ of the samples of 400 magnitude distributions for each of the groups with $n = 10$ to $n = 400$ meteors. Instead of using the table given in [5], we may approximate it for $10 \leq n \leq 400$ by:

$$\sigma_r = 4.07 n^{-0.764} + 0.2 \tag{59}$$

This procedure offers some advantages, such as:

- the possibility to take into consideration the individual perception by shifting the standard function $p(\Delta m)$; and
- the possible choice of a suitable magnitude interval for the regression.

The latter is of interest since we often find only few bright meteors per distribution causing significant statistical uncertainties. The interval for the regression should be chosen such that:

1. there is a sufficient number of meteors per magnitude class ($n \geq 3$),
2. the faintest magnitude classes are not included (that means $\Delta m \geq 2$, or normally $m \leq +4$, or in exceptional cases $m \leq +5$), and
3. for the regression, there are at least 5 magnitude classes available, e.g. $0 \leq m \leq +4$.

The possibility to choose a suitable interval diminishes possible errors. Since it is not possible to perform the criteria 1–3 with one magnitude distribution for one interval, we may add the $\Phi_i(m)$ of several magnitude distributions:

$$\Phi(m) = \sum_i \Phi_i(m) \tag{60}$$

until the magnitude distributions fulfils the criterion for one interval. The calculation of the differences between the observed values $\log \Phi(m)$ and the regression line:

$$v(m) = am + b - \log \Phi(m) \tag{61}$$

allows the detection of systematic errors in the magnitude distributions. Consequently, one can also select erroneous magnitude distributions. In Table 18, we present such values of $v(m)$ and the corresponding relative errors $\Delta\Phi(m)/\Phi(m)$.

Table 18 – Relative errors $v(m)$.

$v(m)$	0.05	0.10	0.15	0.20
$\frac{\Delta\Phi(m)}{\Phi(m)}$	12%	25%	41%	58%

Generally, smaller systematical errors of magnitude estimates, such as the preference of certain magnitude classes, are compensated by the regression. In the case of values $|v| \geq 0.20$ in the regression interval the effected distribution should be omitted. If a given magnitude distribution allows the calculation of more than one regression interval (fulfilling the above mentioned criteria), the regression should be carried out for each of these intervals, connected with a check of the deviations $v(m)$. Finally, we use the index r obtained from the interval with the highest correlation coefficient.

Sometimes it is argued that the use of apparent magnitudes m instead of absolute magnitudes m_{abs} is a general error. Let us have a look at this statement. The index r is defined as

$$r = \frac{\varphi(m_0+1)_{\text{abs}}}{\varphi(m_0)_{\text{abs}}} = \frac{\Phi(m_0+1)_{\text{abs}}}{\Phi(m_0)_{\text{abs}}} \tag{62}$$

This leads to:

$$\begin{aligned}
\Phi(m_0+1)_{\text{abs}} &= r\Phi(m_0)_{\text{abs}} \\
\Phi(m_0+2)_{\text{abs}} &= r^2\Phi(m_0)_{\text{abs}} \\
\Phi(m_0+3)_{\text{abs}} &= r^3\Phi(m_0)_{\text{abs}} \\
&\vdots
\end{aligned}$$

and if we set $m_0 = 0$ we obtain:

$$\Phi(m_{\text{abs}}) = Cr^{m_{\text{abs}}} \tag{63}$$

with C a constant. Within a small altitude interval h_i, we have:

$$m_{\text{abs}} = m + 5\log\frac{d_i}{100\text{ km}} + \varepsilon_i \tag{64}$$

and thus:

$$\Phi_i(m) = \Phi_i(m_{\text{abs}})r^{-5\log\frac{d_i}{100\text{ km}}-\varepsilon_i} \tag{65}$$

Then, we write the equation (63) as follows:

$$\Phi_i(m_{\text{abs}}) = C_i r^{m+5\log\frac{d_i}{100\text{ km}}+\varepsilon_i} \tag{66}$$

Substitution of (66) in (65) yields:

$$\Phi_i(m) = C_i r^m \tag{67}$$

Every total magnitude distribution obtained during an observation results from the superposition of magnitude distributions $\Phi_i(m)$ in separate small altitude intervals h_i. We may write:

$$\Phi(m) = \sum_i \Phi_i(m) = \sum_i C_i r^m = \left(\sum_i C_i \right) r^m = C r^m \tag{68}$$

with C again a constant. This expression (68) is identical with equation (55) and is the initial point of the proposed method. Consequently, we may state that the use of apparent magnitudes does not imply an error.

The error on r, $\sigma_r = f(n)$ as given in equation (59) was determined from simulations. Thus it includes only random errors, while errors such as those from different perception are not taken into consideration. The selection of the most suitable magnitude interval diminishes the contribution of both components of the error. That allows us to regard the $\sigma_r(n)$ as the "true" error on the population index. If we use the *VMDB* to determine the value of r, we find two possibilities:

1. summing up the $\Phi_i(m)$ of all observers of a certain time interval and calculating r using this summarized magnitude distribution $\Phi(m)$, or
2. calculating individual r_i from the distributions $\Phi_i(m)$ of each observer and averaging these r_i for a certain time interval.

We now compare both versions. The total number of meteors included in the analysis is designated n_{tot}. In case 2, we divide n_{tot} into j different magnitude distributions of n meteors each,

$$n = \frac{n_{\text{tot}}}{j} \tag{69}$$

whereas $j = 1$ in case (1). From the j different magnitude distributions we obtain j values of r. These values r_k, $k = 1, 2, 3, \ldots, j$ are normally distributed with expectancy r and standard deviation $\sigma_r(n)$. If we estimate the expectancy r by averaging all individual r_k:

$$\overline{r} = \frac{1}{j} \sum_{k=1}^{j} r_k \tag{70}$$

we find the 68.3% confidence interval to be:

$$\Delta r = \frac{\sigma_r(n)}{\sqrt{j}} \tag{71}$$

or, using (69):

$$\Delta r = \frac{\sigma_r(n)}{\sqrt{\frac{n_{\text{tot}}}{n}}} \tag{72}$$

Applying equation (59) we find then:

$$\Delta r = \frac{(4.07 n^{-0.764} + 0.2)\sqrt{n}}{\sqrt{n_{\text{tot}}}} \tag{73}$$

Of course, we try to find a result which gives a minimal Δr. If we set $\frac{\partial(\Delta r)}{\partial n} = 0$ and find a minimal Δr for $n = 22$, independently of n_{tot}. That means, we obtain the most certain value for the population index r if we average it from $j = n_{\text{tot}}/22$ magnitude distributions. In Table 19, we show Δr as a function of n and n_{tot}. Since equation (59) is not sufficient for $n = 10$,

we take $\sigma_r(n = 10)$ directly from [5]. The numbers n and n_{tot} refer to the regression interval chosen, not to the total number of meteors.

Table 19 – The error Δr as a function of the total number n_{tot} taken into account for the calculation of r and the number n of individual r_i calculated.

n_{tot}	$n = 10$	$n = 15$	$n = 20$	$n = 40$	$n = 100$
20	0.71	0.62	0.61		
40	0.50	0.44	0.43	0.44	
100	0.32	0.28	0.27	0.28	0.32
200	0.22	0.20	0.19	0.20	0.23
400	0.16	0.14	0.14	0.14	0.16
1000	0.10	0.087	0.086	0.089	0.10

In the range $15 \leq n \leq 40$, the amount of Δr varies only little; we find a flat minimum there.

What are the practical conclusions from these findings? If an observer noted a large number of shower meteors (at least 150), it is useful to divide them into (time) intervals with a sufficient number of meteors in each interval. Since it is important to choose a suitable regression interval, we can generally expect about 30 shower meteors being necessary for such an interval. One obtains a number of independent magnitude distributions allowing the choice of a suitable regression interval (cfr. Table 19). Consequently, we calculate a series of values r_k from each interval chosen. On the other hand, we sum the magnitude distributions of single observers who independently do not fulfil the conditions for a calculation of an r_k. Of course, we sum only as many magnitude distributions as necessary to obtain a magnitude distribution according the above mentioned criteria. In the future it seems to be worth testing, if a determination of a r-profile along the cross-section of a shower is possible using the sliding mean of the individual r_k with a suitable sampling period. In such a case, the error Δr has to be calculated using:

$$\Delta r = \frac{\sigma_r}{\sqrt{j}} \tag{74}$$

with j the number of the individual values r_k. Here, it is reasonable to calculate σ_r from the distribution of the r_k (instead of equation (59)), because this represents the actual conditions.

12. Final remark

The concept described here allows the determination of the flux density Q, or the spatial number density ρ, respectively, of meteoroids causing meteors of an absolute magnitude of at least 6.5. Furthermore, we are able to calculate the population index r, or the mass index s, respectively, using visual observations fulfilling the *IMO* standard. For all quantities we may give information concerning the accuracy. The authors would be grateful for any discussion and hints allowing the improvement of the procedures.

Appendix

For calculating d, we find the following expressions:

$$\delta = \arccos\left(\frac{6370 \text{ km} \cos h}{6370 \text{ km} + H}\right) - h \tag{75}$$

and then:

$$d = (6370 \text{ km} + H)\,\frac{\sin\delta}{\cos h} \tag{76}$$

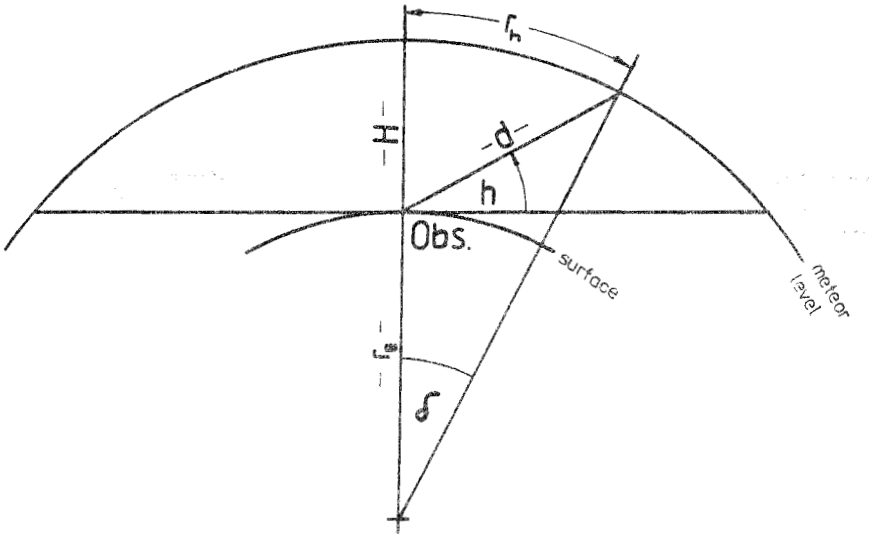

Figure 17 –Calculation of d and r_h.

The radii of the isohypses r_h as given in Tables 3 and 4 are:

$$r_h = (6370 \text{ km} + H)\delta \tag{77}$$

where δ has to be expressed in rad. A very important measure are the limits of the distance classes projected into the meteor level. These limits are the intersection curves of a straight circular cone, where the angle R is half the angular diameter of the field of view. The observer is situated at the narrow end of the cone, the other end is given by the sphere at the meteor level. There is no closed solution of this problem. That is why we calculate the curves point by point as shown in Figures 18 and 19.

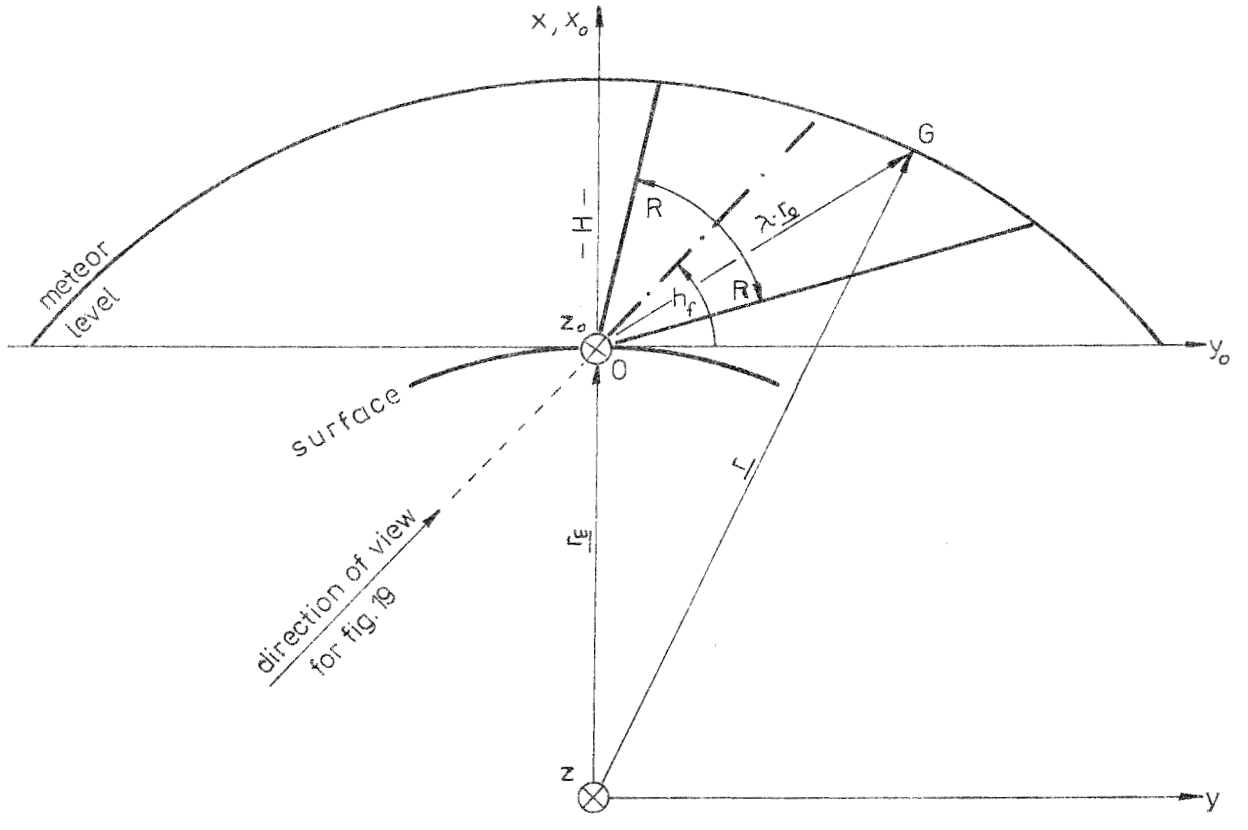

Figure 18 –Calculation of the projection of limits of distance classes onto the meteor level.

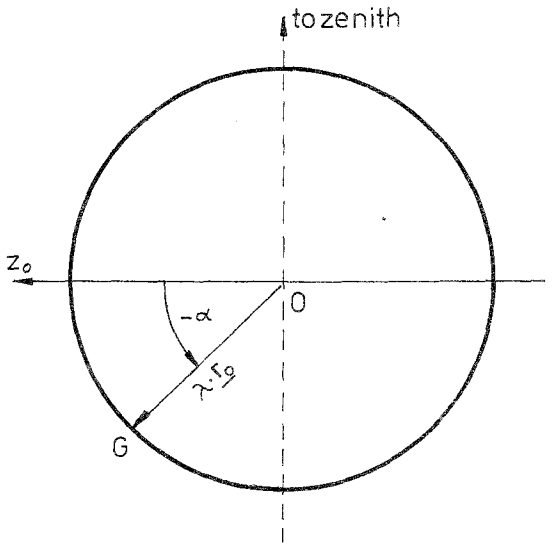

Figure 19 –Calculation of the projection of limits of distance classes onto the meteor level.

Because of symmetry, we have to calculate only half the intersection curve (left of Figure 17). For $-90° \leq \alpha \leq +90°$, we calculate the curve with a step width of 3°. The aim is to calculate the positional vector $\vec{r}$. First, we determine the directional vector $\vec{r}_0 = (x_0, y_0, z_0)$, where $|r_0| = 1$. We find:

$$z_0 = \sin R \cos \alpha \tag{78}$$

$$y_0 = \cos R \cos h_f - \sin R \sin \alpha \sin h_f \tag{79}$$

$$x_0 = \frac{\cos R \cos h_f \sin h_f - \sin R \sin \alpha \sin^2 h_f + \sin R \sin \alpha}{\cos h_f} \tag{80}$$

Using the equation of the straight line we may write:

$$\vec{r} = \vec{r}_E + \lambda \vec{r}_0 \tag{81}$$

and our task is to find λ.

λ can be written as:

$$\lambda = -x_0 \times 6370 \text{ km} + \sqrt{(x_0 \times 6370 \text{ km})^2 - (6370 \text{ km})^2 + (6370 \text{ km} + H)^2} \tag{82}$$

The coordinates of the intersection are then:

$$(x, y, z) = (r_E, 0, 0) + \lambda(x_0, y_0, z_0) \tag{83}$$

with:

$$x = 6370 \text{ km} + \lambda x_0 \tag{83.1}$$

$$y = \lambda y_0 \tag{83.2}$$

$$z = \lambda z_0 \tag{83.3}$$

We transform this into a spherical coordinate system. Its positive z-axis is directed to the pole. Consequently, we obtain:

$$\vartheta = \text{arctg} \frac{\sqrt{x^2 + y^2}}{z} \tag{84}$$

$$\varphi = \text{arctg} \frac{y}{x} \tag{85}$$

$$r = 6370 \text{ km} + H \tag{86}$$

Because of the neglectable curvature ($|\varphi| < 10°$) we may regard he spherical surface at the meteor level to be a plane. In this way, we have to calculate plane coordinates (x_E, y_E). The origin of this coordinate system is situated at the zenith. The positive x-axis then is the projection of the azimuth of the center of the field of view onto the meteor level. In Figure 4, we find this as the straight horizontal line.

With φ and ϑ given in rad we may now write:

$$x_E = r\varphi \tag{87}$$

$$y_E = r\vartheta \tag{88}$$

The areas A_i (as shown in Figure 4) for a certain elevation of the center of the field of view were determined graphically. Therefore the radii of the isohypses corresponding to the elevation angles $h = 4°$, $6°$, $8°$, $10°$, $12°$, $14°$, $16°$, $18°$, $20°$, $25°$, $30°$, $35°$, $40°$, $50°$, $60°$, $70°$, and $80°$ were calculated. The lines for the limits of all distance classes were calculated according to equations (78) to (88).

The isohypses and the latter lines were then plotted at a scale of 1 : 500 000 and 1 : 2 000 000, respectively. This represents the projection of half the symmetrical field of view. The areas situated between the isohypses are then determined for each distance class (cfr. Figure 4). At the plot of 1 : 500 000 we may find only the near-zenith area. This covers a field of 10 cm by 7 cm at the other plot only, where the remaining areas were determined. The scale for the near-zenith area allows a more certain determination for the corresponding areas.

Remember that just these areas deliver a larger contribution to A_{red}. All areas A_i determined by this method are then doubled (for the other half of the field). The whole procedure was carried out for $h_f = 40°$, $50°$, and $65°$ assuming a height $H = 100$ km.

The results are given in Tables 20, 21 and 22.

Table 20 – Composition of the areas as a function of the distance classes R and the elevation h for an elevation of the center of the field of view of $h_f = 40°$ and $H = 100$ km.

h	$R = 5°$	$R = 10°$	$R = 15°$	$R = 20°$	$R = 25°$	$R = 30°$	$R = 35°$	$R = 40°$	$R = 45°$	$R = 50°$
04–06°						0	45808	38144	26384	24536
06–08°						1696	38604	21302	16136	14248
08–10°						14080	19384	12936	10240	9024
10–12°						14880	9304	8176	8000	6096
12–14°				0	2904	9464	5828	5256	4320	4288
14–16°				0	6104	6016	3700	3792	3128	2208
16–18°				208	5160	2984	2604	2624	2232	1880
18–20°				2632	3224	2200	2016	2056	1800	1800
20–25°	0	0	1200	5808	3704	3056	2962	2994	2704	2696
25–30°	0	664	2936	2124	1429	1768	1594	1672	1867	1560
30–35°	306	1545	1072	1032	1018	1002	1010	1032	987	1010
35–40°	902	736	663	662	667	661	678	674	684	691
40–50°	792	1066	962	870	858	864	872	874	890	912
50–60°	0	161	647	844	644	590	562	574	568	586
60–70°	0	0	0	125	504	602	480	427	406	416
70–80°						90	363	430	351	336
80–90°						0	0	75	246	318

Table 21 – Composition of the areas as a function of the distance classes R and the elevation h for an elevation of the center of the field of view of $h_f = 50°$ and $H = 100$ km.

h	$R = 5°$	$R = 10°$	$R = 15°$	$R = 20°$	$R = 25°$	$R = 30°$	$R = 35°$	$R = 40°$	$R = 45°$	$R = 50°$
04–06°								0	55584	44408
06–08°								1800	47544	24236
08–10°								17136	21368	14840
10–12°								19112	11688	9360
12–14°							2784	14192	7040	5016
14–16°							7912	6064	4680	4160
16–18°						253	7824	3912	3300	2880
18–20°						3152	4000	2704	2394	2184
20–25°					1816	7616	4704	3791	3556	3388
25–30°	0	0	0	1096	3902	2584	2188	1968	1922	1792
30–35°	0	0	560	2146	1506	1376	1258	1182	1162	1178
35–40°	0	294	1338	1018	816	818	800	796	784	794
40–50°	648	1186	1024	1024	950	994	984	1018	1002	1018
50–60°	472	648	638	578	544	576	576	590	628	620
60–70°	0	98	424	576	444	426	418	414	446	488
70–80°	0	0	0	90	326	422	356	338	388	600
80–90°						62	238	292	280	61

Table 22 – Composition of the areas as a function of the distance classes R and the elevation h for an elevation of the center of the field of view of $h_f = 65°$ and $H = 100$ km.

h	$R = 5°$	$R = 10°$	$R = 15°$	$R = 20°$	$R = 25°$	$R = 30°$	$R = 35°$	$R = 40°$	$R = 45°$	$R = 50°$
04–06°										
06–08°										
08–10°										
10–12°										
12–14°										5476
14–16°										10728
16–18°									515	10318
18–20°									4832	5520
20–25°								2598	10628	6850
25–30°							1504	6149	3820	3336
30–35°						1022	3735	2344	1990	1910
35–40°					562	2271	1430	1266	1194	1170
40–50°			254	1402	2275	1591	1450	1476	1477	1557
50–60°	100	616	1064	848	769	751	797	868	926	1166
60–70°	563	439	404	437	461	496	559	682	1016	891
70–80°	68	304	408	351	366	412	642	554	131	
80–90°			69	232	305	281	81			

For each distance class we now determine the reduced areas A_R according to equation (1). We take into consideration d_i and ε_i for the corresponding center of the interval, e.g. for the class 04°-06°, we assume 5°.

$$A_R = \sum_i A_i r^{5 \log \frac{100 \text{ km}}{d_i} - \varepsilon_i} \tag{89}$$

The values of A_R are then summed up to the total reduced area A_{red} with:

$$A_{\text{red}} = \sum_{R=5°}^{50°} A_R \tag{90}$$

The result was already shown in Figure 5.

List of symbols

A	true area at the meteor level (km^2)
A_R	reduced area of a given distance class
A'_R	portion of the reduced area of a distance class relative to the total area
A_{red}	reduced area of a field with a radius of $R = 52\overset{\circ}{.}5$
c_i	total correction factor of a ZHR, $c_i = \mathrm{ZHR}_i/n_i$
$c(r)$	correction factor to convert the observed ZHR into the true ZHR
d_i	distance between observer and an area A_i at an elevation h_i (km), cfr. Appendix
ε_i	extinction at an elevation h_i according to [4] in magnitudes
H	altitude of the meteor level, a.s.l. (km)
h_f	elevation of the center of the field of view (°)
h_i	average elevation of an area Ai above the horizon (°)
h_R	elevation of a radiant (°)
HR	hourly rate, corrected for the limiting magnitude
I	intensity of a meteor
k	perception coefficient
lm	visual limiting magnitude (for stars)
$\overline{\mathrm{lm}}$	averaged lm
m	magnitude of a meteor, or magnitude class of one magnitude width
M	mass of a meteoroid (g)
n	number of meteors observed
n_{cum}	cumulative number of meteors observed
p	probability of perception
Q	flux density of meteoroids (km^{-2} h^{-1})
r	population index
R	angular distance from the center of the field of view, or distance class of 5° width
s	mass index
v_0	reference velocity for which particles of 10^{-3} g cause a meteor of magnitude 6.5
V_∞	geocentric velocity of a meteoroid (km/s)
ZHR_o	observed ZHR
ZHR_t	true ZHR
φ	true number of meteors
Φ	true cumulative number of meteors
ρ	spatial number density of meteoroids (km^{-3})

Acknowledgment

The authors wish to thank R. Arlt, A. Knöfel, I. Rendtel, P. Rendtel and H. Seipelt very much for their cooperation. Without their enthusiasm, the double count observations as well as the analysis of the huge amount of data would not have been carried out and thus their contribution would not have been possible now.

References

[7] Roggemans, P., "The 1988 Perseid Meteor Stream and Observer's Perception Coefficients", *WGN* 17:5, 1989, pp. 189–193.

[8] Rendtel, J., "Meteoorwaarnemingen DDR", *Radiant* 7:6, 1985, pp. 130–131.

[9] de Lignie, M., "Calculating Error Bars for ZHRs", *WGN* 18:1, 1990, pp. 3–4.

[10] Kresáková, M., "The Magnitude Distribution of Meteors in Meteor Streams", *Contr. Skalnaté Pleso Obs.*3, 1966, pp. 75–109.

[11] Roggemans, P. (ed.), "IMO Handbook for Visual Meteor Observations", Sky Publishing Co., 1989, pp. 80–81.

On the Cause and Nature of Error in Zenithal Hourly Rates

Peter Brown

A formula is developed which takes limit error of the individual variables in the ZHR function into consideration. The application of the formula to real world ZHR calculations is briefly analyzed and the sources of error within each variable component of the ZHR function are identified.

1. Introduction

One of the key quantities of meteor showers studies by scientists is the zenithal hourly rate (ZHR). This value is quoted by meteor astronomers to give an indication of a showers' relative strength and provide information on the particle distribution and temporal evolution within the meteor stream.

The ZHR is defined as the number of meteors seen each hour by a standard observer watching an unlimited portion of a clear sky, with the shower radiant at the zenith and a limiting magnitude in his field of view of 6.5. The importance of the ZHR in the establishment of key features within a meteor stream cannot be underestimated. It is therefore imperative that an accurate value of the error in the ZHR value be established to prevent misinterpretation of the profile data, leading to incorrect conclusions.

The present widely-accepted formula for measuring the error in the ZHR is ZHR/$\sqrt{n}$ with N the number of meteors that contributed to the ZHR. This is derived from the interpretation of the value for the standard deviation in a Poisson distribution, which gives the percentage error as $1/\sqrt{n}$ to a 68% confidence level for an individual measurement by definition. Note that this formula becomes useless when small hourly rates are involved. In effect, this formula takes into account the statistical variations expected in a random process such as meteor rates. Thus it can be stated that the actual ZHR is within ZHR/$\sqrt{n}$ to a 68% confidence level.

Two things are apparent about this error formula. First, as the number of observed meteors increases the actual percentage error decreases. During high meteor activity the percentage errors may become minuscule. For example, according to [1] the 1985 October Draconid return produced visual hourly rates as high as 300 in Japan. From this the percentage error in ZHR (which was probably close to 400) would have been 5% or roughly 20. This is clearly far to low as limit errors from limiting magnitude measurements, perceptional differences, etc. would contribute far more to the error.

A second underlying assumption is made that the number of meteors appearing in any one small time interval (for example, a minute) during this hour remains constant; more precisely, that the probability for such an event remains constant. This is often not the case as varying radiant heights distort this probability and make the $1/\sqrt{n}$ generalization less applicable.

For both of these reasons a more accurate formulae for deriving uncertainties in ZHR estimates is desired.

2. Method

A ZHR value for any meteor shower is composed of a number of variables such as radiant height, cloud cover, etc. Each of these measured values has an accompanying uncertainty as does any physical measurement. Thus as each variable is used in the ZHR formula the final ZHR value becomes more uncertain as the individual uncertainties accumulate. The ZHR is given as:

$$\mathrm{ZHR} = F r^{6.5-\mathrm{lm}} \cos^{-1}(Z)\, p \frac{n}{T_{\mathrm{eff}}} \tag{1}$$

where F is the correction factor due to obstruction of the field of view and takes the form $F = 1/(1-k)$ where k is the decimal fraction of the field of view obscured, r is the population

index, lm the limiting magnitude in the field of view, Z the zenith distance of the radiant, p the perception factor, n the number of observed meteors and T_{eff} the effective observed time given in hours.

If all these values are known exactly then the only source of error will be the statistical variation, and the form $1/\sqrt{n}$ can be used. But all these values are measured and subject to uncertainties that propagate down to the final ZHR answer.

In general any function of the form $f(x_1, x_2, x_3, \ldots)$ where each variable is subject to independent, random errors $\Delta x_1, \Delta x_2, \Delta x_3, \ldots$ has a global uncertainty according to [2] given by the formula:

$$\Delta f = \sqrt{\left(\frac{\partial f}{\partial x_1}\Delta x_1\right)^2 + \left(\frac{\partial f}{\partial x_2}\Delta x_2\right)^2 + \left(\frac{\partial f}{\partial x_3}\Delta x_3\right)^2 + \cdots} \tag{2}$$

where $\frac{\partial f}{\partial x_1}$ is the partial derivative of the function f with respect to the variable x_1 and so on. Note that the error is found using the method of the quadratic sums or addition in quadrature, which is extensively described in [2].

For the ZHR formula the error formula is of the form:

$$\begin{aligned}(\Delta\text{ZHR})^2 = &\left(r^{6.5-\text{lm}}\cos^{-1}(Z)\,p\frac{n}{T_{\text{eff}}}\Delta F\right)^2 \\ &+ \left(F(6.5-\text{lm})r^{5.5-\text{lm}}\cos^{-1}(Z)\,p\frac{n}{T_{\text{eff}}}\Delta r\right)^2 \\ &+ \left(Fr^{6.5-\text{lm}}\ln(r)\cos^{-1}(Z)\,p\frac{n}{T_{\text{eff}}}\Delta\text{lm}\right)^2 \\ &+ \left(Fr^{6.5-\text{lm}}\sin(Z)\cos^{-2}(Z)\,p\frac{n}{T_{\text{eff}}}\Delta Z\right)^2 \\ &+ \left(Fr^{6.5-\text{lm}}\cos^{-1}(Z)\,p\frac{n}{T_{\text{eff}}^2}\Delta T_{\text{eff}}\right)^2 \\ &+ \left(Fr^{6.5-\text{lm}}\cos^{-1}(Z)\,p\frac{n}{T_{\text{eff}}}\Delta p\right)^2\end{aligned} \tag{3}$$

Thus in theory, given each quantity and its respective error, it is possible to arrive at a final answer for the error in the ZHR caused by the propagation of errors in the individual measurements. Each variable is independent of all the others since no variable is a function of any other variables. Therefore all measurements are independent, satisfying the first criterion for the use of the formula.

The random nature of the errors is not clear. Arguments can be made that some error are likely to be systematic in certain cases and that other methods are more applicable. In general this contention is hard either to prove or to disprove. As a result it will be assumed that the errors involved are random, keeping in mind the limitations of this assumption.

3. Analysis

At first glance, formula [3] may seem quite complex and somewhat unwieldy for practical use. Indeed, taking the formula from the theoretical arena to practical applications requires serious simplifying assumptions. It is hoped that in the end, however, a more accurate formula for general use in ZHR error analysis will be obtained than the one currently employed. In order to analyze the ZHR error function one must look at each of its components separately to arrive at a realistic interpretation of each variable's error and the ease with which this error can actually be determined in the field.

The obstruction correction factor F

The value for F is arrived at by weighing the total amount of the sky covered during a given time period (usually one hour). The observer must make a weighted judgement based on a number of cloud measurements during the time interval if the percentage is varying, or in the case of terrestrial obstruction (trees etc.) determine a single value to correct for the loss of the viewing area.

In practice, most observations are carried out under clear skies. Under these conditions the factor F becomes 1 and the error zero for practical purposes. Thus the factor F often plays no role in contributing to the ZHR error. If cloud is present the amount of sky covered is measured subjectively by the observer. The only way for an error estimate to be made is for the observer to estimate his limit error and record it. However, this error can be greatly reduced by the use of instrumentation or through meteorological training and practice.

The population index r

The population index expresses the ratio of the number of meteors in magnitude class $m+1$ to magnitude class m. As this value varies somewhat from magnitude class to magnitude class through random errors, the value is usually obtained by linear regression.

When applying r values in the ZHR formula, it is desirable to use the magnitude data from the same data set to derive an appropriate r value. In this case the error is simply given by the general formula for the error in the slope of a regression line:

$$(\Delta r)^2 = \frac{N}{N-2} \frac{\sum_{i=1}^{N}(y_i - r - bx_i)^2}{N\sum_{i=1}^{N} x_i^2 - \left(\sum_{i=1}^{N} x_i^2\right)} \tag{4}$$

where N is the number of magnitude classes used in the analysis, y is the number of meteors in magnitude class x (after perceptional corrections) and b is the y-intercept of the regression line. Of course the accuracy of this error is also influenced by the experience of the observers and their ability to estimate magnitudes. Typical values for the error in r in moderately-sized shower databases (more than 1000 observed meteors) are on the order of 0.2 (cfr. [3]). If an r-value is assumed as in [4] then the size of the error in a particular data set is likely to be larger and also more difficult to evaluate.

The limiting magnitude (lm)

This is perhaps the most difficult error factor in the ZHR computation. Accurate estimates of the limiting magnitude lm are particularly important as lm is part of the exponent of a power law factor in the ZHR function, so that small initial errors tend to be amplified in the final ZHR.

The limiting magnitude is determined through two principal methods. In the first, the number of stars in a certain region of the sky are counted and then a chart is consulted giving the corresponding limiting magnitude. The second method simply involves locating the faintest star visible to the naked eye and record this as lm. In recent years most observers have been using the former method which seems to give more accurate results. The error in lm when obtained from either of these methods can only be determined by a limit error estimate by the observer. While generalizations are difficult, the author's personal empirical results give errors typically of 0.2–0.4 over the useful lm-range. Visually lm is unlikely to be determined to any more than 0.2 or 0.3 at best by any but the most experienced observers.

Reducing the errors in lm requires some other than these two simple methods. An ingenious device described by Berry and Pike in [5] called a visual photometer has an accuracy of better than 0.1 according to the authors. The device is non-electronic and permits the observers to more accurately judge his visual lm, reducing subjective limit error. The device is simple to make and could be used for advanced observers participating in specific observing projects.

The altitude correction factor $\cos^{-1}(Z)$

This factor is one of the more difficult to derive an error estimate from. Generally, meteor radiant altitudes are found by using accepted radiant positions and then computing the radiant's height at the midpoint of the hourly observation. Care must be taken to ensure that radiant drift is properly accounted for or large errors may develop. The two principal mechanisms likely to cause error in radiant position are zenith attraction and diffuse meteor radiants.

Zenith attraction is significant only for slow meteor showers, when the radiant is near the horizon. The apparent radiant position, however, can be accurately calculated if the stream geocentric and apparent velocity is known [6]. Typically this kind of error can be screened by calculating the apparent radiant position, or simply waiting until the radiant is higher in the sky before making any observations.

The diffusiveness of meteor radiants is difficult to take into account in the error formula. If the meteors from the shower all have radiant positions evenly distributed within a radius of the given radiant position, it is not unreasonable to assume that the center of this radius represents a fair "average" for the stream. In any case the effect is likely small for most streams.

The perception factor p

This is the most difficult variable to get any kind of accurate estimate for, let alone an accurate error estimate. For this reason many meteor astronomers leave this factor out altogether and make an underlying assumption that $p = 1$, and that the observer in question is a standard observer.

Getting an estimate for the value p for any observer is a time consuming task which requires comparison with other observers. Some methods for determining perceptional coefficients are discussed in [7] and [8].

Even if a reasonable perception value is empirically determined for any observer, the result holds strictly only for the data from which the value is derived as perception likely displays wide variations on different time scales. Over the long term, as an observer ages, the average level of perception is likely to go down. In short term, factors such as fatigue and diet play a role in influencing perception. As well, distraction, such as discussions held during group observing, can lead to effective reductions in perception as attention is diverted away from the task at hand.

For all above reasons, in general it is impractical to arrive at reasonable error limits for perception which remain valid over the long term.

The effective observing time T_{eff}

The useful observing time during an observing session can be recorded with the least error. By using a tape recorder and not taking breaks until the end of a recording interval the observer can reduce the error in T_{eff} to all but zero. If he is recording on paper, estimating the time to record an average individual event and then multiplying by the number of events in a time period and subtracting this from the total length of time the observer can give a good measure of the T_{eff} value.

Ultimately the limit error, if any, in T_{eff} must be estimated by the observer.

4. Conclusions

Statistical variation in meteor rates is only one of several variables which influence the error in the ZHR. Given limit errors in any number of the quantities used to calculate the final ZHR value, formula (3) gives the final ZHR uncertainty.

For practical purposes the formula may be simplified by dropping the perception term and assuming $p = 1$. All the remaining terms have error values which may be easily determined in practice. Simplifications such as assuming $p = 1$, and having the observer make the limit error estimate in each term (which is itself subject to error) reduce the final accuracy of the outcome. This formula does take these obvious errors into account, however, while the old formula ignores them and thus creates a very conservative and erroneous error value.

Combining the uncertainty due to statistical variations and the limit error due to inaccurate measurements gives a true picture of the individual ZHR error.

When many individual ZHRs are combined to produce a final global profile, the error in each measure must affect the final error in the global ZHR. Taking individual ZHRs without proper error and then combining and getting an error out yields a measure of the variation of all the individual ZHRs relative to one another. However, in point of fact, each ZHR measure is merely the midpoint of a range of possible values allowed by their respective error size and so this process will yield error values far too small. Thus analysis of global ZHR error values begin by first accurately determining individual ZHR error values.

References

[1] K. Simmons, "The Draconid Storm Returns over Japan", *Meteor News* 72, January 1986, pp. 1–3.

[2] J.R. Taylor, "An Introduction to Error Analysis", University Science Books, 1982, p. 73.

[3] P. Roggemans, "On the Geminid Meteor Stream in 1985", *WGN* 14:2, April 1986, p. 53.

[4] L. Vanhoeck, D. Koschny, "ZHR Correction Factors", *Proceedings of the International Meteor Weekend*, Luc Vanhoeck (ed.), Hingene, Belgium, 1986, pp. 29–31.

[5] R. Pike, R. Berry, "A Bright Future for the Night Sky", *Sky and Telescope* 55:2, February 1978, pp. 126–129.

[6] D.W.R. McKinley, "Meteor Science and Engineering", McGraw-Hill Book Company, 1961, p. 34.

[7] P. Roggemans, "The 1988 Perseid Meteor Stream and Observers' Perception Coefficients", *WGN* 17:5, October 1989, pp. 189–193.

[8] R. Koschack, "On the Determination of the Probability for Visual Meteors", *WGN* 16:3, June 1988, p. 74.

Constructing a Video-Based Meteor Observatory

R L. Hawkes, Mt. Alisson University

The key elements of a video-based meteor observing system are discussed. A recommended system, consisting of a 50 mm focal length objective lens, a 25 mm microchannel plate (MCP) image intensifier lens coupled to a sensitive monochrome charge coupled device (CCD) video camera is described. Typical performance characteristics for such a system would be a field of view of the order of 16° by 22°, a sensitivity limit of about magnitude 7.5 for stationary astronomical sources, and an effective sporadic meteor rate of the order of 8 per hour.

1. Introduction

Three decades ago (at the December 1960 meeting of the American Astronomical Society) the first report of television-based meteor observations was presented. While low light level television (LLLTV) observations have made significant contributions to our understanding of meteoric phenomena since that time (see [1] for a review), it is only in the past few years that the mass production of video detectors and recorders, and to a lesser degree the image intensifiers required for sensitive observations, have brought prices within the range of serious amateur observers. An article outlining television meteor observations appeared in *WGN* in 1988 [2], and several members of the *IMO* have been conducting video-based meteor detection for the past few years. The primary purpose of this paper is to provide an overview of image intensifier and video technology, and to present some recommendations for those considering setting up a video based meteor observatory. A companion article will suggest specific LLLTV

meteor observations, and initiate a discussion on how the *IMO* can coordinate and standardize video-based meteor observations.

Before we look in detail at the components of an image intensified video detection system, let us consider the performance of a typical camcorder alone for meteor observations. The sensitivity of a typical color camcorder is of the order of a few lux. When such instruments are used with the lens in telephoto setting it is possible to detect stars down to just beyond magnitude +2. This level of sensitivity and the rather small field of view would result in a rate of the order of one sporadic meteor every few hundred hours! While significantly higher rates could be obtained during the major showers, nevertheless a nonintensified color video camera is of very limited use as a meteor detection instrument.

2. Basic components of a video-based meteor observatory

The essential components of a video-based meteor observatory are pictured in the diagram of Figure 1. Little needs to be said about items (E) or (F), except that the difference between North-American and European video frame rates[1], and the continued existence of several popular VCR formats, will make sharing of unprocessed video data within the *IMO* difficult. In this regard it should be mentioned that while the same video tape formats (VHS, Beta and 8 mm) are used around the world, there are three main methods of encoding the video information (NTSC in North and parts of South America; PAL in Europe; and SECAM in Africa and the Pacific region).

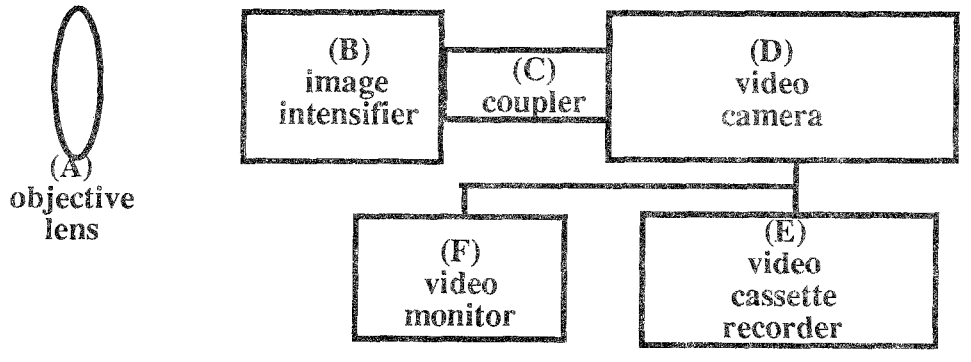

Figure 1 – Key elements of video-based meteor observing system.

3. Vidicon versus CCD video detectors

Let us next consider the video camera itself (D). A wide variety of video detectors have been used for meteor observations, including image orthicon, vidicon, image isocon, SIT (silicon intensifier target), SEC (secondary electron conduction) vidicon, CID (charge injection device) and CCD (charge coupled device). The interested reader is referred to text [3] for a detailed technical discussion of image tubes and solid state devices, and to review [1] for a summary of actual performance as meteor detectors. We will consider only the vidicon tube and solid state CCD sensors here, since the vast majority of current video cameras use one of these detectors.

The faceplate target of the vidicon tube consists of a photoconductive layer which may be considered as a matrix of many parallel resistor-capacitor elements. The presence of light will lower the resistance and allow discharge of the capacitor elements. A beam scans across the tube, and the current required to recharge the capacitors is an indication of the amount of light which has fallen on that region of the sensor since the preceding scan (i.e. during the frame time).

[1] Video detectors work on the principle of scanning across the image, one line at a time. In interlaced mode every other line is scanned on one pass through the image, and this is termed a field. Two fields constitute a complete frame. In North America there are 60 fields and 30 frames per second, while in Europe there are 50 fields and 25 frames per second in an interlaced picture.

The CCD (charge coupled device), invented in 1970, is now the dominant detector for most video applications. The sensor is a MOS (metal oxide semiconductor) solid state device. It can be regarded as a matrix of capacitive "wells" (typical CCD devices employ about 640 by 480 individual elements, or pixels). The presence of light generates charge in these wells. In order to reduce the number of connecting lines (which would, for example, be over 300 000 for a typical CCD sensor!), the charge is shifted from well to well. The following might serve as a useful analogy. Suppose that we wanted to know the rainfall over a large area. We could station people with buckets in a series of lines covering the area. At the end of the collection period, rather than each person measuring the contents of his or her bucket, we could have a scheme where, starting with the rightmost person, each person first empties their bucket to the right and then receives the contents of the bucket on their left. Then one measuring station could serve to provide measurements of the entire line, the number of the sample indicating how far to the left of the station that it originated. A CCD transfers packets of charge, which indicate the amount of light falling on different parts of the sensor, in a similar way.

As a meteor detector we are principally interested in the sensitivity and resolution of the detector. High quality vidicon and CCD detectors are quite comparable in terms of both sensitivity and resolution. For conventional stellar and galactic astronomy the CCD is preferred because of the capability of integrating over long effective exposures while maintaining a quite linear input-output response. The sensitivity of a video detector is usually expressed in terms of the required illumination level (lux)[2]. A typical commercial color camcorder requires 1 to 20 lux for a good quality picture, while the best monochrome CCD-based video cameras can produce a usable picture with as little as 0.02 lux, as can the most sensitive vidicon tubes (trade named newvicon). However, vidicons (operated at low light levels) tend to suffer more from blooming (the spilling of bright images into nearby areas of the picture) and persistence (the presence of a fraction of the previous image in a subsequent frame). Furthermore, the CCD can operate with low voltages, is much more rugged and reliable, and (being solid state) has almost perfect stability (i.e. the distortion of the picture does not change with time or temperature).

In most astronomical applications CCD cameras are cooled to limit background noise. There are two principal sources of noise in a CCD-based video camera—dark current noise (which increases with effective exposure time) and readout noise (which is independent of exposure time). For meteor observations we read the CCD at standard video framing rates (50 or 60 Hz) and readout noise predominates over dark current noise. For this reason there is little advantage in cooling CCD cameras used as meteor detectors.

4. Image intensifiers

An image intensifier is used the increase (often by factors of tens of thousands) the brightness of an image. Image intensifiers have an input photocathode window. A small amount of light falling on this surface will generate electrons by the photoelectric effect, these photoelectrons are then accelerated by a high (typically a 10 000 V) electric potential difference. They then strike an output window phosphor (like a tiny television screen). In so called "first generation" image intensifiers, the electrons were attracted toward the point of a cone shaped anode, which acted essentially like an electronic pinhole camera, with each of these stages having an intensity gain of roughly 50. However one could then add a second similar image intensifier stage. A typical configuration was three coupled first generation image intensifiers in a single package, which would have a luminous gain of roughly $50 \times 50 \times 50$ (assuming 100% transmission between stages) or about 125 000 in total. A second generation of image intensifiers used electron multiplication in a large number of tiny conducting channels, a microchannel plate (MCP), to achieve a high luminous gain in a single stage (typical luminous gains of 25 000). Most commercial image intensifiers are now of this second generation MCP type. Often the input and output windows are of the same size (this need not be so since tapered fiber optics can be used to increase or

[2] Sometimes this is expressed in terms of scene illumination, and sometimes as a faceplate illumination—be careful when comparing manufacturer's claims.

decrease the size of the image), and are of the order of 18 to 25 mm in diameter. Generation 3 image intensifiers essentially differ only from the generation 2 tubes in that they have a more efficient photocathode. Additional details on image intensifier operation can be found in text [2].

It is important to keep the limitations of image intensifiers in mind. First, they have a limited resolution. A good quality second generation MCP tube will have a minimum resolution of the order of 25 line pairs per mm, which, for a 25 mm tube, would correspond to an absolute limit of 625 line pairs across the horizontal dimension of the picture. In addition, all intensifiers suffer to some degree from blooming, which further significantly restricts the actual resolution of the device for bright light sources, and from persistence (largely due to the properties of the output window phosphor). Both blooming and persistence are significantly worse with first generation image intensifier tubes. Although most current image intensifiers incorporate some electronic protection against damage by high light levels, an image intensifier tube can be seriously damaged by exposure to high light levels for even a second, and they must be carefully protected.

5. Coupling

The image on the output window of the image intensifier must in some way be coupled to the input window of the video detector. This can be done in two ways—either by using direct physical connection (usually via a fiber-optic coupling pipe) between the image intensifier output window and the input window of the CCD or the vidicon detector, or by using a coupling lens. The advantage of direct coupling is that virtually none of the luminous intensity is lost. It also results in a shorter and lighter total observing system. The disadvantage is that each new fiber-optic coupling will result in a further loss in resolution. Optical coupling with a high quality lens will result in little loss in spatial resolution, but does result in significant loss in intensity. A couple of points should be mentioned for those considering direct coupling methods. The first is that in order not to suffer a loss in clarity (i.e. making images appear as though they are slightly out of focus) one really needs access directly to the photocathode surface, which means a windowless CCD (which are delicate to handle and need to be specially ordered), or a very thin window vidicon tube. Secondly, one cannot usually directly couple an image intensifier output phosphor to a vidicon tube (i.e. without a fiber-optic coupler) since the electromagnetic fields generated in the intensifier interfere with the scanning in the vidicon. If direct coupling is done, I would recommend use of a high quality optical coupling glue, available from science supply stores. If optical lens coupling is used, one will need either a macro lens, or a conventional lens with extension tubes or the addition of "close up" lens attachments (which attach to the filter ring on the lens). In all cases one should strive to have the coupling lens fast (i.e. a low F number) and physically close to the image intensifier output window so that as little intensity as possible will be lost.

6. Objective Lens

Most video-based meteor observations have used objective lens focal lengths of the order of 25 to 100 mm. To some degree the wider the field of view (i.e. the shorter the lens focal length) the higher the meteor rate. However one eventually reaches the point where the background "noise" (the accumulated light from unresolved stars, skyglow, etc.) in a single pixel becomes great enough that the sensitivity of the system becomes "background limited". This limit will be reached sooner with wide angle lenses, since more of the sky is being directed to a single pixel. Furthermore, the wider the field of view the poorer the spatial resolution (and hence the more uncertainty in such parameters as meteor heights and trail lengths) since each pixel will correspond to a larger angle. Reference [4] provides a more detailed description of the relation between lens parameters and optimization of video detector performance.

We have indicated in Table 1 the expected field of view assuming that a 25 mm active diameter circular image intensifier is optimally (i.e. using largest possible area of intensifier) coupled to

a video detector with a 4:3 aspect ratio. In addition we have indicated the angular resolution (in minutes of arc) assuming a resolution of 500 pixels horizontally, and the background limited sensitivity (in astronomical magnitudes), assuming the night sky brightness quoted in [5], for both 500 and 200 pixel resolutions. The background limit will vary extensively with observing location, weather conditions, and observing orientation.

Table 1 – Effect of objective lens focal length of view, angular resolution and background limited sensitivity for a 25 mm image intensifier optimally coupled to a CCD vidicon detector.

	$f = 25$ mm	$f = 50$ mm	$f = 100$ mm	$f = 200$ mm
Field of view	31°.5 × 42°.0	16°.3 × 21°.7	8°.2 × 11°.0	4°.1 × 5°.5
500 pixel resolution	5′.0	2′.6	1′.3	0′.7
Background sensitivity limit for 500 pixel resolution	+9.2	+10.6	+12.1	+13.6
Background sensitivity limit for 200 pixel resolution	+7.2	+8.6	+10.1	+11.6

The much smaller active surfaces of CCD detectors used without image intensifiers mean that a lens of the same focal length will result in a smaller field of view. For example, a typical CCD has an active area of 8.8 by 6.6 mm, resulting in a field of view of 7°.5 by 10°.1 with a 50 mm focal length lens.

In using the above data it is worthwhile to keep in mind that a typical +5 meteor observed at the zenith (100 km range), making an angle of 45° with respect to the line of sight, would subtend an angle of the order of 5° to 6°. Hence a focal length much longer than 50 mm will result in many partial meteor trails that begin or end outside the field of view.

It is likely that a serious meteor observer will, over the lifetime of the video observing system, want to use several different focal length lenses. Hence it is important to plan your system using a lens mounting system to make this possible. Most standard closed circuit TV systems use a standard screw type "C" lens mounting. A fair variety of lenses are available with this type of mounting. Another alternative is to purchase from a camera supply store a 35 mm camera body lens mount ring, which will then allow one to use any lens offered with that mount (if one chooses a standard lens mount such as Pentax, Canon, Minolta or Nikon this will offer a much wider choice of lenses at prices competitive with C mount lenses). In any case it is critical to make the objective lens as fast as possible. For example an $f/1.8$ lens will yield a meteor rate (for sporadic meteors) less than half that of an $f/1.2$ lens in an otherwise identical observing system.

7. Recommended system

Any sort of sensitive LLLTV meteor observing system will be a major investment. Although a number of companies sell directly coupled composite image intensifier-detector units, one usually pays a very high premium for these ready made specialized devices (typical costs are 10 000 to 15 000 USD). As a rule of thumb the total package costs will be at least double the cost of the intensifiers and video cameras which make up the constituent parts.

I believe that most observers will be best served by purchasing separately a second generation MCP image intensifier, and then using lens coupling to a monochrome CCD camera. The total length and weight of such a system can still be kept quite small—a typical 25 mm diameter MCP image intensifier has a length of about 75 mm, a good coupling lens will only add 50 to 100 mm more, and some CCD cameras are as short as 85 mm. There is nothing technically difficult about lens coupling, since one is simply using the CCD camera and coupling lens to focus on a nearby object (the output window of the intensifier). A suggested configuration, with order of magnitude prices given in US dollars is indicated in Figure 2.

Suggested Moderate Performance LLLTV Meteor Observing System

1. **Objective Lens 50 mm / F1.2 (35 mm camera lens attached to a camera body mount ring; typical cost $250 for lens + $25 for attaching ring).**
2. **Second generation 25 mm MCP image intensifier (gain of at least 20,000) which includes an integral high voltage multiplier and oscillator so that it can be powered with several dry cell batteries (typical cost $1800).**
3. **Lens coupling system permitting 2:1 imaging (i.e. image the full 25 mm intensifier output window on a 12 mm active area width of a typical CCD camera). Recommended method (and exact cost) of coupling will depend on lens mounting arrangment of CCD camera. (cost of the order of $200)**
4. **Monochrome CCD camera with 0.02 lux (or better) rating and at least about 600 by 400 pixels ($600).**
5. **Quality VCR ($450)**
6. **Monochrome video monitor ($140) (could be replaced by standard TV)**

Figure 2 – A suggested configuration, with order of magnitude prices given in US dollars.

As can be seen, an LLLTV meteor observing system is a major investment for an amateur meteor astronomer (although it might be pointed out that the total cost of about 3500 USD is no more than serious amateurs in other areas of astronomy pay for a good quality telescope and accessories). Also, many of those considering setting up a video-based meteor observatory will have items (E) and (F), and quite possibly item (A), which will reduce the total costs. Indeed, one would have a less sensitive (but simple and workable) video meteor system by simply using the macro lens on a home camcorder to view the output window of an image intensifier.

I would urge you to carefully consider alternatives before purchasing a system. Particularly with respect to the image intensifier, prices will vary between companies by at least a factor of three for devices with identical specifications (the other items, being mass produced, will tend to vary much less in price). Some of the main manufacturers of image intensifiers include EEV, Hamamatsu, ITT, Litton, Philips, Thomson, Varian and Varo, while monochrome CCD cameras are manufactured by many companies including Cohu, EEV, Fairchild, GE, Hamamatsu and Philips. Most of these companies will not sell directly (although they will usually provide technical data), and so you will have to locate a local distributor. If you are hesitant to get involved in buying the separate components and mounting them together, you might consider one of the lens coupled systems which can now be bought "off the shelf". For example, Edmund Scientific (101 E. Gloucester Pike, Barrington, NJ 08007-1380, USA) sells a night vision system incorporating a 25 mm MCP for 3400 USD, which can be coupled directly to any C lens mount CCD video camera using their 260 USD TV coupler.

Another option which we have not discussed, would be to purchase a used intensified video camera.

8. Performance Expectations

It is difficult to predict precisely the exact performance of an LLLTV. Reference [1] provides a table indicating the sensitivity of various actual meteor observing systems. The sensitivity will be limited either by the unresolved sky background intensity (discussed earlier), the sensitivity limit of the intensifier-video detector combination (essentially a limit imposed by the total "noise" generated in various electro-optical components), and finally by the discrete nature of light itself (one needs to detect at least several photons in each frame period). As mentioned earlier, the unresolved sky background limit for our recommended system is of the order of +8.5 to +10.5. The quantum limit can be calculated with some precision—e.g. for a lens of active

diameter 50 mm, a first surface quantum efficiency of 0.30, a net lens transmission factor of 0.85, a frame integration time of 1/30 s and a meteor at 100 km range, the quantum limit would be about +11.2 (if 5 photons per frame are required to observe the meteor). If one doubles the lens diameter this limit will improve by about 1.5 magnitudes.

The most difficult parameter to estimate is the sensitivity limit imposed by the camera-intensifier electronics. Let us first consider the sensitivity limit of a nonintensified CCD detector. It can be shown that a CCD camera with a sensitivity of 1 lux, and with 500 pixel horizontal resolution, incorporating a lens with a 25 mm effective diameter would be expected to have a limiting sensitivity of about +1.8. In arriving at this figure we have assumed that all of the light from a stellar source is concentrated onto a single pixel, whereas the 1 lux refers to a picture-averaged illumination rating. A 200 pixel resolution would correspond to an apparent stellar sensitivity limit of about −0.2. Meteors, being moving light sources, will have their intensity spread over a number of pixels, which causes the effective meteor sensitivity to be brighter than the apparent stellar sensitivity by typically 1 to 3 magnitudes.

The MCP image intensifier in our suggested system would have a luminous gain of the order of 20 000 to 30 000. Even viewing the lens coupling in the most conservative manner, we would expect that 1/50 of the image intensifier output window light would reach the video detector, for a net optical gain of the order of 400 to 600, corresponding to an improvement in sensitivity of the order of 6.5 to 6.9 magnitudes, resulting in a system apparent stellar sensitivity of the order of +6.3 to +8.7 (depending on resolution). Additional care in the lens coupling (i.e. using a fast lens as close to the intensifier output window as possible) could result in improvement by a factor of 10, corresponding to 2.5 magnitudes. Therefore it is probably reasonable to assume that the recommended system will be sensitivity limited to approximately +7.5 (for stationary images), with an expected sporadic meteor rate of the order of 8 per hour. Care in design of the coupling system might double this rate, but the overall system would soon reach the background limit of about +8.5. One may also reach the limit of the effective background noise of the image intensifier itself (this is called the EBI or equivalent background illumination).

While the author has not constructed precisely the system recommended here, I have built and used a variety of direct and lens coupled image intensified video observing systems, and I would be pleased to assist members of the *IMO* considering construction of an LLLTV system. Questions may be directed by mail (see address on inside of back cover) by electronic mail (RHAWKES@MTA.BITNET). I would also be pleased to provide reprints of articles [1] or [4].

Acknowledgments

Our video-based meteor research program is sponsored by the Natural Sciences and Engineering Research Council of Canada. I acknowledge useful comments on the first draft of this paper provided by Ms. Candace Wilmot, who is working with me this summer on the construction of two lens coupled image intensified video detection units.

References

[1] Hawkes R.L., Jones J., "Electro-optical meteor observation techniques and results", *Q. Jl. R. astr. Soc.* 27, 1986, pp. 569–589.

[2] Jobse K., "Meteor Observing by Video", *WGN* 16, 1988, pp. 119–120..

[3] Csorba I.B., "Image Tubes", Howard W. Sams & Co., Inc., Indianapolis, 1985.

[4] Hawkes R.L., Jones J., "An inexpensive meteor observing system", *Observatory* 93, 1973, pp. 233–235.

[5] Allen C.W., "Astrophysical Quantities", Athlone Press, London, 1973.

Video-Based Meteor Observation Procedures

R.L. Hawkes, Mt. Alisson University

Coordination and standardization of video-based meteor observations is needed. Suggested reporting forms and procedures are outlined in this article. A television zenithal hourly rate (TVZHR) is defined, along with a number of correction factors applicable to television meteor observations. Useful video-based meteor observations would include determination of shower and sporadic rates, measurements of the population index r, and statistical light curve regularities. More challenging projects include single or double station observations in order to estimate atmospheric heights and orbits of individual meteors.

1. Introduction

In a companion article [1] we have outlined construction of a video-based meteor observatory. The main purpose of the present article is to suggest areas in which the *IMO* can assist with the coordination and standardization of video-based meteor observations. Several specific observing projects, of varying degrees of sophistication, are also suggested.

2. Basic observational data

A low light level television system can be used for meteor observations at a variety of levels of sophistication. At the most basic level it can be used in essentially the same manner as for visual observations. The key advantage, in addition to an improvement in sensitivity, is the ability to replay video tape segments repeatedly in order to record meteor starting and ending points and luminous intensities with some precision. Just as for visual observations, it is critical that certain observing parameters be measured and recorded. There has in the past been very little standardization of video-based meteor observations, and I believe that the *IMO* can play an important role in this regard. As a first step towards standardization I would like to suggest use of the reporting form which is found in Figure 1, and would welcome suggestions on improvements which could be incorporated into a subsequent official *IMO* video reporting form. In devising this form I attempted to keep the procedures as similar as possible to those suggested in Roggemans' *Handbook for Visual Meteor Observations* [2]. Comments on completion of certain aspects of the form are indicated below.

- *Time:* The beginning and ending times should refer to the actual time of video recording, and not the time of initial setup. In the case of multiple tapes, or significant interruptions, on a single night, I would suggest separate forms for each segment. Brief interruptions could be subtracted in obtaining an effective observing time, in the same way as indicated below for cloud interference.
- *Video camera:* Because of widely differing resolution, signal to noise quality, persistence and blooming, it is important to know the equipment used for any set of observations. A typical entry might read "50 mm $f/1.2$ lens; Panasonic monochrome CCD model XY-4 lens coupled to Varo 25 mm MCP intensifier".
- *Video recording:* The main reason to include this is to determine ease of interchange of unprocessed data with other observers. A typical entry might be "Beta I recorded in NTSC".
- *Limiting stellar magnitude:* It is critical that this be estimated as precisely as possible, using visual apparent magnitudes from a star catalogue (e.g. [3,4]). Depending on the spectral response of the image intensifier (and hence the color index value), there may seem to be some inconsistencies when visual magnitudes are compared. Also, most intensifier video systems are somewhat more sensitive in the central portions of the screen. Therefore it is essential to use a selection of stars in estimating the mean limiting stellar magnitude.
- *Observing direction:* We have provided spaces for specifying the observing direction (of the center of the field of view) in both earth-based and celestial coordinates. One can convert from one to the other by knowing the time for the celestial coordinates. Altitude (also called elevation) is measured in degrees (0° along the horizon to 90° straight up at

the zenith) and azimuth (0° to 360°, starting with north and going through E, S and W)[1]. It is critical that the precise time be stated when celestial (right ascension and declination) coordinates are used.

- *Cloud interference:* Here the observer should indicate the effective part of the field of view covered (e.g. an average of 0.4 of screen covered for 5 minutes; plus 0.2 of screen covered for 20 minutes). One can then multiply and add to find the time which should be subtracted in finding the effective observing time (a total of 6 minutes would be subtracted in the above example).

Video Meteor Observation Reporting Form

Date: _____
Time: Beg. Obs. _____ **(UT) End Obs.** _____ **(UT)**
Observer: _____
Mailing Address: _____

Video Camera: _____
Recording: _____
Limiting Stellar Magnitude: _____
Field of View: _____ **degrees**

Location Long. _____ **Lat.** _____ **Ht.** _____
Observing Direction Azimuth _____ **Altitude** _____
Screen Centre Rt. Asc. _____ **Dec** _____ **at** _____ **UT**

Moon: _____ **Weather:** _____
Cloud Interference: _____ **(min)** _____ **(fraction obscured)**
_____ **(min)** _____ **(fraction obscured)**
_____ **(min)** _____ **(fraction obscured)**
time subtracted for cloud interference _____
Total number of meteors observed: _____

SUMMARY OF OBSERVATIONS:
Shower (or sporadic): _____
Unbiased (by part trails) number of meteors (N): _____
Effective Observing Time (T): _____ **(hr)**
r value: _____ **{source:** _____**}**
mean apparent speed: _____ **(pixels/frame)**
limiting magnitude for this shower M_m: _____
V (correction for field of view) _____
C (limiting magnitude correction) _____
K (correction for radiant's zenith distance) _____
TVZHR (video zenithal hourly rate) _____

Figure 1 – Video meteor observation reporting form.

3. Corrections to determine zenithal hourly rates

In the same way that the ZHR (which corrects for clouds, zenith angle of radiant, and limiting magnitude) has become the accepted way of reporting shower meteor rates, it is essential that we

[1] *Note from the editor: in several countries it is customary to measure azimuth starting with south going through W, N and E. Therefore, it might by a good idea to mention to explicitly indicate on the form how the observer is supposed to measure the azimuth.*

have a similar standard for video-based observations. My first inclination was to propose a ZHR correction which would allow direct comparison between visual and video-based observations. This is more difficult to do with precision than one would at first think. The key problem is that the effective field of view for a visual observer is magnitude dependent, being much larger for bright meteors than for faint ones. The correction which should be applied will in turn depend on the population index r of the shower (r is the ratio between the number of meteors of one magnitude class and the number in the class which is one magnitude brighter). Also, the discrimination of video-based systems against fast moving images requires additional correction factors. It seemed to me dangerous to propose calling some corrected video-based observation rate a ZHR prior to proper long term calibration of the video standard against observations by skilled amateur observers.

Hence I am proposing a television zenithal hourly rate (TVZHR). I think that there is value in keeping this standard as similar as possible to the visual ZHR. Therefore we will define it as the number of shower meteors which would be detected by a video-based observing system with a field of view of size 8655 square degrees if the radiant were at the zenith, assuming a limiting sensitivity of +6.5 and a cloudless night. The choice of a 8655 square degrees field of view is based on the work reported in [5] which suggests that the effective field of view of a visual observer is a circle of approximately $52^{\circ}.5$. While this is a very large field of view, and a somewhat poor sensitivity, for a video-based meteor observing system, we have adopted it to maintain consistency with the visual ZHR. Each of the components required in the calculation of the TVZHR is indicated below.

- *Cloud and effective observing time T:* The effective observing time, T, takes into account cloud interference as indicated above.
- *Field of view correction V:* This is a simple geometric correction given by:

$$V = \frac{8655}{wh}$$

  where w and h are the width and height of the field of view (expressed in degrees).
- *Unbiased number of meteors observed N:* The small field of view of most video systems means that one will encounter a large number of partial trails—meteors that either begin or end outside the field of view. These will inflate the effective meteor rate and a correction must be applied. Although it is possible to do this by using the field of view and the effective apparent trail length, a simpler procedure is to count only those meteors which originate within the field of view (or equivalently use only those which end on the field of view, or only those which reach their brightest point on the field of view). We will call this the unbiased number of meteors, N. The best procedure is to add the total number of meteors which begin on the field of view, the number which have their brightest point on the field of view, and the number which end on the field of view (many meteors will belong to two or all three categories), and then divide that number by 3 to get N. If one is studying a particular shower, one should use only those meteors whose radiant and apparent velocity are consistent with possible membership in that stream (see [6] for a more sophisticated way of separating video meteors into different shower categories).

  Before leaving the topic of numbers, we should deal briefly with the question of detecting faint meteors on a somewhat noisy intensified television screen. Automated meteor detection is a challenging task which has not yet been solved satisfactorily. The best detection "system" continues to be a human observer. A valid question to ask is how many times the tapes need to be viewed to find all of the meteors. Experimental evidence suggests that two viewings will detect about 90% of the meteors, and hence we recommend this as a standard to be followed throughout the *IMO*.
- *Limiting magnitude for this shower M_m:* The limiting magnitude for meteors will be somewhat brighter (up to several magnitudes for a fast meteor) than the limiting magnitude for stationary stellar sources. The reason for this is that the light from the meteor will

be spread out over several pixels during a single video frame time. The easiest way to estimate this is to use the single step control on your VCR to obtain two images of the meteor separated by a single frame time. Determine the length of this movement, divide by the total width of the screen, and then multiply by your estimate of the number of resolution elements across the width of your screen. For example if a system had 300 pixel horizontal resolution, and a typical meteor from this shower moved 2 mm in one frame time across a monitor which measured 15 cm horizontally, then the meteor moves 4 pixels each frame time. To obtain the magnitude correction we assume that the intensity is reduced by a factor of 4, which is 1.5 astronomical magnitudes. This is expressed in equation form below where M_m is the limiting "meteor" magnitude (for this shower and observing geometry) and M_s is the limiting sensitivity for stationary sources.

$$M_m = M_s - 2.5 \log \frac{distance \times pixel}{width}$$

Here *distance* represents the distance moved in one frame, *width* the horizontal dimension of the monitor (the units of distance and width must be consistent) and *pixel* is the number of horizontal pixels which can be resolved. If the field of view is near to the radiant point (so that the mean apparent speed will change significantly during a single tape), it may be necessary to break the observing period up into several segments with different correction factors for each. An alternate procedure for correction of the limiting magnitude to account for meteor motion is to move the camera at angular speeds similar to those for typical meteors from the shower under study, and then estimate the faintest "trailed" stars which can be detected.

- *Limiting magnitude correction C:* This correction (to account for different sensitivities) is essentially the same as for visual observations except that we will use the limiting magnitude corrected for apparent motion of meteors from the shower under study, and is given by:

$$C = r^{6.5 - M_m}$$

In this equation r represents the population index for the shower, that is the ratio between the number of meteors of some magnitude and those of one magnitude brighter. A typical r value for sporadic meteors is in the range of 2.5 to 3.5 with showers having values typically in the range 1.8 to 2.8. For most of the major showers this population index is quite reliably known, and can be looked up in standard works[2]. Alternately one can calculate the r-value for a set of video observations by providing careful estimates of the brightness of each meteor, and then computing the r-value which provides the best statistical fit to the observations.

- *Zenithal correction K:* As explained in [2, pp. 48–51] a correction must be applied to account for the zenith angle of the radiant at the time of observations. This is because when the radiant is low to the horizon the meteors are distributed over a much larger effective area of the Earth's atmosphere. This geometric correction is simply given by $\sec Z$, where Z is the zenith angle. However in the case of video-based meteor observations a second dependence on zenith angle comes into play, since a meteor approaching the atmosphere vertically will have its mass ablation (and hence luminosity) spread over a shorter trail length than the same meteor approaching at a low angle to the horizon. This means that meteors with a low zenith angle are favored, since the light will be spread over fewer pixel elements. It is argued in [7] that this, to first approximation, introduces a second $\sec Z$ factor, and hence (for video-based observations) the total zenithal correction is given by

$$K = \sec^2 Z$$

[2] Many meteor articles refer to the *mass distribution index* s rather than the population index r. The relation between s and r is given in [5].

- *TVZHR:* The TVZHR is then obtained from the unbiased meteor rate N and the effective total observing time T from the various correction factors as indicated in the following formula:

$$\mathrm{TVZHR} = VCK\frac{N}{T}$$

4. Recording data for individual meteors

The basic data on each meteor observed could be recorded in a form similar to that shown in Figure 2. M_V refers to the apparent magnitude at the brightest point in the trail. Under stream one would record the shower (if known) using the standard *IMO* abbreviations. Then one would indicate for the beginning point the celestial coordinates (right ascension α and declination δ) and (with a check mark or $\times$) whether the meteor began within the field of view. Similar data are recorded for the maximum luminosity and ending points. The celestial coordinates can be determined fairly accurately (sufficient for shower associations) by replaying the meteor segment repeatedly and interpolating its position on a detailed star map. A preferable method is to digitize the video signal, and then perform digital measurements of the position of the meteor head and a number of reference stars. This method is essential for detailed trajectory/orbit data, and will be the topic of an article in a future issue of *WGN* if there is sufficient interest in video-based meteor observations. The approximate accuracy of the celestial coordinates should be indicated with any set of observations.

Video Based Meteor Observations

time (UT)	M_V	stream	beginning			brightest point			ending		
			on?	α	δ	on?	α	δ	on?	α	δ

Figure 2 – Form for the basic data on individual meteors.

5. Observing projects

Finally, we wish to briefly outline several specific video observing projects. The majority of meteors observed with a sensitive video-based observing system will be sporadic meteors. The reason for this is that the number of sporadic meteors increases with decreasing mass much more rapidly than for members of the major showers (i.e. the population index r is higher). Hence while a strong shower such as the Perseid or Geminid may increase the photographic and visual rates by 5 times or more, it will only increase the rate observed by a television system sensitive to +7.5 meteors by perhaps 20%. Partly for this reason, there has been relatively little detailed study of even many of the major showers utilizing video techniques (see [8] for a detailed review). This means that there is much valuable work which can be done by *IMO* members in the area of shower meteors. Since a typical video meteor is several hundred times smaller in mass than the bright meteors observed by photographic and visual methods, they can yield valuable data on the physical nature of the smaller meteoroids. Furthermore, since more

detailed and accurate data can be obtained (compared with visual or telescopic observations) fewer meteors are needed for valid conclusions. Several specific observing projects are indicated below.

(a) I would urge members of the *IMO* who are skilled visual observers to carry out simultaneous video and visual observations in order to provide a(n r dependent) conversion relationship between ZHR and TVZHR. Such observations could also be used to measure the precision of visual observers' estimates of brightness, starting/ending points and trail orientation.

(b) TVZHR data for the major and minor showers would help astronomers better determine the structure and total mass content of these streams, and hence answer questions regarding their origin and evolution. Careful measurements would permit determination of the radiant radius for these faint meteors.

(c) The population index is not well established for fainter meteors (it is not necessarily mass-independent). Most of the data used for mass-number distributions come from radio studies which are plagued by biases. Careful determinations of r (or s) values would be a valuable contribution (but a difficult one, considering that relatively few shower meteors are observed with sensitive television equipment).

(d) The light curves (distribution of luminous intensity along the trail) of faint meteors seem quite variable, even among members of a given shower (see e.g. [7]). One can obtain statistical measures (e.g. where along the trail is the point of maximum luminosity) even from single station sporadic data, and indeed with some assumptions derive average trail lengths from such data [9].

(e) With a digitized measurement system it is possible to derive heights and velocities from single station observations (see [6]). Heights are particularly important since the variation of the height of ablation with mass can serve as a useful measure of the physical structure of the meteoroid.

(f) Dual station observations are preferable since one can obtain height, velocity and orbital information from individual meteors (by using triangulation). Optimum spacing of the two stations is of the order of 40 to 120 km, and with careful measurements it is possible to measure heights with an accuracy of better than 1 km. Time information (required for coincidence determination) can be provided either as a standard time signal on the audio track of the VCR, or, preferably, by a video time-date generator which superimposes the information on the recorded video signal. A large sample of double station television meteors, which demonstrates the trajectory and orbital data which can be obtained in such work, is described in [10,11].

6. Concluding remarks

Sensitive video-based meteor observation equipment is not difficult to assemble, but it is expensive [1]. The analysis of low light level television data is time consuming, and a computer-based video digitizing system adds significantly to the total system cost. However, with sensitive video systems one can study truly tiny meteoroids (down to 10^{-6} kg), and provide a wealth of data on individual meteors (a typical meteor will be recorded on 8 or so different video frames, each of which can be analyzed in detail). Even though image intensified video systems have been around for several decades, there still remains much to be done and amateur or professional members of the *IMO* can make a valuable contribution.

There is not a "Video Commission" within the *IMO*. As a first step toward seeing if there is sufficient interest to warrant such a proposal, I would ask that those who have already conducted (or are seriously considering) television-based meteor observations to write to me, briefly indicating the equipment used (or planned), performance (e.g. limiting sensitivity, typical sporadic meteor rate), and observations which have been made (I am not asking for detailed observations at this point, but rather simply a short summary). I would also welcome suggestions regarding whether a video commission would be worthwhile, and if so the role it should play.

Acknowledgment

Our Mount Allison video-based meteor research program is sponsored by the Natural Sciences and Engineering Research Council of Canada.

References

[1] Hawkes R.L., "Constructing a Video-based Meteor Observatory", *WGN* 18:4, August 1990, pp. 145–151.

[2] Roggemans P., "Handbook for Visual Meteor Observations", Sky Publishing Co., 1990.

[3] Smithsonian Astrophysical Observatory, "Star Catalog", Smithsonian Institution, Washington, 1971.

[4] Hirschfeld E., Sinnott R.W. (ed.), "Sky Catalogue 2000.0", Cambridge University Press, Cambridge, 1982.

[5] Koschack R., Rendtel J., "Determination of Spatial Number Density and Mass Index from Visual Meteor Observations (I)", *WGN*18:2, April 1990, pp. 44–58.

[6] Duffy A.G., Hawkes R.L., Jones J., "The determination of shower meteor parameters from single station observations", *Mon. Not. R. astr. Soc.* 228, 1987, pp. 55–75.

[7] Duffy A.G., Hawkes R.L., Jones J., "Television observations of the 1984 Orionid shower", *Mon. Not. R. astr. Soc.* 234, 1988, pp. 643–654.

[8] Hawkes R.L., Jones J., "Electro-optical meteor observation techniques and results", *Q. Jl. R. astr. Soc.* 27, 1986, pp. 569–589.

[9] Jones J., Hawkes R.L., "Television observations of faint meteors – II: light curves", *Mon. Not. R. astr. Soc.* 171, 1975, pp. 159–170.

[10] Sarma T., Jones J., "Double station observations of 454 TV meteors – I: trajectories", *Bull. Astr. Insts. Czechosl.*36, 1985, pp. 9–24.

[11] Jones J., Sarma T., "Double station observations of 454 TV meteors – II: orbits", *Bull. Astr. Insts. Czechosl.* 36, 1985, pp. 103–115.

A Simple Binocular Mount for Meteor Work

Godfrey Baldacchino

The design may first of all be conceived as a *quadpod*, a four-legged platform intended to be used in combination with a deckchair, sunlounger or a low-lying chair.

1. A matter of mounting

The particular advantages of telescopic and binocular meteor watching over the more traditional visual method by amateurs has already been amply elaborated upon by Malcolm Currie in this journal and elsewhere in recently published literature[1]. The positional accuracy which telescopic and binocular meteor watching enjoys and which therefore makes possible the very exact reproduction of meteor trails and the subsequent derivation of radiant position, radiant drifts, multiple and complex radiant structures, etc. depends however ultimately also on the stability of the observing instrument. As telescopic users are well aware, high magnifications and resolving powers are meaningless unless accompanied by sturdy mounting. Indeed, the higher the magnification used, the more vital it becomes to invest in reliable mounting equipment.

[1] For example, *WGN* 17:5, pp. 175–183, and Appendices to Newsletters of the British Astronomical Association Meteor Section (BAAMS) nr. 30 (October 1988), nr. 31 (December 1988), and Nr. 32 (March 1989).

The more common variant for mounting a low-power telescope (or high powered binoculars) is the tripod. The tripod structure seeks to combine a low-weight, skeletal structure which makes the structure portable, with the possibility of movement, the more common being an altazimuth or equatorial arrangement. Add to these a holding clasp such as a cradle to secure the light-gathering instrument properly. Unfortunately tripods are designed with two assumptions concerning the observer who would be using them:

1. That the observer is standing, in an upright position;
2. That the observer is relatively free to adjust his or her body position; his or her eye can be brought in line with the light passing through the light-gathering instrument with relative ease.

Such assumptions do not readily hold in the context of telescopic or binocular meteor watching. The observer is expected to maintain regular vigil over a specific strategically selected telescopic or binocular field for an average of 20 minutes or so. A watch of such a duration would not be effective if carried out in an upright, standing position: the observer would soon become tired, not only because of the standing position but also because of the difficulty of maintaining oneself fully stationary such as to glimpse the subtle intrusion of faint shooting stars through the field observed. Indeed, a crucial component of effective telescopic or binocular meteor watching is comfort. A comfortable, non-straining observing position reduces stress on the body physique, permitting greater concentration on the visual activity. And let us face it, comfort also improves the likelihood of perseverance in any form of voluntary activity as is telescopic or binocular meteor work. Particularly where amateurs are concerned, this is a factor not to be dismissed lightly. There is no doubt that relative ease of undertaking visual meteor watching goes a long way to explain the attraction and perseverance of observers in this field.

2. Experiences from Malta

Some of these assumptions were confirmed during the first telescopic and binocular meteor project carried out by the Astronomical Society of Malta in July and August 1989 in connection with the Aquarid-Capricornid summer meteor shower complex. This was also the target of an *IMO* project[2]. Only one binocular mount (whose construction is described below) was built specifically for meteor work and was used by two observers in this period: Anna and Godfrey Baldacchino. In 8^h20^m of effective observing time, 47 meteor trails were reported, using a modest 7×50 binoculars. The other eight Maltese observers who participated in this project:

> Stephen Abela, Bernard Bonnici, Edwin Camilleri, Martin Debattista, David Gatt, Franco Gatt, Antoine Grima, Jean Paul Mifsud

utilized conventional telescopic mounts and photographic camera tripods on which they mounted binoculars. Securing between them around 11^h of observing time, only 22 meteor trails were reported. The latter group of observers also complained of low rates, eye strain, neck cramp and back pains resulting from uncomfortable seating positions[3]. These complaints in part explain the low observing time secured (or should one say tolerated?) by this second set of observers. The inappropriate equipment also explains the significantly lower meteor counts reported by this second group. The story is thus likely to have been different had more appropriate equipment been used by this second observing team.

3. The Binocular mount prototype

The binocular mount used in this project by the two relatively more successful and satisfied observers was built on the basis of a model belonging to Malcolm Currie, *IMO* Telescopic Coordinator. The latter kindly lent a 35 mm slide of this prototype for consideration.

---

[2] *WGN* 17:3. No mention of the great advantages of binocular or telescopic coverage with respect to this shower complex were however alluded to. Details of the Astronomical Society's contribution to this project are found in the BAAMS Newsletter nr. 35 (January 1990).

[3] A summary, preliminary report of the Maltese project is reproduced in "The Big Bang", (Astronomical Society Quarterly, Malta), nr. 24, p. 4. Copies are available on request.

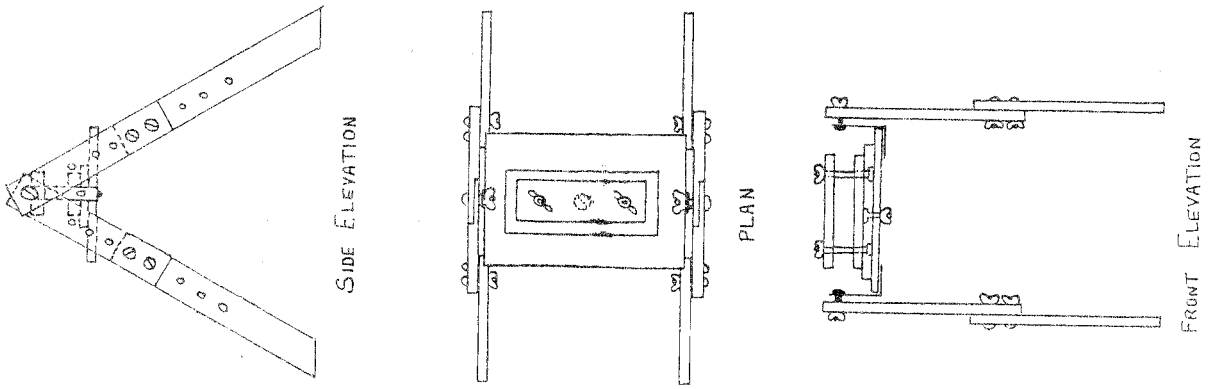
SIDE ELEVATION
PLAN
FRONT ELEVATION

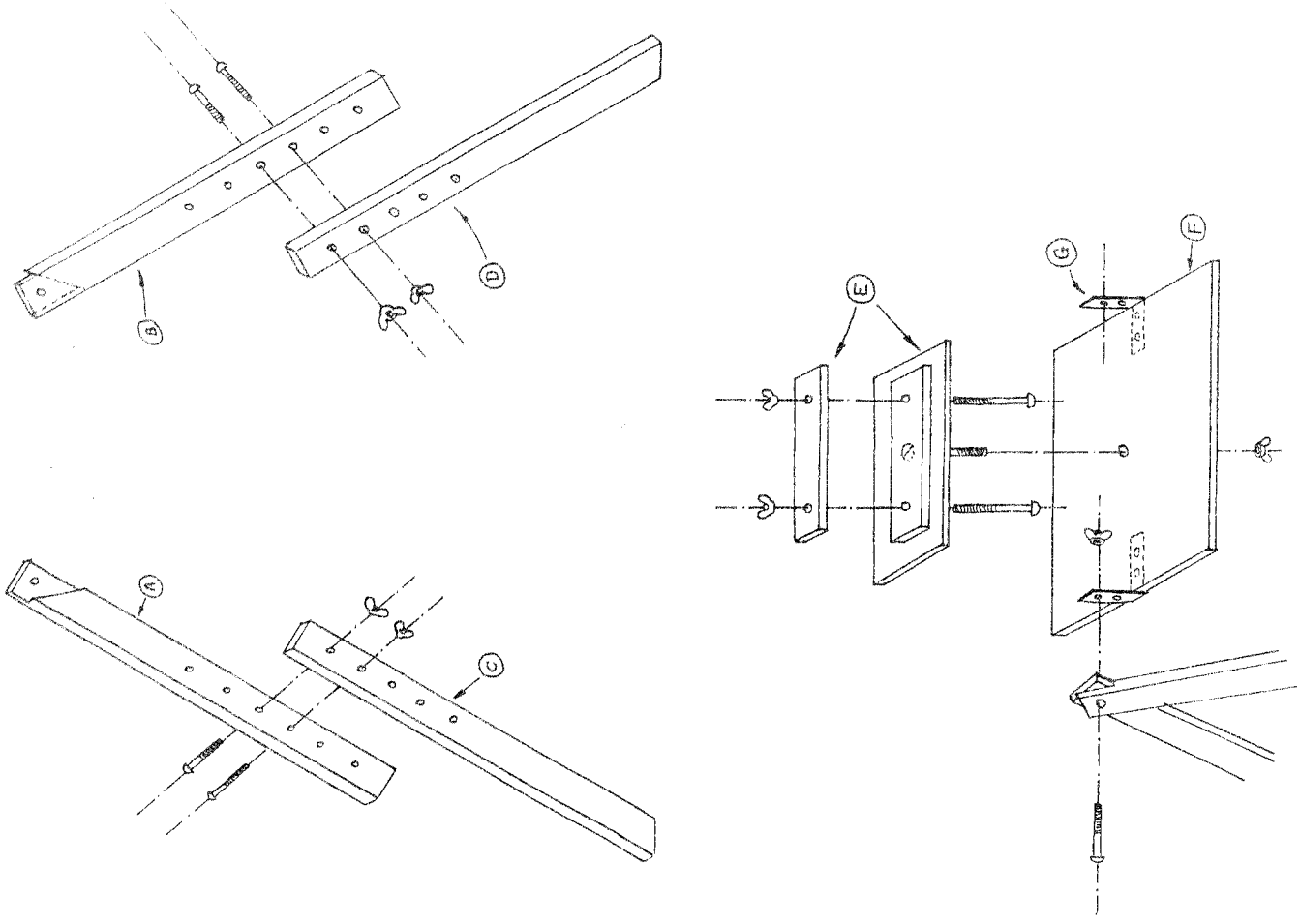
A
B
C
D
E
F
G

Figure 1 – (left) The binocular mount

Materials required:

A 80 × 2 × 4 cm (2 pieces) white deal
B 80 × 2 × 4 cm (2 pieces) white deal
C 80 × 2 × 4 cm (2 pieces) white deal
D 80 × 2 × 4 cm (2 pieces) white deal
E 10 mm plywood
(dimensions according to size of binoculars used)
F 58 × 20 cm (10 mm plywood)
G metal bracket (7 cm high)

- platform E allows azimuth motion
- platform F permits altitude adjustment
- foam strips may be glued between clamping jaws of platform E.
- variable height may be achieved by varying the position of the bolts and wing nuts in the two pairs of legs

This model was selected and taken up mainly because of its relatively simple construction requiring no professional carpentry, mechanical, electrical or other expertise. Other prototypes, though readily available, were discarded because of insufficiently explained construction details. These also often involved rather sophisticated mechanical and electrical devices likely to be beyond the grasp of various meteor watchers[4]. The cost factor was also kept under consideration. In fact, the raw material for the model selected consisted of just eleven pieces of wood (of which eight are identical), two metal brackets and a dozen bolts plus wing nuts in all. The total cost to produce was less than 15 USD ... and all wood in Malta is imported!

The technical drawing accompanying this article (Figure 1) should make the following description of the binocular mount easier to follow. The design may first of all be conceived as a *quadpod*, a four-legged platform intended to be used in combination with a deckchair, sunlounger or a low-lying chair. The eventual choice would depend ultimately on availability but also on the mean altitude of the particular area of the sky to be observed. A camp-bed or sunlounger with an adjustable back would serve very nicely as an all-purpose, all-altitude seater for telescopic and binocular meteor work.

4. Structure of the mount

The quadpod may be conceived as made up of three self-contained parts. First, there are two adjustable capital "A" sections in the vertical plane, each section having two arms (the two legs of the quadpod) each consisting of two wooden beams. The portion of the beams riding over each other is adjusted by means of bolts. This allows one to fix the height of the quadpod from the ground accordingly. The greater the portion of the beams overriding each other, the shorter the quadpod height from the ground. The third and final part of the quadpod is a flat and broad capital "U" section in the horizontal plane, riding in between the two "A" sections. The "U" section is connected to each of the two "A" sections by means of a metal, L-shaped bracket. The size of this "U" section would depend on the width of the deckchair or sunlounger in combination with which the mount is intended to be used. 60 cm would be a good fit for standard-sized, commercial seating models of this kind. On the center of this "U" section lie two horizontal plywood strips, between which the actual pair of binoculars is mounted. Foam or other shock-absorbing material may be glued to the inner parts of the two plywood strips to cushion the grip on the binoculars as well as to prevent scratching. A long bolt keeps this cradle-of-sorts fixed to the base of the "U" section, permitting at the same time a circular motion which corresponds to azimuth.

5. Adjustments

[4] Other ideas for constructing binocular mounts, also supplied by Malcolm Currie, include Meteor Notes nr.6 (BAAMS, 1979) and various extracts from Sky and Telescope magazine (January 1971, pp. 51-53; February 1981, pp. 162–164; July 1982, p. 89; July 1988, p. 38).

The two bolts holding each of the two "A" sections to the "U" section via the metal brackets also permit further refinements in altitude/height of the quadpod. This can be done by changing the angle subtended at the apex of each "A" section. A larger angle means lower height from the ground, and vice-versa. Otherwise, one may simply tilt upwards or downwards the long wooden base of the "U" section. These fine adjustments may be carried out while the actual meteor watch is in progress. All they involve is the loosening of the two bolts (one to the left, one to the right of the observer's head), carrying out the adjustments and re-tightening the bolts. All this can be performed in a few seconds, and with the observer's eyes never leaving the field under observation. Another fine adjustment is to slide the binoculars backwards and forwards some centimeters on the "U" section for full comfort, changing the distance between the eyepieces and the observer's eyes. This is however usually a once-only adjustment carried out at the start of every watch.

6. Recommendation

This kind of binocular mount has proved itself in observation. It requires practically zero technical, mechanical or woodworking skills. Indeed, the parts may be ordered ready cut and planed from any carpentry shop. The mount can be assembled or disassembled slowly in about 15 minutes for maximum portability. When all the wooden parts are placed in a specially made rexene carrying bag, the whole lot weighs 5 kilos and can be carried about with ease. One may prefer using a shoulder strap to leave both hands free.

Acknowledgments

May I thank Malcolm Currie for inspiring the construction of this binocular mount... and hopefully, via this article, many others like it. To his credit also goes the kindling of interest in binocular or telescopic meteor work among members of the Astronomical Society of Malta. May I also thank wholeheartedly Joseph Schembri for building the mount in his spare time, Mario Schembri for completing the accompanying technical diagram, and my wife cum observing companion Anna for designing and sewing the binocular mount's carrying bag.

Observational Results

The 1990 Quadrantids in Czechoslovakia

Beata Čabáková and Peter Zimnikoval

An overview is given of 1990 Quadrantid observations in Czechoslovakia.

The conditions for the observation of the Quadrantids meteor shower were not very good in West and Central Europe this year. At the longitude of our observatory (1^h17^m E) the maximum occured at 21^h local time and the altitude of the radiant was only 10°. So, the values of the ZHR correction are too high. Moreover, the Moon in first quarter caused a very low limiting magnitude (about 4.5 at the beginning and 5.5 near the end). Under this conditions it was impossible to determine a correct ZHR value, but we were happy to see several beautiful Quadrantids.

During the four intervals (18^h55^m–19^h55^m, 20^h27^m–21^h27^m, 22^h00^m–23^h00^m, and 23^h33^m–00^h33^m UT) 49 Quadrantids and 32 sporadic meteors were registered. This number is the total of four observers (J. Fabricius, J. Škvarka, P. Zimnikoval, and D. Očenáš) with the help of B. Čabáková. The ZHR curve is on Figure 1.

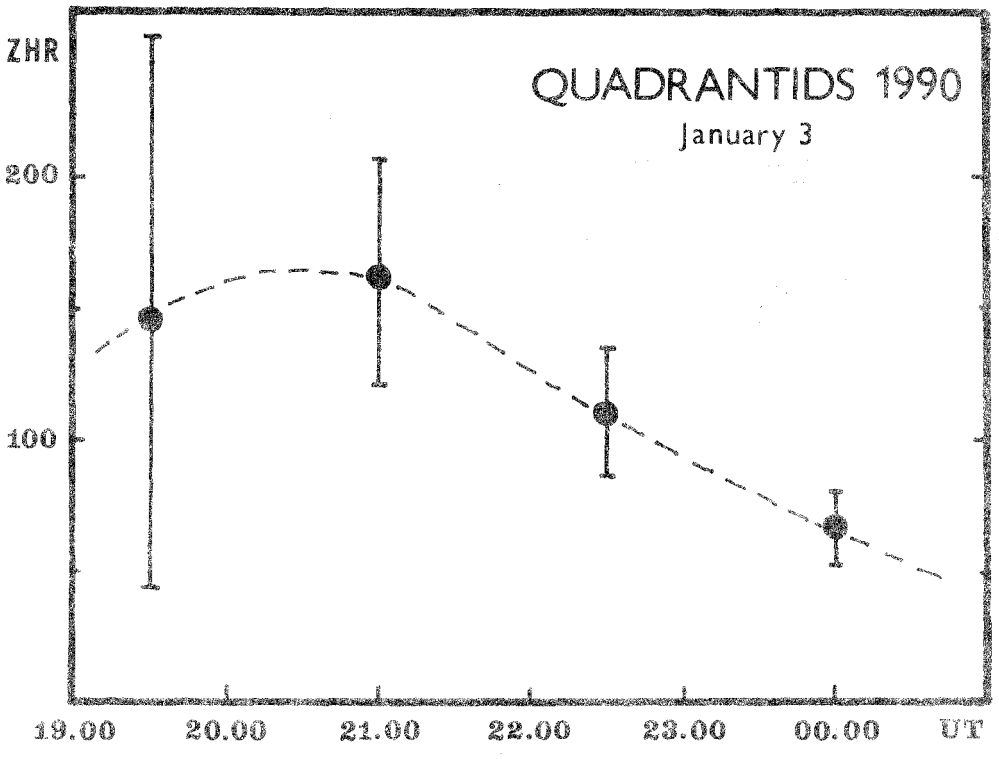

Figure 1 – ZHR profile of the 1990 Quadrantids

The number of Quadrantids was corrected to a standard sky at magnitude 6.0. Zenithal attraction was not considered for determining the ZHR. Despite of the bad conditions of the observations the result look relatively good.

For the following article, the reader may want to read again Dr. Šimek's comment on a previous paper of the same author and the author's reply in WGN 18:3, pp. 74–75 as well as the comments of Jeroen Van Wassenhove in this issue's letter section (ed.)

Visual Level Radio Counts of the 1989 and 1990 Quadrantids

T.R. Manley

An overview is given of the author's radio observations of the 1989 and 1990 Quadrantids.

Paul Roggemans states in [1] that *an attempt to reconstruct overall activity counts for 1 hour intervals comparable to radio observation histograms, but based on visual rates led to no results at all, or better to as many results as there are cases, unfortunately all different.* This is not surprising, because radio lows correspond to visual ZHR highs. Furthermore, correct interpretation of radio data requires that diurnal variations be taken into account. These factors alone account for the results found in his study. Roggemans' excellent, comprehensive reporting of facts has enabled me to discern why he obtained completely negative results with radio meteor data.

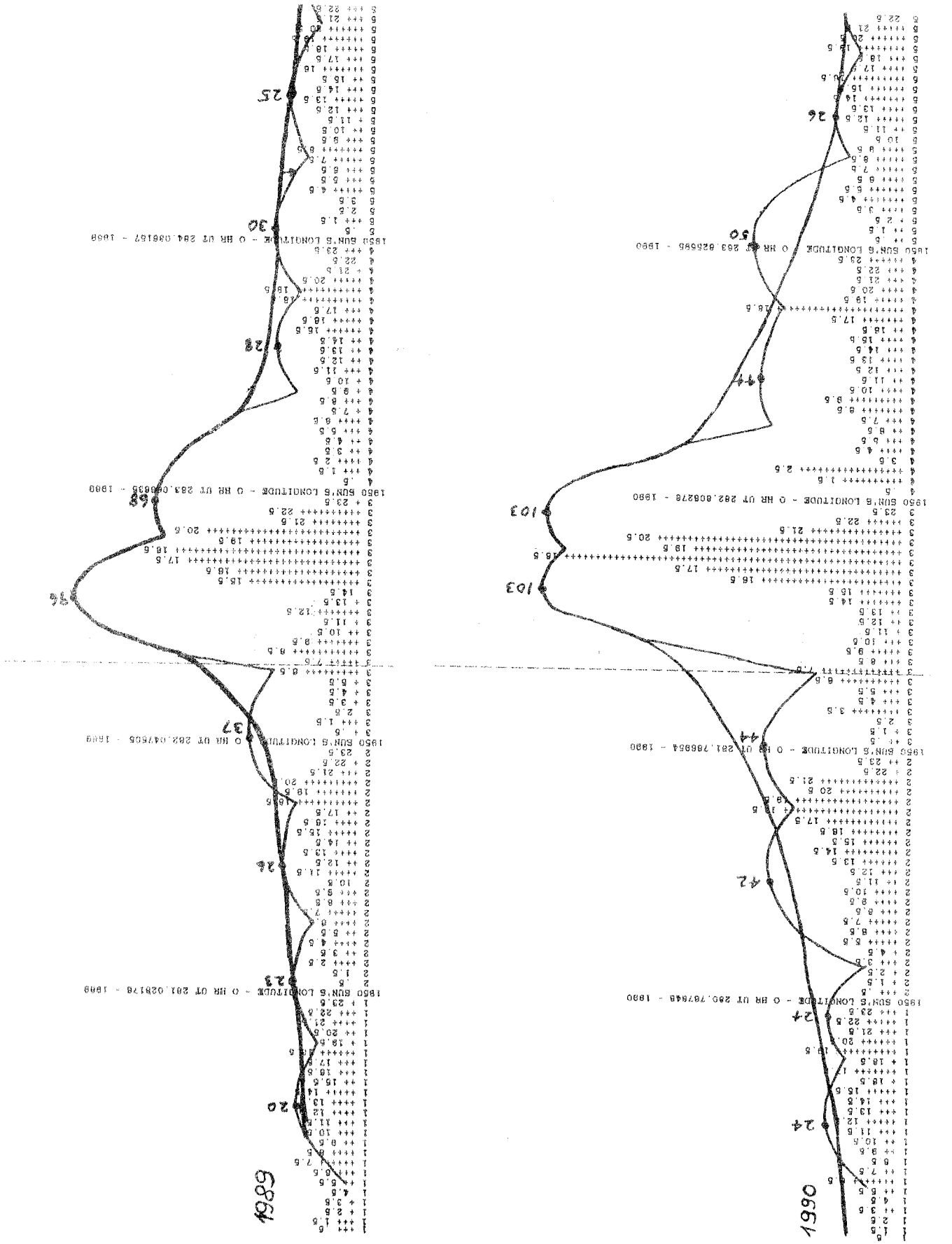

Figure 1 – Radio observations of the 1989 and 1990 Quadrantids, corrected for "missing values" and then averaged.

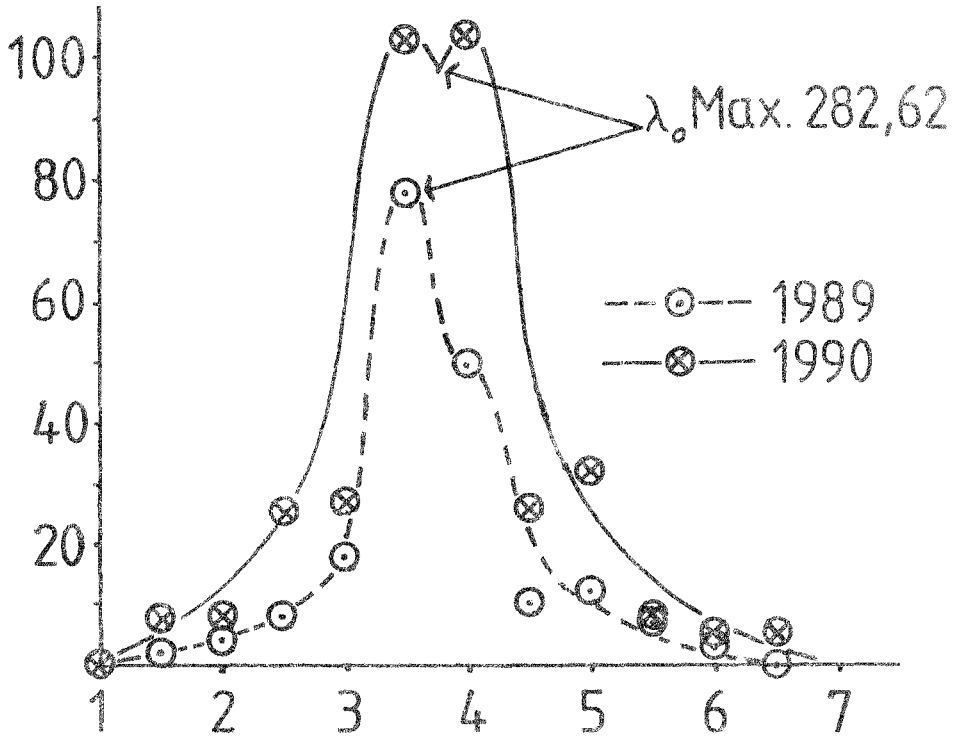

Figure 2 – Rate profiles of the 1989 and 1990 Quadrantids obtained from visual level radio counts from Sebring, Florida.

My 1989 Quadrantid graph corresponds well with Figure 4 of [1]. It shows the Quadrantids with a sampling period of 6 hours and a maximum correction factor of 2. The summary graphs in Figure 2 were made by subtracting 18 background counts off my 1989 data and 17 off my 1990 data. However, the computer printouts of my hourly graphs show much more detail (Figure 1). A study of my hourly graphs reveals the reasoning that must go into radio data before it can be utilized by the scientific community. My previous articles published in the *Radio Observer* have put forth the necessary concepts for the interpretation of radio meteor surveys. Hopefully, these graphic methods can be computerized in the future.

My experience with seismic, resistivity and magnetic surveys has taught me that the best use of geophysical surveys is in the extrapolation of known factors or results. Radio meteor data might be called an astrophysical survey and the best use of it is also in extrapolation. One of the reasons for this is that interpolation is necessary in all types of geophysical and astrophysical surveys. However, there are times when this type of survey can stand alone. The data must be well known and repeatable.

Reference

[1] P. Roggemans, "The 1989 Quadrantid Meteor Stream", *WGN* 18:1, Feb. 1990, pp. 12–18.

The 1990 Lyrids from Spain

José Trigo

An overview is given of the 1990 Lyrids seen in Spain.

During 5 nights in April 1990, the observer saw 210 meteors in 14.10 hours of observing. Among these, there were 7 α-Scorpids, 7 α-Virginids, 5 ψ-Bootids and 4 δ-Draconids. Information concerning the Lyrids, the α-Bootids and the sporadics is contained in Table 1.

Table 1 – Magnitude distributions of the 1990 Lyrids, α-Bootids and sporadics, observed in Spain. (The average limiting magnitude was 6.45.)

Shower	−4	−3	−2	−1	0	+1	+2	+3	+4	+5	+6	Tot	$\overline{m}$
Lyrids	1	0	2	1	1.5	4	15.5	19	20	13.5	1.5	79	3.03
α-Bootids	0	0	0	0	0	1	4.5	7.5	5.5	3	0.5	22	3.30
Sporadics	0	0	0	0	1.5	0.5	8.5	30.5	21.5	19	2.5	84	3.63

Recent Meteor Observations in Alberta

Peter Brown

An overview is given of meteor observations carried out in Alberta between September 1989 and June 1990.

Without doubt the aurora has become the major obstacle towards dark sky meteor work. With solar activity increasing, this is to be expected and the trend will not likely reverse for several more years. Cloud and poor weather has been typical for the province during 1989–90 so far which means that only one out of every 4–5 nights is clear enough for useful work.

The first session of the period took place from Miquelon Lake to the southeast of the city of Edmonton. I had the pleasure of being joined by Marc Zalcik, another ardent Alberta meteor observer, for this session which looked initially to promise cloud-free and aurora-free skies. However, within one hour the aurora has become active to the North and an ominous cloud band lurked to the west. By the time half of the next hour had passed, the sky was virtually overcast, the wind was blowing and the aurora had enveloped the small patches of clear remaining. Taurid activity did not really come in full force as the radiants were still fairly low and sky conditions were less than ideal through most of this session. No Orionids were seen as the radiant had not had the opportunity to rise by the time the session ended.

The next session took place on the summit of Maqua Lake on December 29–30 and conditions here made the October Miquelon Lake session look tropical. The aurora was active and this time I only managed to get half an hour into the session before the clouds rolled in from the North accompanied by a bitter breeze. No Quadrantids were seen as the radiant was far too low to produce activity.

The session on March 3–4 took place again from Miquelon Lake with Mark along as well. Conditions were quite favorable with the aurora quiet to the North and no cloud to interfere except some local ice fog. None of the early minor spring showers produced any noticeable activity with only 1 δ-Leonid being logged as a shower member. However, the late character of the session became apparent when the final hour saw no less than 18 sporadic meteors, a level comparable to what I normally see in July and not bad for a month known usually for its low sporadic activity. The final session on March 17–18 took place again from Miquelon Lake and again with Mark. This session got off to a very good start when 4 minutes into the first hour a brilliant −6 fireball appeared low on the SSW horizon briefly lighting things up with its terminal burst. Curiously the final phases of the fireball appeared distinctly green in color, a phenomenon I have only rarely seen before. The fireball ended only a couple of degrees above the horizon so people in Southwestern Alberta undoubtedly got the best view of the event. The only other activity present on this night was a lonely Virginid and one slow Camelopardalid attesting to the generally low activity characteristic of most of the spring minor showers.

The International Meteor Organization

Council

President: Jürgen Rendtel, Gontardstrasse 11, DDR-1570 Potsdam, *GDR*

Vice-Pres.: A. McBeath, 12A Priors Wk, Kirkhill, Morpeth, Northumberld. NE61 2RF, *Engl.*

Secretary-General: Paul Roggemans, Pijnboomstraat 25, B-2800 Mechelen, *Belgium*, tel. 32 (15) 41 12 25

Treasurer: Ann Schroyens, Stuivenbergvaart 48, B-2800 Mechelen, *Belgium*, postal (giro) account number: 000–1601407–34

Other council members:
Peter Brown, 181 Sifton Ave, Ft. McMurray, *Alberta T9H 4V7, Canada*
Malcolm Currie, 25, Collett Way, Grove, Wantage, Oxon. OX12 0NT, *England*
Marc Gyssens, Heerbaan 74, B-2530 Boechout, *Belgium*
Robert Hawkes, Mt. Allison Univ., Physics Dept., Sackville, *N.B. E0A 3C0, Canada*
Detlef Koschny, Ostpreussenstrasse 51, D-8000 München 81, *FRG*
Masahiro Koseki, 4-3-5 Annaka, Annaka-shi, Gunma-ken 379-01, *Japan*
Vasilii Martynenko, Astronomical Observatory of the Crimean Regional Young Technicians Station, P.O. Box 52, Simferopol, *Crimea* 333 000, *USSR*
D. Olsson-Steel, Univ. of Adelaide, Dept. of Physics, Gpo. Box 498, *S.A. 5001, Australia*
Christian Steyaert, Dr. Van de Perrestraat, B-2440 Geel, *Belgium*
Gabor Süle, Egry 47/B III.11, H-8200 Veszprém, *Hungary*
A. Terentjeva, Astr. Council USSR Acad. Sci., Pjatnitskaja 48, Moscow 109 017, *USSR*
Casper ter Kuile, Akker 145, NL-3732 XD De Bilt, *the Netherlands*
Jeff Wood, 37 Hodgson Street, Tuart Hill, *West-Australia 6060, Australia*

Commission Directors

Visual Commission: Ralf Koschack, Wilhelm-Pieck-Strasse 33, DDR-7580 Weisswasser, *GDR*

Telescopic Commission: Malcolm Currie

FIreball DAta Center: André Knöfel, Anton-Fischer-Ring 96, DDR-1580 Potsdam, *GDR*

Radio Commission: Jeroen Van Wassenhove, 's-Gravenstraat 66, B-9730 Nazareth, *Belgium*

Computer Commission: Christian Steyaert

WGN — The Journal of the International Meteor Organization and Observational Report Series

Editor-in-chief: Marc Gyssens, tel. 32 (3) 455 68 18

Editorial board: Peter Brown, Masahiro Koseki, Jürgen Rendtel, Jeff Wood, and Trond Erik Hillestad, Stengelsrud, N-3600 Kongsberg, *Norway*

Typesetting: Urania, the Public Observatory of Antwerp

Printing: André Gabriël

Other author's addresses

Dirk Artoos, Nattenhofstraat 74, B-2800 Mechelen, *Belgium*
O. Belkovich, Engelhardt Astronomical Observatory, *SU-422 526 Kazan, USSR*
A. Levina, A. Grushchenyuk, Astronomical Observatory of the Crimean Regional Young Technicians Station, P.O. Box 52, Simferopol, *Crimea* 333 000, *USSR*
Ulrich Sperberg, Südbockhorn 59, DDR-3560 Salzwedel, *GDR*
Godfrey Baldacchino, "Sirius" Triq Il-Migbha, Marsascala, *Malta*
Peter Zimnikoval, Micinska Cesta 70, CS-974 00 Banska Bystrica, *Czechoslovakia*
Thomas R. Manley, 614 Killarney Drive, Sebring, *Florida 33872, USA*
José Trigo, Avda Antic Regne de Valencia 35, 9 aptda, E-46005 Valencia, *Spain*

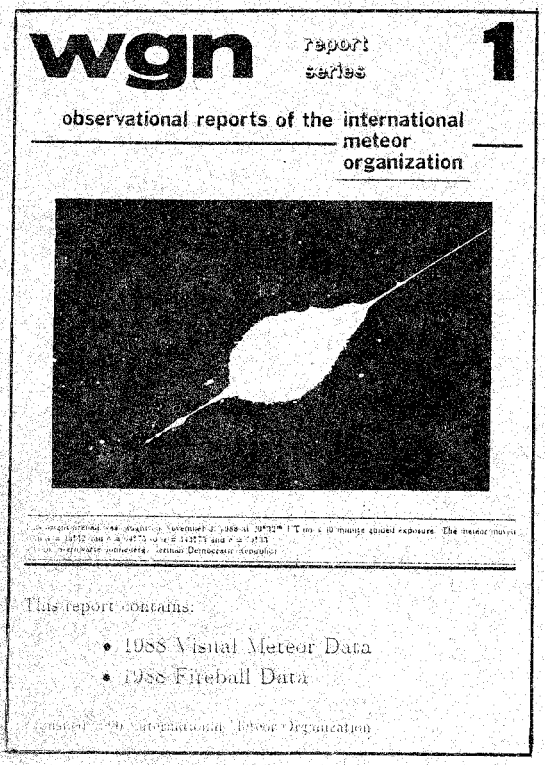

New Observational Report Series.

edited by Marc Gyssens

The first volume contains 148 pages with all *IMO* visual and fireball observations of 1988! In total, you will find 100 408 visual meteors seen during 4867 hours in 256 calendar dates by 264 observers from 16 different countries, as well as 197 entries on fireballs!

An invaluable work for meteor workers wishing to carry out further analyses or for meteor observers wanting know how their contributions fit in on a global scale.

Do not miss this first issue of a new series and order this book; only 300 BEF post paid! (surface mail delivery)

Now available: Proceedings

International Meteor Weekend 1989

Balatonföldvár, Hungary, October 5–8, 1989

The proceedings of this International Meteor Weekend are now available. The book contains more than 20 articles in about 80 pages, about various fields of meteor astronomy—almost entirely covering the conference. Included are: visual and photographic observations, radio meteor work, new techniques in meteor observation, data processing, computerization of meteor astronomy, databases, investigations on meteorite events in the past, and the International Meteor Organization itself.

These proceedings are a common publication of the *International Meteor Organization*, the *Hungarian Amateur Astronomical Association* and the *Hungarian Meteor Fireball Observing Network*. They can be ordered at 250 BEF per copy. For more information, see pp. 97–98 of this issue.